The Josephson effects in weakly coupled superconductors

J R WALDRAM

Cavendish Laboratory, University of Cambridge, Madingley Road, Cambridge CB3 0HE, UK

Abstract

The effects described in this review arise as a consequence of two terms calculated by Josephson in the expression for the electrical current flowing between a pair of weakly coupled superconductors. One of these terms is present at zero voltage and represents a supercurrent which can cross such barriers as thin layers of insulator or normal metal; the other is an extra component of resistive current. Both terms are periodic in ϕ, the phase difference across the barrier of Ψ, the complex order parameter. It is the periodic dependence of the current on ϕ which leads to the Josephson effects themselves, a unique group of phenomena which arise through the quantum-mechanical dependence of ϕ on the voltages across the barrier and on the magnetic fields near to it.

This review sets out sufficient theoretical background to allow readers with no previous knowledge of superconductivity to understand the basic physics of the effects. It also caters for those wishing to learn enough to understand devices based on Josephson effects, and no more. Although the potentially most useful applications are described, the article concentrates on fundamentals, and early and recent experimental and theoretical developments in the understanding of Josephson weak links of all types are emphasized.

This review was completed in April 1976.

Contents

	Page
1. Introduction	755
2. The Josephson supercurrent as a simple quantum-fluid property	755
2.1. What are the Josephson effects?	755
2.2. The Josephson supercurrent as a pair transition	757
2.3. The free energy of the weak link	758
2.4. The order parameter and electric and magnetic fields	759
3. The background to Josephson's calculation	760
3.1. The BCS condensed state	760
3.2. The complex order parameter in BCS theory	763
3.3. Excitations of the superconducting state	764
3.4. Single-particle tunnelling	765
4. Josephson's first calculation for tunnel junctions	767
4.1. The method of Cohen, Falicov and Phillips (1962)	767
4.2. The currents between superconductors	769
5. The basic Josephson effects	773
5.1. Josephson's predictions	773
5.2. Early observations of the Josephson effects	775
6. Quantum interference	778
6.1. The connection between magnetic flux and superconducting phase	778
6.2. Two small junctions in parallel	780
6.3. The Bohm–Mercereau experiment	780
6.4. Quantum interference in a single junction in an applied field	780
6.5. Self-field limiting and flux lines in large junctions	781
6.6. Single junction in a superconducting loop	784
7. Time-dependent effects for the shunted-junction model	785
7.1. Use of current sources and the RSJ model	785
7.2. Reduced variables	785
7.3. Constant current applied to a small junction of negligible capacitance	785
7.4. The effect of capacitance on the I–V curve for small junctions	787
7.5. The effect of series inductance on small junctions	788
7.6. Small-signal inductance of a junction at zero voltage	788
7.7. The plasma resonance in small junctions	788
7.8. The effect of high-frequency input on small junctions	789
7.9. The effect of noise voltages on I–V characteristics	791
7.10. Time-dependent effects in large tunnel junctions	791
7.11. Self-excited structure in large tunnel junctions	794
7.12. Time-dependent effects in large SNS junctions	794
8. Further developments for tunnel junctions	795
8.1. Werthamer's formulation of the tunnel current	795
8.2. Evidence for the existence and sign of the $\cos\phi$ term	798
8.3. Observations of the Riedel peak	799
8.4. Quantum noise in tunnel junctions	800
9. Other weak links	801
9.1. Josephson's generalized calculation	801

9.2. The microbridge 802
9.3. The Wyatt–Dayem effect in microbridges 806
9.4. SNS junctions and related devices. 807
9.5. Modified tunnel junctions 808
9.6. Point contacts 809
9.7. Current–phase measurements 809
9.8. Josephson effects in superfluid helium 810
10. Applications using quantum interference 811
10.1. The DC SQUID 811
10.2. RF SQUIDS 813
10.3. Josephson devices as computer elements 814
11. Applications using the AC effects 815
11.1. Precision measurements of e/h and voltage 815
11.2. Microwave mixing 816
11.3. Parametric amplification 818
Acknowledgments 818
References 818

1. Introduction

In the fourteen years since B D Josephson made his predictions of the effects which now carry his name, an enormous body of work (including a book, several important specialist reviews and many hundreds of papers) has been published developing and expounding them. In preparing this account of the Josephson effects I have therefore tried particularly to write for the general audience of non-specialist physicists for whom this journal is published. I have, for instance, (at the risk of some bias) deliberately restricted my list of references to key papers and general articles so as to avoid overwhelming the newcomer to the subject with an impossible mass of further reading. I have also concentrated on giving an account of the essential physics, and only treated rather briefly in the final two sections a few of the most important or potentially important applications, leaving the interested reader with references to some of the more technical reviews which are available. Within this framework the subject falls naturally into two parts, which may interest different groups of people and which I have tried to keep reasonably well separated. The reader who wants to know simply what the Josephson effects are and what uses can be made of them will probably wish to read quickly §2 and then come to grips with §§5, 6 and 7, which between them cover most of the essential ideas which are involved in the practical applications of Josephson effects. The reader interested in the fundamental theory of the effect, in how it is modified in devices other than tunnel junctions or at high frequencies, and in how fully it has been confirmed and developed may prefer to concentrate on §§3 and 4 which describe the original theory itself and §§8 and 9 which describe later developments. A feature of the subject is the extreme economy of Josephson's own papers. To the expert they are most illuminating, but to the newcomer the essential physical arguments which make them fascinating and original are so gently referred to that they are easily missed altogether. For this reason I have been at pains to expound the essence of Josephson's original theory. This is why I have included §3 which emphasizes the significant features of the BCS description on which he built; I hope that this section will explain enough of BCS theory to allow readers to whom it is unfamiliar to follow the development without further reading.

Brian Josephson was a research student at the Royal Society Mond Laboratory, Cambridge, at the time when he made his discoveries, working on an experimental project quite unconnected with tunnelling. It is a great pleasure to me as one of his contemporaries there to present to a wider audience the spare-time activity for which he was awarded a Nobel Prize.

2. The Josephson supercurrent as a simple quantum-fluid property

2.1. What are the Josephson effects?

When a superconductor passes below its transition temperature T_c, a second-order phase transition occurs and a new type of ordering appears. The metal behaves as though it contained two fluids, a normal fluid of electron-like excitations, and a superfluid or quantum fluid which has many strange properties. The quantum fluid is in some respects like a Bose condensate of electron pairs. It carries no entropy. Electrons

can enter the condensate, in pairs, and always at the same energy which, if the condensate is considered to be in equilibrium with a reservoir of electrons at chemical potential μ, must be just 2μ. The condensate is described by a complex order parameter $\Psi(\boldsymbol{r})$ which has many of the properties of a wavefunction for pairs. For instance, in the absence of magnetic fields the supercurrent carried by the condensate is given by

$$\boldsymbol{J}_S = -\frac{e\hbar}{2im}(\Psi^*\nabla\Psi - \Psi\nabla\Psi^*) \tag{2.1}$$

which can be re-written as†

$$\boldsymbol{J}_S = -2en_p\boldsymbol{v}_S = -\frac{en_p\hbar}{m}\nabla\theta \tag{2.2}$$

where n_p is the pair density $\Psi\Psi^*$ and θ is the phase of Ψ. The pair density rises steadily from zero at T_c to a finite value at low temperatures.

When two superconductors are well separated, they are quite independent and can be considered separately. When they have a substantial superconducting contact they form a single superconductor, to which the above results apply: they are said to be *strongly linked.* There are, however, intermediate cases in which electrons can flow from one superconductor to the other, but only so weakly that each superconductor can be regarded as essentially still in static equilibrium. This happens, for instance, where the superconductors are separated by a thin layer of oxide through which electrons can tunnel quantum-mechanically, or by a thin layer of normal metal or semiconductor, or by a very small bridge of superconducting material. In such situations one sometimes finds that a small supercurrent (i.e. DC current at zero voltage) can flow through the link and that the magnitude of this supercurrent is given, not by (2.2), but by the relation

$$I_S = I_1 \sin\phi \tag{2.3}$$

where ϕ is the phase difference, $\theta_1 - \theta_2$, between the superconducting wavefunctions on the two sides of the link‡. This is the Josephson supercurrent in its simplest form. When this relation (or some similar periodic dependence on ϕ) holds, the two superconductors are said to be *weakly linked.*

In his original letter Josephson (1962a) presented an economical but fundamental argument which demonstrated theoretically that (2.3) must hold for the special case of a tunnel junction. This argument went directly to the heart of the detailed microscopic theory of superconductivity and illuminated features of that basic theory which had previously been obscure or incompletely understood. This part of his achievement can only be understood in terms of the concepts of the microscopic theory itself, and we shall try to indicate what he did and why it was so significant in §4. Quite separate from this is the remarkable range of *consequences* of (2.3), mostly also predicted briefly in the original letter, and also known as 'Josephson effects'. These consequences all follow from the fact that, according to (2.3), the supercurrent through a weak link is *periodic* in the phase difference ϕ, in contrast to the supercurrent through a strong link which, according to (2.2), is *linear* in ϕ. This periodic dependence allows the Josephson effect to be used as an instrument which makes the quantum-fluid nature of the superelectrons conspicuous. It is these fascinating consequences of the Josephson

† We assume $e = |e|$ and is positive: note that $\nabla\theta$ is in the direction of the electron *momentum* and is in the *opposite* direction to the electric current.

‡ Note the sign of the definition: ϕ is *minus* the phase difference measured across the junction in the forward current direction. With this definition I_1 is positive.

effect which give it its practical importance, and to understand them we do not need the detailed theory which lies behind Josephson's prediction of (2.3). It will be enough if we can see in simple, general terms why a relationship of this form might be expected to arise. This is our aim in this section. Readers not interested in the microscopic implications of Josephson's work may like, after reading this section, to jump to §5, where we begin our consideration of the Josephson effects which arise as a consequence of (2.3).

2.2. The Josephson supercurrent as a pair transition

Perhaps the simplest picture of the Josephson supercurrent is to regard it as due to the quantum-mechanical transition in which a *pair* of electrons leaves the superfluid on the right and enters the superfluid on the left. In this picture we ignore the details of what goes on in the barrier region between the superconductors and regard the barrier simply as a mechanism which allows such transitions to occur. The nature of the Josephson effect can then be illuminated by considering the results of ordinary time-dependent perturbation theory, where one finds that the rate of change of occupation of the jth state is given by

$$\frac{\mathrm{d}}{\mathrm{d}t}|a_j|^2 = \sum_i -\frac{\mathrm{i}}{\hbar} a_j^* V_{ji} a_i + \mathrm{cc} \tag{2.4}$$

where V_{ji} is the matrix element of the perturbation. Ordinarily, we are interested in the case where a_j is small and the system is close to one of its original eigenstates; in this case, as is well known, the transition rate is proportional to the density of final states and to the *square* of the matrix element. This applies, for instance, to the tunnelling of ordinary electrons between normal metals at a finite voltage, where we may have occupied states on the right and empty states at the same energy on the left (figure 2(*a*)) and we wish to calculate the current. But if we start with a *mixed* state in which, say, $|a_j|^2 = |a_i|^2 = \frac{1}{2}$, and for simplicity take V_{ji} to be real, then (2.4) reduces to

$$\frac{\mathrm{d}}{\mathrm{d}t}|a_j|^2 = \frac{1}{\hbar} V_{ji} \sin\phi \tag{2.5}$$

where ϕ is the phase difference between a_j and a_i. In such a case the transition rate is proportional to the matrix element itself and to the sine of the phase difference between the states. It is this form of the theory which applies to the Josephson supercurrent and it does so because the starting state is a mixed state in which the effective pair wavefunction Ψ is finite on both sides of the barrier. From this point of view the form of the Josephson supercurrent is exactly what one should expect for a mixed state according to simple perturbation theory.

We shall examine a detailed calculation of the supercurrent as a pair transition in §4 where we shall see that, not surprisingly, the matrix element for transferring a *pair* across the barrier is proportional to the *square* of the matrix element for transferring a single electron. This fact originally led physicists to believe that pair tunnelling through insulators would be so small as to be unobservable, and indeed for this reason Josephson himself was looking for phase-dependent terms in the *normal* current when he made his calculation (see Josephson 1974). But we now see from our remarks above that this was incorrect because the supercurrent is *linear* in the pair matrix element, and thus of the same order in the electron transmission factor as the normal current. This is why the tunnelling supercurrent is observable.

2.3. The free energy of the weak link

The point of view of the previous subsection, in which we regard the weak link simply as a transmission mechanism, has the merit of simplicity and is close in spirit to the tunnel Hamiltonian method originally adopted by Josephson. But for weak links, such as layers of normal metal of the order of 10^{-7} m in thickness or superconducting bridges 10^{-6} m long, this attitude becomes rather artificial because the link is large enough for much interesting physics to be happening inside it, and indeed, in such weak links the order parameter Ψ has a well defined value varying from point to point inside the link. Can we say anything about how Josephson effects can arise in such a case?

We can do so by considering the *energy* in the link. We assume that the amplitude and phase of Ψ in the two superconductors is not disturbed by the small current in the link and that the phase difference ϕ can be externally controlled. Suppose now that ϕ is gradually increased by 2π. The boundary conditions on the link have now returned to their initial condition. If the link itself then returns to the same state, we can regard it as a true weak link, for the free energy must be a *periodic*† function of ϕ, and we can deduce the Josephson effect by the following argument. Since the energy of the pairs is 2μ, we assume that $\dot{\theta}$ is given by $\hbar\dot{\theta} = -2\mu$. We can thus change ϕ slowly by applying a very small voltage V to the link. If V is small enough, the normal current induced can be ignored in comparison with the supercurrent and the electrical work done can be taken to be equal to the increase in free energy. Thus

$$\begin{aligned} I_S V &= \dot{F} \\ &= F'(\phi)\dot{\phi} \\ &= F'(\phi) 2eV/\hbar \end{aligned} \tag{2.6}$$

where $V = (\mu_2 - \mu_1)/e$ is the forward voltage across the link. On cancelling the voltage from this equation, we find that *the supercurrent is a periodic function of* ϕ. This is a generalized form of the Josephson effect. In the simplest case where the free energy is an even sinusoidal function of ϕ, we have $F = -F_0 \cos\phi + \text{constant}$, and using (2.6) we obtain Josephson's relation once again, with $I_1 = 2eF_0/\hbar$.

One can use this result to discuss the effect of electrical noise on the observability of the Josephson effect. If the free energy F_0 becomes comparable with or smaller than kT, the thermal fluctuations in ϕ will become large and the Josephson currents will be smeared out. It follows that the effect will be unobservable if the critical current I_1 is much smaller than $2ekT/\hbar$. Unless the electrical leads to the junction are very carefully screened, the electrical noise will correspond to room temperature and the corresponding minimum observable critical current will be a few μA. For very well screened junctions, critical currents of the order of 10^{-7} A are visible. We shall see later that for tunnel junctions and microbridges the maximum value of I_1 is $\pi\Delta/2eR$, where Δ is the gap parameter, typically of the order of 10^{-22} J; in such junctions we see that R must be less than about 100 Ω. In practice, Josephson effects are normally observed in tunnel junctions having low resistances, in the range 1–10 Ω.

The argument given here for the Josephson effect depends on the assumption that on increasing ϕ by 2π, the link returns to the *same* state. Under what circumstances will this happen? For a long, thin superconducting wire, for instance, we would *not* expect this behaviour. There is a finite value of Ψ in the wire at all points and the effect

† If the link is symmetrical the function must be an even function of ϕ also.

of increasing ϕ by 2π is simply to set up a phase gradient along the wire. For a link to behave as a weak link the phase gradient along the link must be, as it were, cut and rejoined with a phase change of 2π and it is not difficult to see that this can only occur if at some stage the *magnitude* of Ψ falls to zero at the centre. From our present point of view, this is the criterion for the Josephson effect. If the link can effectively resist the tendency of Ψ to fall to zero at the centre when $\phi=\pi$, it will not show true weak link behaviour. If, on the other hand, Ψ can fall to zero when $\phi=\pi$, the link will return smoothly to its starting state when $\Psi=2\pi$ and the Josephson effect will occur. We shall examine this picture further in §9.2.

2.4. The order parameter and electric and magnetic fields

In discussing the Josephson effects we shall need to refer to a number of general properties of the superconducting order parameter Ψ introduced in §2.1, which we collect together here for convenience. Discussion of the microscopic meaning of Ψ is deferred to §3.2.

We first note that in the presence of a magnetic field described by a vector potential $\boldsymbol{A}$, a term $-2e^2\Psi\Psi^*\boldsymbol{A}/m$ must be added to the right-hand side of (2.1), so that (2.2) becomes

$$\Lambda \boldsymbol{J}_S = -\frac{\hbar}{2e}\nabla\theta - \boldsymbol{A} \tag{2.7}$$

where $\Lambda = m/(2n_p e^2)$. It follows that

$$\nabla \wedge (\Lambda \boldsymbol{J}_S) = -\boldsymbol{B}. \tag{2.8}$$

This is the second London equation, which shows that a constant supercurrent is associated with magnetic field rather than electric field and from which we can show that external magnetic fields only penetrate a distance $\lambda = (\Lambda/\mu_0)^{1/2}$ below the surface of a superconductor; λ is of the order of 10^{-7} m. If we take the time derivative of (2.7) we find that

$$\begin{aligned}\Lambda \dot{\boldsymbol{J}}_S &= -\frac{\hbar}{2e}\nabla\dot{\theta} - \dot{\boldsymbol{A}} \\ &= \frac{1}{e}\nabla\mu - \dot{\boldsymbol{A}}.\end{aligned} \tag{2.9}$$

This is the first London equation and shows that an electric field, or more strictly a gradient of electrochemical potential, produces an *acceleration* of the supercurrent. We have here used the fact that the rate of change of θ is given by

$$\hbar\dot{\theta} = -2\mu \tag{2.10}$$

as one would expect for a wavefunction for pairs of energy 2μ. This relation will be important in understanding the Josephson effect itself. Finally, if we consider a bulk superconductor threaded by a hole, then by considering a line integral round the hole on a path deep in the metal on which $\boldsymbol{J}_S$ is zero (for supercurrent is always concentrated into a small skin depth near the surface), we find that the magnetic flux in the hole is quantized, for

$$2e \oint \boldsymbol{A}.\mathrm{d}\boldsymbol{l} = 2\pi n\hbar$$

or

$$\Phi = n\Phi_0 \tag{2.11}$$

where Φ is the magnetic flux passing through the hole and Φ_0 is the flux quantum, $h/2e$, equal to $2{\cdot}07\times10^{-15}$ Wb. In some circumstances a superconductor may contain a line along which Ψ is zero and around which the phase increases by 2π. When this happens, supercurrents encircle the line and generate a magnetic field near and parallel to the line. The field and current only exist near the line and are screened from regions in the bulk distant from the line. Such a line is analogous to a vortex line in a non-viscous liquid and is known as a *flux line*. The above argument can be applied to a flux line as well as to a real hole and we see that the flux line is associated with one quantum of flux.

If we examine (2.7) we see that the phase of the order parameter, like the phase of a pair wavefunction, must be gauge covariant: if $\boldsymbol{A}$ is changed to $\boldsymbol{A}+\nabla\chi$, then θ must be changed to $\theta-2e\chi/\hbar$. In this connection we must note that in the presence of a magnetic field the ϕ which appears in Josephson's relation (2.3) must be defined as

$$\phi=\theta_1-\theta_2-\frac{2e}{\hbar}\int_1^2 \boldsymbol{A}.\mathrm{d}\boldsymbol{l} \tag{2.12}$$

where the integral is to be taken along the direct path perpendicular to the junction. This gauge-invariant phase difference is analogous to the 'gauge-invariant phase gradient' expressed by (2.7) which determines the supercurrent in bulk material.

3. The background to Josephson's calculation

We shall present Josephson's first calculation of the tunnelling supercurrent in §4. In this section we aim to outline enough of the microscopic theory of superconductivity both to explain his formalism and to make clear the nature of his discovery. Readers already familiar with the BCS theory should note the particular attention paid to questions of phase and particle number in what follows.

3.1. The BCS condensed state

As is well known, the theory first proposed by Bardeen *et al* (1957, referred to as BCS) has successfully explained the fundamental features of superconductivity. The theory starts from the idea that in some metals there is an effective *attraction* between electrons near the Fermi surface. This attraction is described by a term in the Hamiltonian†

$$H_{\mathrm{int}}=-\sum_{k',k} V a_{k'}^{\dagger}a_{-k'+q}^{\dagger}a_{-k+q}a_k \tag{3.1}$$

which shows that a pair of electrons in states $\boldsymbol{k}$, $-\boldsymbol{k}+\boldsymbol{q}$ can be scattered by their mutual attraction into states $\boldsymbol{k}'$, $-\boldsymbol{k}'+\boldsymbol{q}$ having the same total momentum. BCS showed that when such an attractive interaction is present the usual Fermi-sea ground state

$$\psi_{\mathrm{Fermi}}=\prod_{k<k_{\mathrm{F}}} a_k^{\dagger}\psi_{\mathrm{vac}} \tag{3.2}$$

is unstable and they suggested that there are low lying condensed states having the form‡

$$\psi_{\mathrm{BCS}}=\prod_{\mathrm{pairs}} (u_k+\mathrm{e}^{\mathrm{i}\theta}v_k a_k^{\dagger}a_{-k+q}^{\dagger})\psi_{\mathrm{vac}} \tag{3.3}$$

† The details of the BCS theory are set out in several textbooks (see, for instance, Rickayzen (1965)). We are assuming for simplicity that the matrix element V may be treated as constant; this is a good approximation for many superconductors.

‡ In the full theory the paired states have opposite spin. We omit spin indices for simplicity. Following Anderson (1958) we give careful emphasis to the often ignored phase factor $\mathrm{e}^{\mathrm{i}\theta}$.

where u_k, v_k are real, $u_k^2+v_k^2=1$ and the phase θ is arbitrary. We note that in this wavefunction electron states are occupied in pairs having a common momentum $\hbar\boldsymbol{q}$ (which is zero when the supercurrent is zero). The probability that a particular pair is

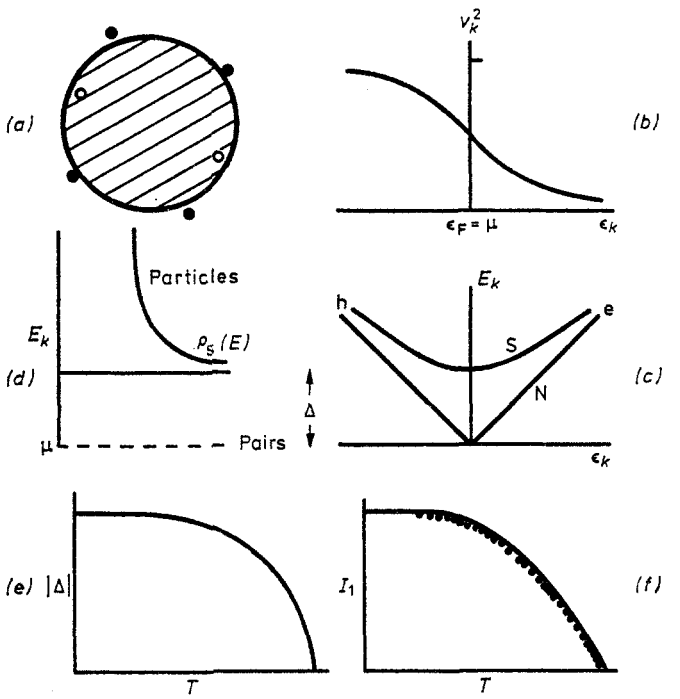

Figure 1. The BCS state with zero supercurrent. (*a*) Typical pairs occupied in the condensate. (*b*) Probability v_k^2 of pair occupation near the Fermi surface. (*c*) One-particle excitation energies on electron and hole branches near the Fermi surface. (*d*) Corresponding density of states. (*e*) Temperature dependence of $|\Delta|$. (*f*) Theoretical temperature dependence of Josephson current compared with results of Fiske (1964).

occupied is v_k^2, which falls smoothly from one below the Fermi surface to zero above it (figure 1(*b*)). Clearly, such a state has a greater kinetic energy than the Fermi sea, but the interaction energy is negative and given by

$$\begin{aligned} E_{\text{int}} &= -V \sum_{k,k'} u_k v_k u_{k'} v_{k'} \\ &= -\sum_{k'} u_{k'} v_{k'} \sum_{k} V u_k v_k \\ &= -\sum_{k'} u_{k'} v_{k'} |\Delta| \end{aligned} \tag{3.4}$$

where we have introduced the *order parameter* or *gap parameter*, $|\Delta|$. We notice that this negative interaction energy depends on the fact that the pair states are neither definitely occupied nor definitely empty; E_{int} would be zero if either u or v was always zero, as in the Fermi sea. BCS used the chemical potential μ as the origin of energy, which is equivalent to treating the superconductor as being in equilibrium with a reservoir of electrons of energy μ, electrons not in the superconductor being in the reservoir. They found that their state ψ_{BCS} could have a lower total energy than

ψ_{Fermi}, and by minimizing the energy with respect to u_k, v_k they showed that

$$\begin{aligned} v_k^2 &= \tfrac{1}{2}(1-\epsilon_k/E_k) \\ u_k^2 &= \tfrac{1}{2}(1+\epsilon_k/E_k) \end{aligned} \tag{3.5}$$

where

$$E_k = |(\epsilon_k^2 + |\Delta|^2)^{1/2}|$$

and ϵ_k is the one-electron energy in the normal state, measured from the Fermi energy, μ. (We shall see in the next section that E_k has an important significance as an excitation energy.) If we combine the definition of $|\Delta|$ in (3.4) with (3.5) we find the self-consistent relation

$$\begin{aligned} |\Delta| &= \sum_k V u_k v_k \\ &= \sum_k V|\Delta|/2E_k \end{aligned} \tag{3.6}$$

which can be solved to find $|\Delta|$. At finite temperatures one-particle excitations (which we shall discuss in the next section) may be present and they have the effect of preventing some of the paired states from contributing to the interaction energy. This reduces $|\Delta|$, which falls as the temperature rises and reaches zero at a critical temperature, T_c (figure 1(*e*)). At this point the BCS state is identical with the Fermi sea. We notice that the characteristic feature of ψ_{BCS} is the *mixture* between occupied and empty pair states near the Fermi surface. Equations (3.5) show that the degree of mixing increases as $|\Delta|$ increases; $|\Delta|$ is a measure of the degree of mixing.

We must emphasize here certain points which are particularly important when we turn later to understanding the Josephson effect. The BCS wavefunction (3.3) is unusual in the sense that it is *not* an eigenfunction of particle number. There is nothing formally incorrect in this. The Hamiltonian commutes with the number operator, and consequently simultaneous eigenfunctions of both must exist, but if the Hamiltonian has *degenerate* eigenfunctions then, although it must be possible to resolve them into eigenfunctions of the number operator, energy eigenstates which are not number eigenstates can also exist. Indeed, if we regard the BCS state as being in contact with a reservoir of energy μ, then for such a system a linear combination of states in which different numbers of electrons are in the reservoir is perfectly natural. We must note that the phase factor $e^{i\theta}$ which appears in ψ_{BCS} is entirely arbitrary, and thus the BCS state is indeed highly degenerate. This corresponds to the fact that it can be resolved into a large number of degenerate components, each containing a definite number of pairs, N, and having a phase factor $e^{iN\theta}$. At this point in the argument, the fact that the BCS state is not an eigenstate of particle number appears simply as a convenient artifice: we choose to work with BCS states which are not eigenstates of particle number because they are mathematically convenient, knowing that we can always reconstruct from them states of definite occupation if we need them.

When we come to consider tunnelling, it is confusing to imagine each superconductor in contact with a reservoir and we must ask how ψ_{BCS} is modified if we are dealing with an *isolated* superconductor. The answer can be seen by noting that the components of ψ_{BCS} corresponding to occupation of exactly N electrons remain good solutions, but since we must now exclude the reservoir energy from the Hamiltonian, instead of being degenerate, the states corresponding to different pair occupations differ in energy by 2μ. The effect on ψ_{BCS} is that the phase factor $e^{i\theta}$ becomes time-dependent and can be written as $\exp[i(\theta_0 - 2\mu t/\hbar)]$; otherwise nothing is changed.

3.2. The complex order parameter in BCS theory

In microscopic theory it has become usual to combine the concepts of the BCS gap parameter $|\Delta|$ and the complex order parameter Ψ into a single complex quantity defined as

$$\Delta(\boldsymbol{r}) = V(\boldsymbol{r})\langle\psi(\boldsymbol{r})\psi(\boldsymbol{r})\rangle \tag{3.7}$$

where V is the BCS interaction parameter and $\psi(\boldsymbol{r})$ is the usual Fermi operator. If we apply this definition to the BCS state (3.3), for instance, we find that

$$\begin{aligned}\Delta(\boldsymbol{r}) &= V\sum_{k,k'}\exp\left[\mathrm{i}(\boldsymbol{k}+\boldsymbol{k}')\cdot\boldsymbol{r}\right]\langle a_k a_{k'}\rangle \\ &= V\sum_{k} u_k v_k \exp\left[\mathrm{i}(\boldsymbol{q}\cdot\boldsymbol{r} - 2\mu t/\hbar + \theta_0)\right]\end{aligned} \tag{3.8}$$

and we see that the *magnitude* of Δ is just the gap parameter given by (3.6), while the *phase* of Δ varies in space and time as the phase of Ψ would be expected to vary, and at $\boldsymbol{r}=0$, is the same as the phase θ appearing in the BCS wavefunction (3.3).

In what sense can $\Delta(\boldsymbol{r})$ be regarded as an effective pair wavefunction? In the formalism of second quantization the operator pair $\psi(\boldsymbol{r}_1)\psi(\boldsymbol{r}_2)$ takes the place in a many-particle system of the wavefunction $\Psi(\boldsymbol{r}_1, \boldsymbol{r}_2)$ for a pair of particles. It follows that *if* such a pair of operators could be replaced by a macroscopic expectation value the system would behave like a system of independent pairs of fermions† each in the state $\Psi(\boldsymbol{r}_1, \boldsymbol{r}_2)$. The expectation value $\langle\psi(\boldsymbol{r})\psi(\boldsymbol{r})\rangle$ which appears in the definition of $\Delta(\boldsymbol{r})$ can be regarded as the centre-of-gravity part of $\Psi(\boldsymbol{r}_1, \boldsymbol{r}_2)$ if we identify $\boldsymbol{r}$ as $\frac{1}{2}(\boldsymbol{r}_1+\boldsymbol{r}_2)$. Thus $\Delta(\boldsymbol{r})$ would be identified with an effective wavefunction for pairs and the superconducting properties discussed in §2.4 would follow automatically. Unfortunately, the truth is more complicated. The existence of such a macroscopic expectation value is certainly connected with the appearance of superconductivity, and the appearance of the factors of 2 (for pairs) in the fundamental equations (2.7) and (2.10) determining the effects of electric and magnetic fields on the phase of Δ is also justified by its definition (3.7). But when we come to calculate the effective value of n_{p} in the expression for the supercurrent (2.2), we find that it is not related in any simple way to $\Delta(\boldsymbol{r})$. The reason is simply that there are other contributions to the supercurrent besides that calculated from the expectation value of $\langle\psi\psi\rangle$ (there is, for instance, a back-flow of excitations at finite temperatures). The amplitude of the *effective* wavefunction has therefore to be calculated microscopically. We shall see later that the same is true of the Josephson supercurrent: it depends in the expected way on the *phase* of Δ but its amplitude requires a special calculation.

We must here notice an important point. Because the operator pair $\psi\psi$ reduces the number of particles by two, $\Delta(\boldsymbol{r})$ as defined by (3.7) only has a definite meaning if we work with a state like (3.3) in which the number of pairs is indeterminate. This is no accident. The part of ψ_{BCS} containing exactly N pairs includes a factor $\mathrm{e}^{\mathrm{i}N\theta}$, so we see that $-\mathrm{i}\partial/\partial\theta$ is the operator for N. Consequently, $\hbar\theta$ and N are a canonical pair of quantities and there is an uncertainty principle of the form

$$\Delta\theta\Delta N \gtrsim 1. \tag{3.9}$$

Thus the phase of the order parameter is only well defined where N is uncertain, and vice versa. As Josephson (1962b) emphasized in his Fellowship dissertation, we have

† For bosons we could have considered the simpler equivalence of $\langle\psi(\boldsymbol{r})\rangle$ to an effective one-particle wavefunction $\Psi(\boldsymbol{r})$, but for fermions the exclusion principle prevents such an expectation value from reaching a macroscopic value.

here a case of *broken symmetry*, the appearance at a phase transition of an ordered state having lower symmetry than the Hamiltonian which produced it†. Just as in a ferromagnetic transition a magnetic moment appears which may point in any direction so, in the BCS wavefunction, a phase appears which can take any value. As, in the ferromagnet, the asymmetry may be removed by working with an ensemble of states having all possible directions of the magnetic moment so, in the superconductor, the phase may be blurred by working with states of fixed N, if we wish. In a superconductor the *absolute* phase is probably not of great importance, and this means that we can work with states having a fixed *total* number of particles and not miss any important phenomena. But the *phase difference* between points in space is another matter. It is these phase differences which are responsible for the superconducting properties and to understand them it is *essential* to use wavefunctions in which the particle density at a given place is indeterminate. Josephson was intrigued by the possibility of directly measuring the phase difference between two superconductors and it was this idea which led him to calculate the current across a weak link as a function of the phase difference. This meant using wavefunctions in which the division of pairs between the two sides was indeterminate. As we shall see, the use of this type of wavefunction proved crucial in the correct derivation of the currents.

3.3. Excitations of the superconducting state

As well as describing the ground state, the BCS theory also provides a framework for discussing the excited states of the system. It is found that there are operators, first written down by Bogoliubov, which create or destroy excitations analogous to electrons above the Fermi surface and holes below. These operators take the form (when $q=0$)

$$\begin{aligned} \alpha_k^{\dagger} &= u_k a_k^{\dagger} - \mathrm{e}^{-\mathrm{i}\theta} v_k a_{-k} \\ \alpha_{-k}^{\dagger} &= u_k a_{-k}^{\dagger} + \mathrm{e}^{-\mathrm{i}\theta} v_k a_k \end{aligned} \tag{3.10}$$

with conjugate annihilation operators. We notice that far above the Fermi surface, where u tends to 1 and v to 0, the operators are pure electron operators, while far below the Fermi surface they are pure hole operators. Near the Fermi surface they have mixed character and change smoothly from being electron-like to being hole-like. The excitation energy is the quantity $E_k = |(\epsilon_k^2 + |\Delta|^2)^{1/2}|$ which was mentioned in the last section. The variation of excitation energy with ϵ_k is shown in figure 1(c) for normal metals as well as superconductors. We notice that in the superconductor the minimum excitation energy is $|\Delta|$—there is an energy gap in the excitation spectrum. The peculiar nature of the excitation operators means that matrix elements for electron processes are modified when we consider the analogous processes in superconductors. Normally the matrix element is multiplied by a factor depending on u_k, v_k and known as a *coherence factor*. The coherence factors explain the abnormal microwave resistance, ultrasonic attenuation and spin relaxation times seen in superconductors, for instance.

As was emphasized by Anderson (1958) before the appearance of Josephson's theory, the Bogoliubov operators do not exhaust the possible ways in which electrons can be added to or removed from superconductors, for one can also add electrons in pairs to the condensate by making small increases in the v_k^2 values for a large number of pair states. Because the BCS energy is a minimum with respect to such small changes, such electrons must always enter at the reservoir energy μ. The density of states of

† Anderson (1964) also emphasized the significance of this idea.

excitations in a superconductor is therefore as shown in figure 1(*d*). Excitations can be added onto either the electron-like or the hole-like branch at energies above $|\Delta|$; since the states are uniformly distributed in ϵ_k and $E_k^2 = \epsilon_k^2 + |\Delta|^2$ there is a sharp peak in the density of quasiparticle states just above the gap. Pairs of electrons can also be added without limit to the condensate at the Fermi energy. In considering this latter process, it is convenient to define a *pair operator* S^+, in the following way. We imagine the BCS state resolved into normalized components of definite occupation as follows:

$$\psi_{\mathrm{BCS}} = \ldots a_{N-2}\psi_{N-2} \exp\left[\mathrm{i}(\tfrac{1}{2}N-1)\theta\right] + a_N\psi_N \exp\left(\tfrac{1}{2}\mathrm{i}N\theta\right) + a_{N+2}\psi_{N+2} \exp\left[\mathrm{i}(\tfrac{1}{2}N+1)\theta\right] \ldots. \quad (3.11)$$

We then define the pair operator and its inverse as having the properties

$$\begin{aligned} S^+\psi_N &= \psi_{N+2} \\ S\psi_N &= \psi_{N-2} \end{aligned} \quad (3.12)$$

for all N. Clearly S and S^+ commute and $S^+S = 1$. In the BCS state the coefficients a_N are very slow functions of N, though a_N will peak at a value of N corresponding to the Fermi level. Consequently, to a close approximation we can write $S^+\psi_{\mathrm{BCS}} = \mathrm{e}^{-\mathrm{i}\theta}\psi_{\mathrm{BCS}}$ and $S\psi_{\mathrm{BCS}} = \mathrm{e}^{\mathrm{i}\theta}\psi_{\mathrm{BCS}}$. These pair operators were used by Josephson in his tunnelling formalism.

3.4. Single-particle tunnelling†

The idea that particles can tunnel through potential barriers in the form of an evanescent wave is as old as quantum mechanics and was applied to metal–insulator–metal junctions by Sommerfeld and Bethe as early as 1933. The invention of the Esaki diode in 1957 aroused active interest in practical investigations of tunnelling in solid-state physics, and in 1960 Giaever published the first results on tunnelling involving superconductors. The idea is that an insulating barrier between two metals (usually oxide grown *in situ*) behaves like a potential barrier whose height is of the order of the band gap in the insulator, about 1 eV. If the kinetic energy of electrons at the Fermi surface in the metal is of the same order of magnitude, then one can show, using elementary quantum mechanics, that the transmission coefficient for electrons is of the order of $\exp(-2\lambda a)$, where λ is the decay constant of the evanescent wave and a is the thickness of the oxide. As a rule of thumb for most junctions one can say that the transmission coefficient is about $\exp(-x/\text{Å})$. Typical tunnel junctions are between 10 Å and 20 Å thick and have resistances between 1 Ω and 10^4 Ω.

The calculation of the tunnel current is very simple in principle. When a voltage is applied to a junction, the distribution of occupied states is as shown in figure 2(*a*). Clearly there will be a conventional current from left to right given by the usual golden rule

$$\begin{aligned} I &= (2\pi\rho_{\mathrm{R}}\rho_{\mathrm{L}}eT^2/\hbar) \int_{-\infty}^{\infty} [f_{\mathrm{R}}(\epsilon - eV) - f_{\mathrm{L}}(\epsilon)]\, \mathrm{d}\epsilon \\ &= (2\pi\rho_{\mathrm{R}}\rho_{\mathrm{L}}T^2/\hbar)e^2V \end{aligned} \quad (3.13)$$

where ρ_{R}, ρ_{L} are the electron densities of states on the two sides (assumed constant near the Fermi level) and f_{R}, f_{L} are the corresponding Fermi factors. T^2 is an effective matrix element for transmission from one side to the other, which can be calculated

† Single-particle tunnelling both in normal metals and in superconductors has been reviewed extensively elsewhere (see Solymar 1972). Here we limit ourselves to essentials.

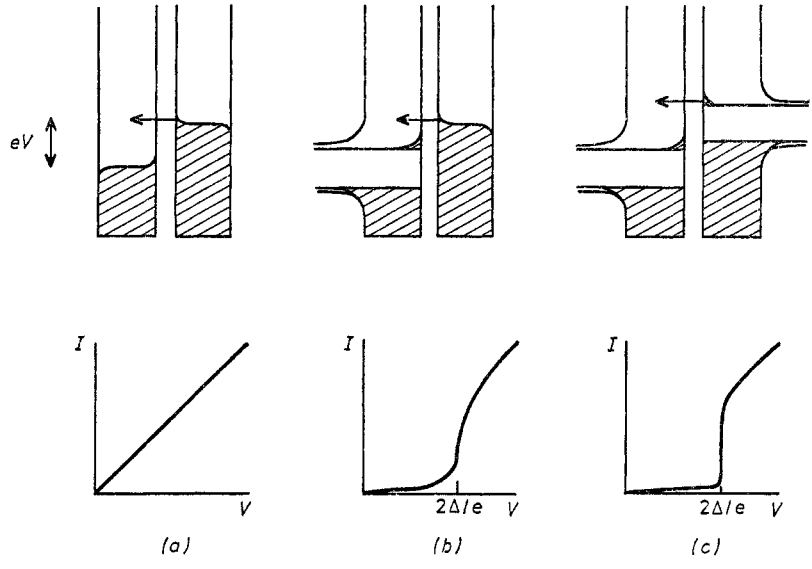

Figure 2. Single-particle tunnelling, showing densities of states in the semiconductor model when a voltage V is applied and the corresponding I–V characteristics for (*a*) NIN, (*b*) SIN and (*c*) SIS junctions.

from the simple theory, and is also assumed to be independent of energy. It is clear that the junction behaves like a simple resistance which is independent of temperature.

This theory has been extended in various ways, of which we might note two. The question of the variation of the tunnelling matrix element with energy was investigated by Harrison (1961) who showed that, at least if the barrier potential rises sufficiently slowly at the edge of the metal, the variation of T^2 with energy exactly cancels the variation of the density of states. Thus placing the factor $\rho_R\rho_L T^2$ as a constant outside the integral in (3.13) is justified over a wide energy range. It follows that in normal metals tunnelling gives no information about the density-of-states function, though it can be used to find band edges, etc. We should also note that tunnelling really involves three-dimensional wavefunctions in the band gap of the insulator. It is found that, typically, only electrons moving within about 5° of a preferred direction have an appreciable chance of tunnelling and that the preferred electrons are probably those whose wavevector is normal to the interface (Dowman *et al* 1969). This selection by direction has been used to investigate anisotropy of the gap structure in superconductors.

When Giaever (1960) and others started to make tunnelling experiments on superconductors a surprising and beautiful fact emerged. The tunnel current appeared to be given by

$$I=\frac{2\pi T^2 e}{\hbar}\int_{-\infty}^{\infty}[f_R(E-eV)-f_L(E)]\rho_R(E-eV)\rho_L(E)\,dE. \qquad (3.14)$$

In other words, the current behaved as if a 'semiconductor version' $\rho(E)$ of the BCS density of states (which is a rapid function of energy and shows an energy gap) replaced the normal density of states and everything else was unchanged (figure 2). The types of I–V curve which were found for SIN and SIS tunnelling are also shown in the figure. The results could be used at once to identify and measure the energy gaps in superconductors as a function of temperature (and later as a function of orientation, magnetic

field, magnetic impurity, proximity effects and many other parameters). Even more importantly, once the validity of (3.14) was established, it was easy to show by differentiating it that for tunnelling from a normal metal on the right into a superconductor on the left

$$\frac{\mathrm{d}I}{\mathrm{d}V}=\frac{2\pi T^2}{\hbar}\,e^2\rho_{\mathrm{N}}\int_{-\infty}^{\infty}-f'(E-eV)\rho_{\mathrm{S}}(E)\,\mathrm{d}E. \tag{3.15}$$

At low temperatures $-f'(E)$ becomes essentially a δ function and consequently a simple measurement of the differential resistance of a tunnel junction as a function of bias allows the superconducting density of states to be plotted as a function of energy. At the time, this was used to check the validity of the BCS expression for $\rho_{\mathrm{S}}(E)$. Later, it became even more important when it was realized that certain small departures from the BCS form for $\rho_{\mathrm{S}}(E)$ near the Debye energy were a direct measure of the quantity $\alpha^2(\omega)F(\omega)$, which is the electron–phonon coupling constant multiplied by the phonon density of states. The observed structure in $\rho_{\mathrm{S}}(E)$ agreed with the known structure in $F(\omega)$ and the values of α^2F were used to check the theory of strongly coupled superconductors itself (see McMillan and Rowell 1969).

The simple result (3.14) was, however, mystifying for several reasons. It looked as though the BCS excitations were forgetting about their mixed electron–hole character and were carrying exactly one electron across the barrier in real processes whose matrix elements contained no coherence factors. It was obvious that the explanation of this unexpected simplicity was not trivial and must lie in a proper treatment of tunnelling for BCS excitations. The hunt for such a treatment was now on. We shall see in §4 how this problem was solved and how the idea of Josephson tunnelling itself first grew out of the solution which appeared.

4. Josephson's first calculation for tunnel junctions

I have thought it best to describe in some detail Josephson's (1962a) first calculation rather than one of the more general later formulations, partly for historical reasons, but mainly because it is more easily followed by the reader unfamiliar with Green's functions, and because it brings out particularly clearly the nature of Josephson's innovation. It must be remembered, however, that it is limited to tunnel junctions and also to weak superconductors in which the excitations are well defined. More general calculations have been given by Ambegaokar and Baratoff (1963a, b), by Josephson (1965, see §9.1) and by Werthamer (1966, see §8.1).

4.1. The method of Cohen, Falicov and Phillips (1962)

We have noted that the experimental facts on single-particle tunnelling in superconductors were surprising to theoreticians and a number of attempts to explain them were made. The first successful calculation was made by Cohen *et al* (1962) and it was by an extension of their formalism that Josephson was led to his predictions. We shall therefore look closely at their method.

They considered a system of two metals separated by a tunnel barrier and took the Hamiltonian to be $H_{\mathrm{L}}+H_{\mathrm{R}}+V$, where H_{L} and H_{R} are the ordinary Hamiltonians for the metals to left and right of the barrier and V is given by

$$V=\sum_{\mathrm{R,L}}\left[T_{\mathrm{R,L}}a_{\mathrm{R}}{}^{\dagger}a_{\mathrm{L}}+T_{\mathrm{L,R}}a_{\mathrm{L}}{}^{\dagger}a_{\mathrm{R}}\right] \tag{4.1}$$

where the sum is over all electron states in both metals. This extra term they called the tunnel Hamiltonian. Neither Cohen *et al* nor Josephson discussed its significance, but we note briefly here that it has the desired property of transferring electrons between the two sides and is the appropriate term to describe a barrier of negligible width which couples together the boundary conditions for the one-electron states on the two sides. It has been discussed in more detail by Prange (1963) and should be valid for tunnel junctions when V is small. How far it can properly be applied to other weak links is uncertain.

Cohen *et al* calculated the conventional current from left to right in terms of the rate of increase of electron number on the left by using the following operator relations:

$$\begin{aligned} I = e\dot{N}_{\mathrm{L}} &= \frac{e}{\mathrm{i}\hbar}[N_{\mathrm{L}}, H] \\ &= \frac{e}{\mathrm{i}\hbar}[N_{\mathrm{L}}, V] \\ &= \frac{e}{\mathrm{i}\hbar}\sum_{\mathrm{L,R}} (T_{\mathrm{L,R}} a_{\mathrm{L}}^{\dagger} a_{\mathrm{R}} - T_{\mathrm{R,L}} a_{\mathrm{R}}^{\dagger} a_{\mathrm{L}}) \end{aligned} \tag{4.2}$$

where we have used the fact that N_{L} commutes with H_{L} and H_{R}. If we treat V as a perturbation, then naturally the current in the unperturbed state is zero. They therefore calculated the perturbation introduced by V to first order and then used (4.2) to calculate the current in the perturbed state. In calculating the perturbation we have to remember that even in the absence of V a superconducting junction having an applied voltage is not in a stationary state (the phase difference between the two sides is changing) and consequently we must use time-dependent theory in calculating the perturbation. We do so by using Schrödinger's equation to write $\mathrm{d}\psi$ as $(-\mathrm{i}H/\hbar)\psi(t)\,\mathrm{d}t$ and we find that the first-order perturbation at time t can be written formally as

$$\delta\psi = \int_{-\infty}^{t} \exp\left[-\mathrm{i}H_0(t-t')/\hbar\right] \frac{V}{\mathrm{i}\hbar} \exp\left(-\mathrm{i}H_0 t'/\hbar\right)\psi_0(0)\,\mathrm{d}t' \tag{4.3}$$

where $H_0 = H_{\mathrm{L}} + H_{\mathrm{R}}$ and ψ_0 is the unperturbed state. The current at time t is then given to first order as

$$\begin{aligned} I(t) &= \langle\psi_0(t)|I\delta\psi\rangle + \mathrm{cc} \\ &= \int_{-\infty}^{t} \left\langle \psi_0(t)|I \exp\left[-\mathrm{i}H_0(t-t')/\hbar\right] \frac{V}{\mathrm{i}\hbar} \exp\left[-\mathrm{i}H_0(t'-t)/\hbar\right]\psi_0(t)\right\rangle \mathrm{d}t' + \mathrm{cc}. \end{aligned} \tag{4.4}$$

When we are dealing with normal metals we note that both V and I consist entirely of terms which *change* the energy by a definite amount, δE, and that for such terms the effect of the exponentials in H_0 is simply to introduce a factor $\exp[\mathrm{i}\delta E(t'-t)/\hbar]$ for any ψ_0. If, for instance, we pick out the term in $a_{\mathrm{L}}^{\dagger}a_{\mathrm{R}}$ in V and the term in $a_{\mathrm{R}}^{\dagger}a_{\mathrm{L}}$ in I and insert them into (4.4) we find after making the thermal average over quasiparticle occupation numbers a contribution to $I(t)$ equal to

$$\frac{T^2 e}{\hbar^2} f_{\mathrm{R}}(1-f_{\mathrm{L}}) \int_{-\infty}^{t} \exp\left[\mathrm{i}(\epsilon_{\mathrm{L}} - \epsilon_{\mathrm{R}} - eV - \mathrm{i}\delta)(t'-t)/\hbar\right] \mathrm{d}t' + \mathrm{cc} \tag{4.5}$$

where the infinitesimal δ is included to indicate that the perturbation was switched on

gradually in the past. On performing the integral and summing over similar contributions we find that

$$I = -\frac{eT^2}{i\hbar}\sum_{L,R}\frac{f_R - f_L}{\epsilon_R - \epsilon_L + eV + i\delta} + \text{cc.} \tag{4.6}$$

If we now replace the sum over R by an integral over the density of states, the principal parts cancel and we are left with

$$I = \frac{2\pi e T^2}{\hbar}\rho_L\rho_R\int_{-\infty}^{\infty}[f(\epsilon - eV) - f(\epsilon)]\,d\epsilon \tag{4.7}$$

from the residues. The fact that only the residues contribute shows that the current is due solely to real transitions and indeed (4.7) can be interpreted simply as the sum of the transition rates for electrons crossing the barrier calculated according to Fermi's golden rule where V is the perturbation (we have treated T^2 as constant and independent of spin for simplicity: these simplifying assumptions introduce no important errors). This is the simple result for normal metals which we discussed in §3.4.

4.2. The currents between superconductors

In calculating the tunnel current by the same method when superconductors are involved we must first express V and I in terms of excitation operators which add a definite energy to the superconductor. At this point Josephson noted that the Bogoliubov operators (3.10) do not add exactly one electron to the system and this means that they only add a definite energy if all energies are measured from the Fermi level. In the tunnelling situation we cannot do this on both sides of the barrier simultaneously when the voltage is finite and consequently the Bogoliubov operators cannot be used as excitation operators. To meet this difficulty Josephson proposed the use of a modified operator. A typical Josephson operator has the form

$$\alpha_k^\dagger = u_k a_k^\dagger - v_k a_{-k} S^+ \tag{4.8}$$

in place of (3.10), where S^+ is the normalized pair operator which we defined by (3.12). The new operator adds exactly one electron† and it remains a valid excitation operator of energy $E_k + \mu$, whatever origin is used for the energy. In terms of these new operators, terms such as $a_L^\dagger a_R$ which appear in V and I can be expanded as

$$\begin{aligned} a_L^\dagger a_R &= (u_1\alpha_1^\dagger + v_1\alpha_{-1}S_1^+)(u_r\alpha_r + v_r\alpha_{-r}^\dagger S_r) \\ &= u_1u_r\alpha_1^\dagger\alpha_r + v_1v_r\alpha_{-1}\alpha_{-r}^\dagger S_1^+ S_r + u_1v_r\alpha_1^\dagger\alpha_{-r}^\dagger S_r + v_1u_r\alpha_{-1}\alpha_r S_1^+ \end{aligned} \tag{4.9}$$

where an operator with a negative suffix such as α_{-1} refers to a time-reversed state. Clearly we now have a wider range of intermediate states to consider in calculating the current using (4.4), but the calculation is essentially similar to what we did for normal metals. This time the intermediate states in (4.4) may involve pair creation and annihilation as well as transfer of excitations, as shown in figure 3.

When we consider the various terms in (4.4) it is at first sight natural to assume‡ that the term in $\alpha_1^\dagger\alpha_r$ in V can only be paired with the term in $\alpha_r^\dagger\alpha_1$ in I. With the analogous assumption for each of the four types of operator appearing in (4.4), we find

† Josephson also used operators which remove exactly one electron, but we shall not need to refer to them.

‡ This crucial assumption excludes the Josephson effect, as we shall see.

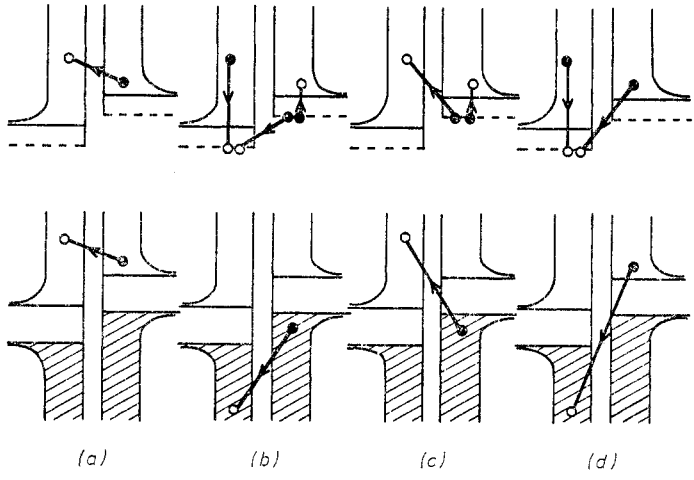

Figure 3. Processes in superconductive tunnelling in which one electron passes from right to left corresponding to the four terms of (4.9). Above: Josephson's description; below: formal semiconductor description. The Fermi factors and energy denominators for the four terms appear in (4.10).

that I should be given by

$$I=I_0=-\frac{eT^2}{i\hbar}\sum_{l,r}\left(\frac{u_l^2u_r^2(f_r-f_l)}{E_r-E_l+eV+i\delta}+\frac{v_l^2v_r^2(f_l-f_r)}{-E_r+E_l+eV+i\delta}\right.$$
$$\left.+\frac{u_l^2v_r^2(1-f_r-f_l)}{-E_r-E_l+eV+i\delta}+\frac{v_l^2u_r^2(f_r+f_l-1)}{E_r+E_l+eV+i\delta}\right)+\text{cc}. \quad (4.10)$$

This result can be simplified in two respects. The sum has to be taken over hole and electron branches on both the left and right of the junction, and remembering that u and v are interchanged for the hole-like branch (and that $u^2+v^2=1$), we see that on summing over the two branches the coherence factors all disappear. The four terms correspond to the four processes shown diagrammatically in figure 3. Examination of the energy denominators and Fermi factors shows that the four processes have simple interpretations in the 'semiconductor representation' also shown in the figure, in which we return to the notion of filled states below the Fermi level for negative values of E. Thus equation (4.10) may be reduced to

$$I_0=-\frac{eT^2}{i\hbar}\sum_{L,R}\frac{f_R-f_L}{E_R-E_L+eV+i\delta}+\text{cc} \quad (4.11)$$

as in the normal metal, provided the sum is now taken over 'semiconductor' states including negative values of E_L, E_R and identified by capital suffixes. As in the normal metal the principal parts cancel and we are left with the simple integral

$$I_0=\frac{2\pi eT^2}{\hbar}\int_{-\infty}^{\infty}[f(E-eV)-f(E)]\rho_R(E-eV)\rho_L(E)\,dE \quad (4.12)$$

the result corresponding to real tunnelling processes which Giaever's experiments had already suggested. Cohen *et al* (1962) realized that there were difficulties about the assumption mentioned above, and in fact limited their calculation to the case in which

only one metal was superconducting. They obtained a result equivalent to (4.12), which is correct in that situation. This actually left open the question of what happens when two superconductors are involved, but it was widely assumed by physicists at the time that the calculation had, apparently very satisfactorily, explained quite generally why the coherence and charge factors cancel out in tunnelling between superconductors. What really happens when two superconductors are involved we must now discuss. We must recognize at this point that the tunnel Hamiltonian method developed by Cohen *et al* (1962) provided Josephson with the formal framework to describe tunnelling supercurrents for which he was already searching, and therefore played a major role in the new developments.

Josephson's crucial contribution to the calculation was to point out that the assumption made above is only valid if the states involved are eigenfunctions of the electron number. This in turn implies that the phase difference across the junction must be indeterminate, on account of the uncertainty principle mentioned in §3.2. But as we saw in the same section he was searching for effects which would arise when the phase difference was well defined, in which case the pair occupation on each side would be indeterminate. For this purpose it was essential to use states of mixed occupation of the BCS type. For such a wavefunction it follows from the discussion following (3.12) that a term in I such as $(-T_{-1,-\mathrm{r}}v_{-1}v_{-\mathrm{r}}S_1^{+}S_{\mathrm{r}})\alpha_{\mathrm{r}}^{\dagger}\alpha_1$ can be replaced by $(-T_{-1,-\mathrm{r}}v_1v_{\mathrm{r}}\,\mathrm{e}^{-\mathrm{i}\phi})\alpha_{\mathrm{r}}^{\dagger}\alpha_1$ where ϕ is the superfluid phase difference between the two sides. Such a term in I could now be paired with the term $(T_{1,\mathrm{r}}u_1u_{\mathrm{r}})\alpha_1^{\dagger}\alpha_{\mathrm{r}}$ in V and on adding the four new types of cross term we find an extra contribution to the current given by

$$I_{\mathrm{J}}=-\frac{eT^2}{\mathrm{i}\hbar}\sum_{\mathrm{L,R}}\frac{4u_{\mathrm{L}}v_{\mathrm{L}}u_{\mathrm{R}}v_{\mathrm{R}}(f_{\mathrm{R}}-f_{\mathrm{L}})\,\mathrm{e}^{-\mathrm{i}\phi}}{E_{\mathrm{R}}-E_{\mathrm{L}}+eV+\mathrm{i}\delta}+\mathrm{cc} \tag{4.13}$$

where, as in the previous section, the sum over hole and electron branches has been performed and four terms have been combined into one by using the semiconductor representation in which negative values of E_{R}, E_{L} are to be included in the sum and the product uv is regarded as negative when E is negative. We have also assumed time-reversal symmetry by writing $T_{-1,-\mathrm{r}}=T_{\mathrm{r},1}{}^{*}$. In this case the presence of the phase factor $\mathrm{e}^{-\mathrm{i}\phi}$ means that the principal parts do not, in general, cancel and we are left with an extra current

$$I_{\mathrm{J}}=I_1(V)\sin\phi+\sigma_1(V)\cos\phi\,V \tag{4.14}$$

with

$$I_1(V)=\frac{2eT^2}{\hbar}\rho_1\rho_{\mathrm{r}}P\int_{-\infty}^{\infty}\mathrm{d}\epsilon_1\int_{-\infty}^{\infty}\mathrm{d}\epsilon_2\,\frac{\Delta_1\Delta_2}{E_1E_2}\,\frac{[f(E_1)-f(E_2)]}{E_1-E_2+eV} \tag{4.15}$$

coming from the principal parts and

$$\sigma_1(V)V=\frac{2\pi eT^2}{\hbar}\rho_1\rho_{\mathrm{r}}\int_{-\infty}^{\infty}\mathrm{d}\epsilon\,\frac{\Delta_1\Delta_2}{(E-eV)E}[f(E-eV)-f(E)] \tag{4.16}$$

from the residues. The first term is what is usually regarded as the *Josephson supercurrent*. I_1 is finite at zero voltage, and when $\Delta_1=\Delta_2$ is given by (figure 1(*f*))

$$I_1(0)=\frac{\pi\Delta(T)}{2eR_N}\tanh\frac{\Delta(T)}{2kT}. \tag{4.17}$$

We see that at $T=0$ the critical current is just the current which would flow in the *normal* junction at an applied voltage of $\frac{1}{2}\pi\Delta/e$. The calculation of $I_1(T)$ in the general

case was given by Ambegaokar and Baratoff (1963a, b). It is clear from inspection of (4.15) that $I_1(V)$ increases with increasing V, peaks where $eV=2\Delta$ and then falls steadily: the details of this effect will be discussed in §8.3. The second term, in $\cos\phi$, is zero at zero voltage and can be regarded as an extra phase-dependent contribution to the *ordinary* quasiparticle conduction of the junction. We shall examine this term in more detail in §8.2.

Let us consider the zero-voltage supercurrent as a quantum process. It is a *second-*order process in the tunnel Hamiltonian which transfers a condensate pair across the junction. A typical intermediate state is shown in figure 4(*a*) and we see how pairs

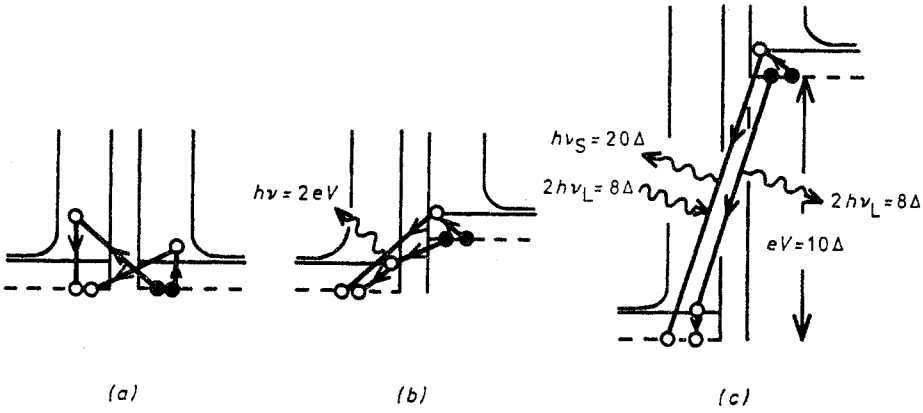

Figure 4. DC Josephson currents as a second-order quantum process. (*a*) Typical transition involved in DC supercurrent at low temperatures. (*b*) Stimulated emission in the presence of microwave excitation, corresponding to the first DC supercurrent step of figure 11; the case drawn has $h\nu=4\Delta$, corresponding to the Riedel peak. (*c*) Example of very-high-frequency fifth harmonic mixing taking advantage of the Riedel peak and involving high-order stimulated emission in the presence of a strong LO signal; ν_S is the signal frequency, ν_L the LO frequency and the IF is treated as DC output (see §11.2).

cross the barrier in two steps of the type appearing in (4.9). What is peculiar is that, although this is a second-order process, the current is still proportional to T^2 and not T^4 (in which case it would not have been observable in most junctions). The reason for this was discussed in general terms in §2.2 and we can usefully remind ourselves here that the Josephson current can be regarded as the pair current due to second-order tunnelling *between states which are mixed in the sense that a given pair in the condensate is equally likely to be on either side of the junction.* From this point of view again we see that the uncertainty in location of the pairs is crucial to the appearance of the Josephson current.

We have still not made completely clear why Josephson was right in believing that in practice the condensate will have well defined phase and indeterminate number density, rather than the other way round. The answer is to be found in the boundary conditions. If one had a *perfect* voltage source, then there is no reason why the phase across a junction should be well defined. In practice, however, all ordinary sources have some internal impedance. If we connect such a source to a superconducting junction it behaves as a pure current source and the phase difference across the junction is forced to adjust itself so that the junction delivers the correct current. Thus

if we start with a wavefunction where n is definite and ϕ indeterminate, the components of different ϕ will change in such a way that the phase differences become identical. In this process the currents flowing across the junction for the different components will be different and the number distribution will become indeterminate. Thus in practice the boundary conditions ensure that ϕ is well defined, as Josephson assumed. Exactly the same process ensures that phase differences from point to point in a bulk superconductor are also well defined.

5. The basic Josephson effects

In his original letter Josephson (1962a) predicted in outline a surprisingly large number of physical consequences of his theory. Discussion of these consequences will take up much of the rest of this review. In this section we shall discuss briefly what the original predictions were and examine some of the early experiments which first confirmed his ideas.

5.1. Josephson's predictions

It will be useful to begin by summarizing the basic equations governing a weak link. It is worth emphasizing again that they all depend on the quantum character of the superfluid and thus on the existence of the order parameter Ψ (or Δ) which is gauge-covariant in the same way as a wavefunction for particles of charge $-2e$. The equations are

$$\phi = \theta_1 - \theta_2 - \frac{2e}{\hbar}\int_1^2 \boldsymbol{A}.\mathrm{d}\boldsymbol{l} \tag{5.1}$$

which defines the gauge-invariant phase difference across the junction. In the presence of a magnetic field, the integral is to be taken along the direct path perpendicular to the junction. Closely related to this is the time-dependent equation

$$\hbar\dot{\phi} = 2(\mu_2 - \mu_1 - e\int_1^2 \dot{\boldsymbol{A}}.\mathrm{d}\boldsymbol{l})$$

or

$$\hbar\dot{\phi} = 2eV \tag{5.2}$$

where V is the forward voltage across the junction. In the presence of a changing magnetic field V is to be measured along the direct perpendicular path. This result depends on (2.10), a microscopic proof of which has been given by Gor'kov (see Abrikosov *et al* 1963). The precise validity of this relation has been examined in connection with the measurement of e/h (§11.1). It is generally agreed that it is exact and that V is the voltage across the junction measured by an ordinary voltmeter. Finally we have the Josephson relation itself, which we shall write in simplified form as

$$I = I_S + I_N$$

or

$$I = I_1 \sin\phi + V/R. \tag{5.3}$$

This equation is not exact. We have already seen that for weak links in general we merely expect the supercurrent to be periodic in ϕ and not necessarily sinusoidal; and indeed, if Josephson's calculation for tunnel junctions is carried to higher order, more general periodic terms do appear. Moreover, as we have already seen for tunnel

junctions, I_1 and R are in general both voltage-dependent and R is also phase-dependent. The somewhat crude model represented by (5.3) in which we treat I_1 and R as constants does however show most of the important effects. It is known as the *resistively shunted junction or RSJ model* and we shall from now on use it frequently, for simplicity.

A surprisingly large number of physical effects follow from these three equations, almost all of them noted briefly but explicitly in Josephson's original letter (1962a) and all developed in his Fellowship dissertation and his Doctoral dissertation, which were not published at the time. Some of these will be described briefly now.

5.1.1. The DC Josephson effect. When the voltage across the junction is strictly zero then ϕ is constant according to (5.2). Thus according to (5.3) the junction can carry a DC supercurrent depending on the value of ϕ, but lying in the range $-I_1 > I_S > I_1$. The DC I–V characteristic therefore has a 'supercurrent spike' at zero voltage.

5.1.2. The AC Josephson effect. At a finite voltage we can integrate (5.2) and find that $\phi = (2eV_0/\hbar)t = \omega_V t$. Then (5.3) shows that there is no DC supercurrent but an AC supercurrent of amplitude I_1 flows in addition to the normal DC current. The frequency of oscillation is known as the Josephson frequency and takes the value of $4{\cdot}836 \times 10^{14}$ Hz per volt DC applied.

5.1.3. The inverse AC Josephson effect. If an AC voltage of the form $V_S \cos(\omega_S t)$ is superimposed on the DC voltage V_0, integration of (5.2) shows that ϕ varies as $\omega_V t + (2eV_S/\hbar\omega_S) \sin(\omega_S t) + \phi_0$. On inserting this variation into (5.3) we find that the supercurrent is phase-modulated, having components at the frequencies $\omega_V \pm n\omega_S$. In detail we find that

$$I_S = \sum_n I_1 J_n(2eV_S/\hbar\omega_S) \sin(\omega_V t \pm n\omega_S t + \phi_0) \tag{5.4}$$

where the J_n are ordinary Bessel functions. Thus the junction mixes multiples of the applied frequency with the natural Josephson frequency. In particular, when $\omega_V = n\omega_S$ (that is, when $V = n(\hbar\omega_S/2e)$) there is now a DC supercurrent in addition to the normal current (see figure 4(*b*)). Like the supercurrent at zero voltage this DC supercurrent can have a range of values, depending on the phase ϕ_0. Thus the I–V characteristic should now have 'spikes' of zero slope-resistance at all of these voltages. The size of the spikes is given by the corresponding Bessel functions and oscillates with the magnitude of the AC excitation; the original zero-order spike also oscillates. At very large microwave powers the Bessel functions all tend to zero and all the supercurrent behaviour is suppressed.

5.1.4. The quantum-interference effect. If two junctions are connected in parallel by superconducting leads then, as we shall show in detail in §6, it follows from (5.1) that

$$\phi_B = \phi_A + \phi_M \tag{5.5}$$

where ϕ_A and ϕ_B are the phase differences at the two junctions and ϕ_M is a magnetic phase difference equal to $2\pi\Phi/\Phi_0$, Φ being the magnetic flux threading the loop which connects the two junctions and Φ_0 the flux quantum $h/2e$. The total supercurrent passing through the joint system is equal to

$$I_S = I_{1A} \sin\phi_A + I_{1B} \sin(\phi_A + \phi_M). \tag{5.6}$$

This formula is analogous to the expression for the wave amplitude produced by the two slits in a Young's interference experiment, with ϕ_M playing the role of the path phase difference. It follows that the *critical current of the combination varies in the same way with magnetic flux as does the amplitude of the Young's slit diffraction pattern with position.* The idea can be extended to explain the effect of magnetic fields on single junctions. The effect is perhaps the most beautiful and direct demonstration of the wave nature of electrons yet devised. It is also the basis of several of the most useful devices which employ the Josephson effect (see §10).

5.1.5. The self-field effect. When we have a large junction the currents flowing in it may themselves generate fields which induce serious quantum interference. As we shall see in §6.5 this ensures that in a large junction the currents are limited to strips at the edges of the junction having a characteristic width (the Josephson penetration depth) which is typically a fraction of a millimetre.

5.1.6. The plasma resonance. If a small tunnel junction is on open circuit, current flowing across the junction can enter the capacitance C of the junction. On differentiating (5.2) with respect to time and ignoring normal currents we find that

$$\hbar\ddot{\phi} = 2e\dot{V} = -(2eI_1/C)\sin\phi$$

or

$$\ddot{\phi} \simeq -(2eI_1/\hbar C)\phi \tag{5.7}$$

for small displacements. Thus the junction has a natural oscillation frequency which is analogous to a plasma resonance. On inserting appropriate values for I_1 and C one finds that the resonant frequency is typically 10^9 Hz. The resonance is, of course, damped by the normal current (§7.7).

Apart from these effects, the original letter also commented on or carried implications for three questions which arise when we try to improve on (5.3).

5.1.7. The Riedel peak. We have already pointed out that I_1 varies with voltage and has a maximum when $eV = 2\Delta$, that is, when the Josephson frequency is equal to twice the gap frequency. This idea was developed later by Riedel (1964) and Werthamer (1969) (see §8.1).

5.1.8. The quasiparticle interference current. Josephson's prediction (4.14) shows that there is a phase-dependent contribution to the real quasiparticle current (the Josephson $\cos\phi$ term: see §8.2).

5.1.9. Proximity-effect weak links. Josephson pointed out that effects similar to what he had predicted for SIS junctions would be expected in SNS junctions also (see §9.4).

We shall now examine some of the early confirmations of these predictions.

5.2. Early observations of the Josephson effects

5.2.1. Observation of the DC Josephson effect by Anderson and Rowell (1963). It is certain that many experimenters must have seen the Josephson effect in tunnel junctions without realizing what they were seeing: anyone who finds supercurrent flowing across a thin oxide layer is very likely to conclude that he has a pinhole in the oxide and a superconducting short-circuit. It must also be noted that Meissner was convinced that he and his students had seen supercurrents flowing through insulators some years

before the effect was theoretically predicted and generally accepted (Dietrich 1952, Meissner 1960)†. But such observations were treated with some scepticism by many physicists and their significance was not understood. Once Josephson had made his prediction, the climate was changed, and within a year Anderson and Rowell (1963) had published observations which established the existence of the DC effect (the flow of DC supercurrent across a tunnel barrier). They started with two substantial advantages. Anderson had discussed the theory with Josephson, was convinced by it, and knew what to look for experimentally, while Rowell was very experienced in making reliable tunnel junctions. They knew before they started that it was essential both to use low-resistance junctions, so that electrical noise would not blurr the phase, and to screen the Earth's magnetic field, since even one flux quantum in the junction was enough to remove the effect. Their arguments that the supercurrent which they quickly saw was indeed a Josephson current and not due to pinholes were:

(i) The effect was destroyed by quantum interference in a field of a few gauss, as expected.

(ii) The critical current density was within a factor of ten of the maximum current predicted by Josephson.

(iii) They calculated that a pinhole having the necessary critical current (the alternative explanation) would have a readily measurable conductance when normal, which was not observed.

(iv) The critical currents were reproducible and could not be 'burnt out' without destroying the complete junction (in contrast to the behaviour of pinhole contacts commonly observed in thicker oxide layers).

5.2.2. Observation of the inverse AC effect by Shapiro (1963). Once Anderson had made clear the importance of working with low-resistance junctions, the field was open and many observations of the Josephson effect in tunnel junctions followed rapidly. The first to observe the effect of applying microwaves to a junction was Shapiro (1963). The junctions were Al–Al_2O_3–Sn tunnel junctions of small area and resistance between 5 Ω and 20 Ω, and they were mounted in a cavity resonant at 9·3 GHz and at 24·8 GHz. He saw extra current spikes at the voltages predicted by Josephson when a few mW of microwave power was applied to the junction. He confirmed that the magnitude of the spikes oscillated with microwave power as expected, and that at a suitable power level the original supercurrent at zero voltage was completely suppressed. At high powers the I–V characteristic appeared normal.

5.2.3. Observation of quantum interference in single junctions by Rowell (1963). Almost simultaneously, Rowell (1963) published an extension of his first observations, with two important developments. The first was that he succeeded in making junctions in which the critical current density was within a factor of two of the theoretical maximum predicted by Josephson. The second was the demonstration of the quantum-interference effect. We shall see in §6.4 that in a junction containing a uniform magnetic field the critical current as a function of magnetic field parallel to one of its edges should be identical with the familiar diffraction pattern of a slit, of the form $\sin(B/B_0)(B_0/B)$, where πB_0 is the field which introduces one flux quantum into the junction. Rowell's results are shown in figure 5. Considering the difficulty of fabricating perfectly uniform junctions, the agreement with the expected diffraction pattern is

† Meissner and Smith *et al* (1961) had also observed that supercurrent could cross thin layers of normal metal.

good (note the vertical logarithmic scale); the position of the zeros also agreed exactly with the value of B_0 calculated from the flux quantum and dimensions of the junction.

Rowell's and Shapiro's results between them confirmed the essential features of Josephson's prediction—that the supercurrent is periodic in ϕ and that the space

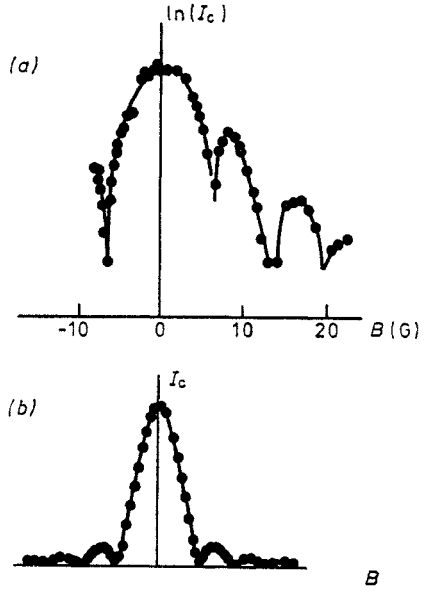

Figure 5. Quantum interference in a single junction. (*a*) First results of Rowell (1963). (*b*) Showing quality of agreement with theory in a very good sample (Matisoo 1969a).

dependence and time dependence of ϕ were connected with the magnetic potential and the chemical potential as expected for an effective pair wavefunction. They swept away most of the remaining doubts about the validity of Josephson's prediction and began a burst of experimental activity which still continues.

5.2.4. Observation of the AC effect by Yanson et al (1965) and by Giaever (1965). The direct AC effect—the generation of very-high-frequency supercurrents when a fixed voltage is applied to a weak link—was not observed so soon. The reason is easy to understand. When a fixed DC voltage is applied, the weak link behaves roughly as an AC current source of amplitude I_1 in parallel with its normal resistance R. Josephson's theory shows that the upper limit on the product I_1R is $\frac{1}{2}\pi\Delta/e$ which is typically about 1 mV. At optimum coupling the power available is $\frac{1}{8}RI_1^2$. If we take 0·5 Ω as the lowest resistance of available junctions small enough to avoid self-field effects the *maximum* power available would be about 10^{-7} W. In practice, however, the product I_1R is often an order of magnitude smaller than Josephson's maximum and, more importantly, it is extremely difficult to match simultaneously the large capacitance (of the order of 10^{-9} F) and small resistance of the typical junction to a conventional microwave circuit. If no matching is attempted the effect is typically to make the microwave power available of the order of 10^{-14}–10^{-16} W. Not surprisingly, it proved difficult to detect power levels of this order.

The first published detection of the effect was by Yanson *et al* (1965) who simply

placed a junction in a resonant cavity without any elaborate precautions to optimize the coupling. They detected output from the cavity of about 10^{-14} W at the Josephson frequency.

At almost the same time Giaever (1965) published results obtained differently. He removed the matching difficulty by using as detector a second tunnel junction lying immediately above the generating junction, with the leads so arranged that there was strong microwave coupling between the two. His generator junction also had very low resistance and a critical current reasonably near the Josephson limit. The microwave field was detected in the second junction both by the appearance of photon-assisted conventional tunnelling and (when the second junction was made thin enough to exhibit Josephson effects) by the appearance of the inverse AC effect in the detector. The power detected was reasonably near the theoretical maximum.

5.2.5. Other observations. The predicted temperature and gap dependence of the critical current in tunnel junctions was confirmed experimentally by Fiske (1964, figure 1(*f*)). A number of other important observations will be discussed in more detail later. The first observation of quantum interference in an external loop by Mercereau and his group in early 1964 (Jaklevic *et al* 1964a) is discussed in §6.2. Large junction effects and the 'Fiske steps' due to internal resonances in large junctions first reported at the Colgate Conference in 1963 (Coon and Fiske 1965) appear in §7.11. The first investigations of microbridges by Dayem (Anderson and Dayem 1964), point contacts (Levinstein and Kunzler 1966) and SNS junctions (Clarke 1969) are discussed in §9, as are the first reported observations of Josephson effects in superfluid helium (Richards and Anderson 1965). The plasma resonance was first investigated by Dahm *et al* (1968, see §7.7). The Riedel peak was first measured experimentally by Hamilton and Shapiro (1971, see §8.3) and the quasiparticle interference current by Pedersen *et al* (1972, see §8.2). Thus all of Josephson's original predictions have been examined experimentally.

6. Quantum interference

In this section we shall discuss quantum interference as it applies to the equilibrium states and critical currents of Josephson devices in various configurations. What happens when the critical current is exceeded is dealt with in the following section and useful devices based on quantum interference are discussed in §10.

6.1. The connection between magnetic flux and superconducting phase

The fundamental connection between flux and phase arises as a direct consequence of (5.1). We imagine two bulk superconductors which at two or more points are brought into close contact so as to form weak links (figure 6(*a*)). Let the phase difference across the first link be ϕ_0; we use this as a reference phase. Then it is easy to show that the phase ϕ at the second contact is given by

$$\phi = \phi_0 + \phi_M \tag{6.1}$$

where the 'magnetic phase difference' ϕ_M is just 2π times the number of flux quanta in the loop. The proof is as follows. The downward magnetic flux in the loop is given by the line integral

$$\Phi = \oint \boldsymbol{A} . \mathrm{d}\boldsymbol{l}. \tag{6.2}$$

We may break up the path of the integral into four parts. For the path involving the first junction equation (5.1) shows that the contribution is $(\hbar/2e)(\theta_4-\theta_1-\phi_0)$, and similarly for the second junction we have a contribution $(\hbar/2e)(\theta_2-\theta_3+\phi)$. For the

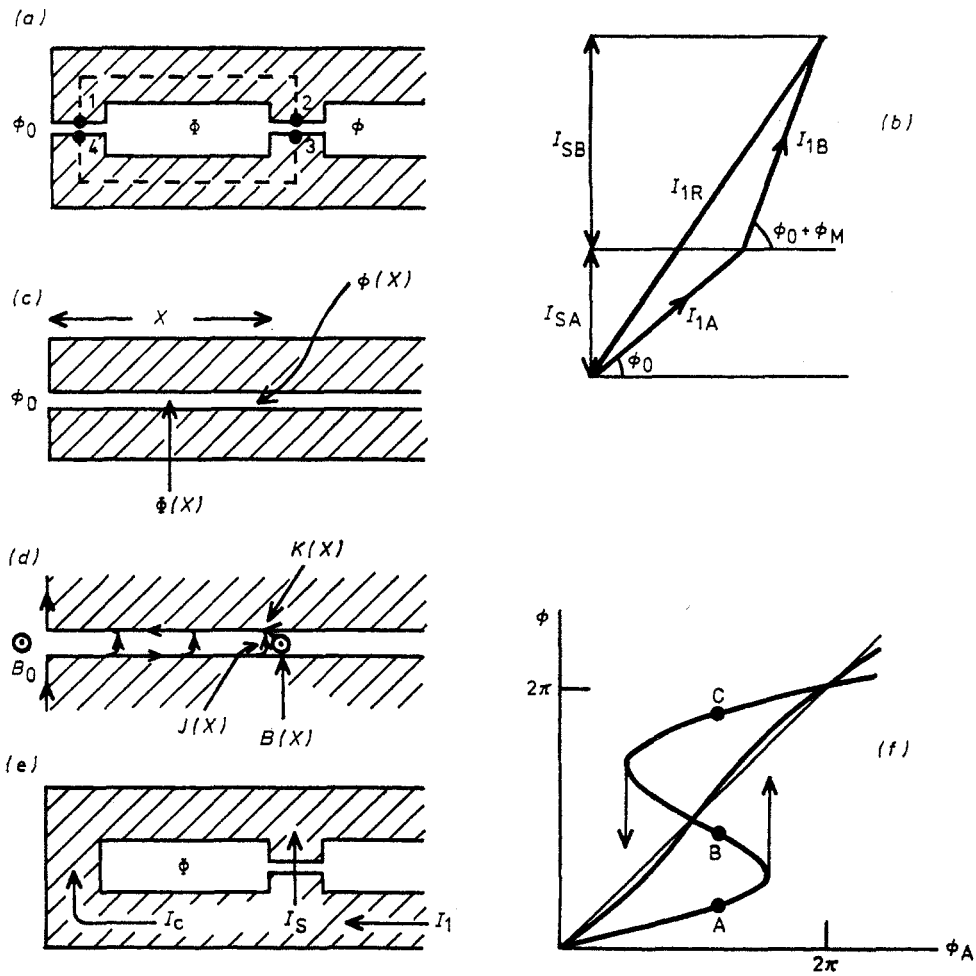

Figure 6. Quantum interference. (*a*), (*b*) Two small junctions in parallel and corresponding phase diagram (see §6.2). The positive direction of flux is into the paper. (*c*) Uniform junction of finite size in external field B (see §6.4). (*d*) Self-field effects in large uniform junction (see §6.5). (*e*), (*f*) Single junction in superconducting loop and corresponding plot of junction phase against applied phase (see §6.6).

paths in the bulk we appeal to the fact that supercurrents only penetrate a very short depth below the surface of a superconductor so that the supercurrent on the bulk paths may be taken to be zero. Then using (2.7) we find that their contributions are $(\hbar/2e)(\theta_1-\theta_2)$ and $(\hbar/2e)(\theta_3-\theta_4)$. On adding the four contributions, equation (6.1) follows.

If the superconductors are so thin that the supercurrent on the bulk path cannot be taken to be zero, then Φ must be replaced in (6.1) by London's 'fluxoid', defined as

$$\Phi' = \oint (\boldsymbol{A}+\Lambda \boldsymbol{J}_S)\cdot \mathrm{d}\boldsymbol{l}. \tag{6.3}$$

6.2. Two small junctions in parallel

If we take the configuration just discussed, then the total supercurrent through the two weak links is given by

$$I_S = I_{1A} \sin \phi_0 + I_{1B} \sin (\phi_0 + \phi_M) \tag{6.4}$$

where I_{1A} and I_{1B} are the corresponding critical currents. We may plot these supercurrents on a phase diagram (figure 6(*b*)) and we see that the problem of finding the critical current of the joint system is mathematically identical to the problem of finding the resultant amplitude in a Young's slit experiment. Each weak link contributes a supercurrent given by the projection onto the vertical axis of the corresponding vector in the phase diagram. The phase difference ϕ_M corresponds to the path difference in the Young's slit experiment and fixes the magnitude of the resultant vector, I_{1R}. In the optical case, the resultant is rotating and its magnitude gives the amplitude of the corresponding wave after interference. In the case of quantum interference ϕ_0 is a constant which we are free to vary. By varying ϕ_0 we can make the projection on the vertical lie between I_{1R} and $-I_{1R}$; clearly, I_{1R} gives the amplitude of the critical current of the joint system. The joint critical current will oscillate with the flux in the loop in the same way as the amplitude oscillates with the path phase difference in a Young's slit experiment.

This effect was first observed in double junctions by Mercereau and his collaborators (Jaklevic *et al* 1964a) and is commonly known as the Mercereau effect. The fact that the critical current is a periodic function of the applied flux makes the device a very useful and sensitive flux detector and this principle is applied in the device known as the DC SQUID (see §10.1).

6.3. The Bohm–Mercereau experiment

The argument of §6.1 which connects phase and flux shows a novel feature. The phase shift is a function of the flux within the loop, which may be present (if suitably screened) without any of the electrons experiencing the magnetic field directly. It is as though we are forced in this instance either to recognize the physical reality of the $\boldsymbol{A}$ field (which is normally regarded as an abstraction of no physical significance) or to accept the idea of direct action at a distance of the $\boldsymbol{B}$ field on the electrons. This idea is not however special to superconductivity, nor is it new. In 1949 Ehrenberg and Siday had pointed out that similar considerations apply to interfering electron beams *in vacuo* and Aharonov and Bohm (1959) emphasized the paradoxical nature of the conclusion. In 1960 Chambers had used a Young's slit arrangement in an electron microscope to demonstrate the shift of the interference pattern produced by a magnetized iron whisker placed between the interfering beams and having a very small stray field. The analogous experiment for superconductors was first reported by Jaklevic *et al* (1964b). They examined the critical current of a double bridge as a function of the enclosed flux generated in the loop by a very small, long solenoid having a negligible stray field and they found the usual variation of critical current with flux.

6.4. Quantum interference in a single junction in an applied field

If we have a *single* junction of uniform thickness in a strong external field B parallel to the plane of the junction, then the junction itself may contain an appreciable magnetic flux (figure 6(*c*)). In fact, the flux up to distance X from the boundary will be

equal to $B(t+\lambda_1+\lambda_2)X$ where $t+\lambda_1+\lambda_2$ is the 'magnetic thickness', equal to the thickness of the oxide plus the two magnetic penetration depths. Then the argument used above shows that at this point

$$\begin{aligned}\phi(X) &= \phi_0 + [2\pi B(t+\lambda_1+\lambda_2)/\Phi_0]X \\ &= \phi_0 + kX \end{aligned} \tag{6.5}$$

where k is proportional to the applied field B. If the Josephson current density per unit length at point X is $J_1(X)$, the total supercurrent carried will be

$$I_S = \int_0^a J_1(X) \sin(kX+\phi_0)\, dX. \tag{6.6}$$

This is a Fourier transform analogous to the transform which appears in Fraunhofer diffraction in optics. $J_1(X)$ plays the role of the transmission coefficient. If J_1 is constant, *the critical supercurrent as a function of magnetic field will be identical with the diffraction pattern of a slit of finite width as a function of angle.*

We have already seen that this prediction was confirmed by Rowell in 1963 for a tunnel junction (figure 5). The effect has also been confirmed in small SNS junctions (Clarke 1969). Both tunnel junctions and SNS junctions are very sensitive to small magnetic fields. In the smaller devices such as bridges and point contacts the effect requires larger fields and the more complicated geometry usually makes it less easy to interpret.

6.5. Self-field limiting and flux lines in large junctions

We have so far treated the magnetic field as being equal to the applied field, ignoring the screening effect of the currents flowing in the junction. To allow for this effect, refer to figure 6(*d*), which shows the edge of a large junction carrying current from bottom to top. The current enters the junction as a surface current of density K_0 per unit length flowing within the bulk penetration depth λ. It then crosses the junction with a density $J(X)$ per unit area (given by the Josephson equations) and finally leaves the junction again as a surface current. Note first that it follows from Ampère's rule and the fact that the magnetic field is zero inside the superconductor that the magnetic field inside the junction points *upward* normal to the plane of the diagram and that $B(X)=\mu_0 K(X)$ (and that similarly the field B_0 at the edge of the function is equal to $\mu_0 K_0$).

We then easily derive the following equations for the magnetic phase as a function of position:

$$\frac{\partial\phi}{\partial X} = -(2ed/\hbar)B(X) = -(2ed\mu_0/\hbar)K(X)$$

so

$$\frac{\partial^2\phi}{\partial X^2} = (2ed\mu_0/\hbar)J(X)$$

or

$$\frac{\partial^2\phi}{\partial X^2} = \frac{1}{\lambda_J{}^2}\sin\phi \tag{6.7}$$

where the length λ_J is equal to $(\hbar/2e\mu_0 dJ_1)^{1/2}$, d being the magnetic thickness of the junction, $t+\lambda_1+\lambda_2$. The significance of this result was first noted by Anderson and analysed in detail by Ferrell and Prange (1963). Equation (6.7) is a nonlinear screening equation and shows that ϕ, and hence B, decays to zero inside the junction over a

length of the order of λ_J, which is known as the *Josephson penetration depth.* For typical tunnel junctions λ_J is of the order of 1 mm, and for typical SNS junctions it is an order of magnitude smaller. Thus only rather small junctions can be assumed to contain a constant field and to have the same value of ϕ at all points.

In a wide junction the solutions of this equation are both complicated and fascinating. Their general nature can be visualized by noting that (6.7) is also the equation

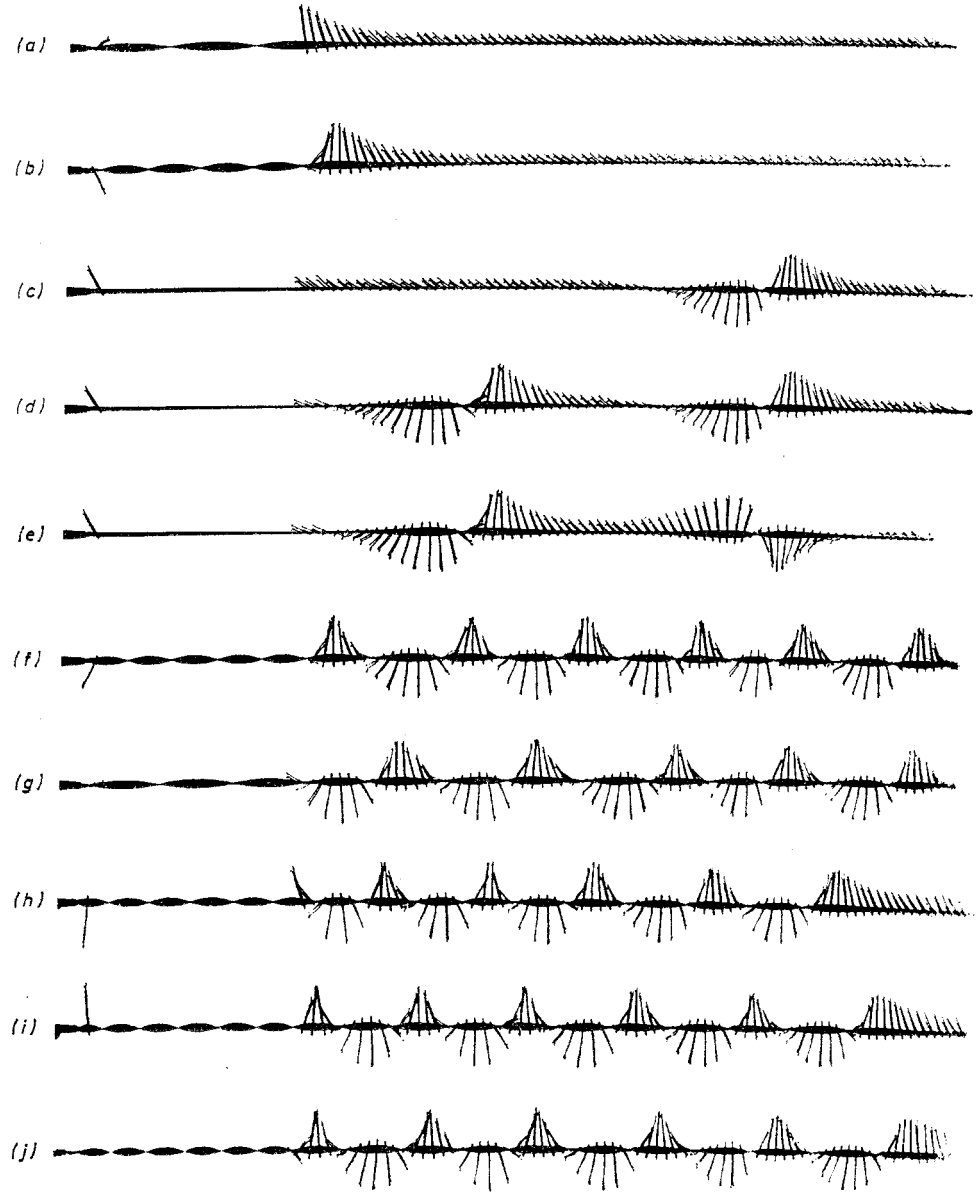

Figure 7. Mechanical analogue for self-field effect seen from above. (*a*), (*b*) Field and current screened from interior. (*c*) Flux line. (*d*), (*e*) Similar and opposed flux line pairs. (*f*), (*g*) Stationary flux in junction showing upper and lower critical fields. (*h*), (*i*), (*j*) Three stages in motion of flux lines from left to right (after Waldram *et al* 1970; see §6.5).

obeyed by a continuous line of identical pendulums hanging from a torsion wire. In this analogue, $\phi(X)$ is the angle from the vertical of the pendulum at position X, the magnetic field is the couple in the torsion wire, and the supercurrent density is the projection of the pendulum onto the horizontal plane (figure 7). Analytic solutions of (6.7) can be written down in the form

$$F[\tfrac{1}{2}(\pi-\phi)\backslash\alpha] = \pm\tfrac{1}{2}(X-X_0)(\partial\phi/\partial X)_{\max} \tag{6.8}$$

where F is an elliptic integral of the first kind and $\sin\alpha = 2(\lambda_J\,\partial\phi/\partial X_{\max})^{-1}$. These solutions have been extensively analysed by Owen and Scalapino (1967) and others. Some important features are as follows.

(i) For a junction in zero applied field the critical current increases with width but saturates at a value of $4J_1\lambda_J$ when the width exceeds about $5\lambda_J$ ('self-field limiting').

(ii) The dependence of the *total* current on the phase at the edge of the junction is no longer given by the Josephson relation. In the limit of a very wide junction the current carried at one edge is equal to $2J_1\lambda_J \sin(\frac{1}{2}\phi)$ and the junction becomes internally unstable when ϕ exceeds π.

(iii) A wide junction can contain a set of *flux lines*, which are analogous to the flux lines in bulk type II superconductors and correspond to twists in the line of pendulums (figure 7(*c*)). Flux lines contain exactly one flux quantum. Flux lines of the same sign repel each other and flux lines of opposite signs attract and may annihilate each other.

(iv) The plot of critical current as a function of applied field for a wide junction has overlapping branches corresponding to different numbers of flux lines in the junction (figure 8) and, although reminiscent of the small junction behaviour (figure 5), is quite different in detail.

(v) As in bulk type II superconductors, there is a lower critical field for the entry of flux lines into the barrier. For a wide barrier the thermodynamic critical field is equal to $(4/\pi)J_1\lambda_J$. There is, however, as in bulk type II behaviour, a surface barrier and

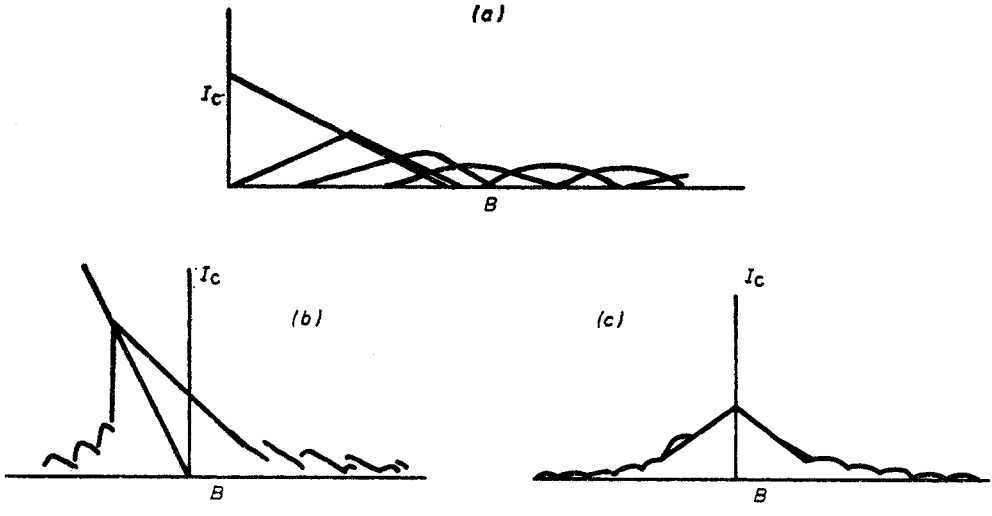

Figure 8. Critical current of a wide symmetrical junction as a function of applied field. (*a*) One-dimensional calculation for $L = 10\lambda_J$ (Owen and Scalapino 1967). (*b*) Experimental results for tunnel junction with $L \simeq 6\lambda_J$ (Matisoo 1969a; the axes are tilted because the ground plane used makes the junction asymmetric). (*c*) Results for a square SNS junction with $L = 8{\cdot}5\lambda_J$ (Clarke 1969).

hysteresis: the barrier only becomes unstable in an external field of $2J_1\lambda_J$, and once the flux has entered it only leaves the barrier when the external field is reduced to zero. There is no upper critical field of the barrier itself, which remains superconducting until the superconductors surrounding the barrier are themselves driven normal by the applied field.

In comparing these predictions with experiment (figure 8), two important points must be borne in mind. Firstly, although there is no difficulty in principle in extending the calculation to two dimensions, all the results referred to are for a one-dimensional analysis. Most experiments, however, have been performed on junctions in which ϕ varies in more than one direction and thus can only be expected to fit the predictions qualitatively. A genuine one-dimensional arrangement requires the use of a ground plane. Secondly, it must be remembered that the behaviour of the two-dimensional junction still depends on the boundary conditions at *both* edges and precautions must be taken to ensure that they are properly controlled. Experiments in which attention was given to these considerations include the work of Matisoo (1969a) on tunnel junctions and, very recently, that of Lumley (1974) on SNS junctions, who measured the current–phase relation and the I–V characteristic as well as the critical current. Both authors found rather good agreement with the theory just described.

The *motion* of flux lines and its effect on the I–V characteristics of large junctions are discussed in §7.

6.6. *Single junction in a superconducting loop*

We complete this section by considering the self-field effects for a single small junction inserted into a superconducting loop (figure 6(*e*)). This is equivalent to short-circuiting the first junction in figure 6(*a*), and we see from (6.1) that there is now a direct connection between the phase ϕ at the remaining junction and the total flux Φ in the loop, $\phi = 2\pi\Phi/\Phi_0$. It is interesting to enquire what happens if a current I_1 enters the system from the right. If I_1 divides, I_S passing through the junction and I_c circulating around the loop, then if we allow both for the externally applied flux Φ_E and for the flux generated by I_c we have

$$\phi = \frac{2\pi}{\Phi_0}(\Phi_E + LI_c). \tag{6.9}$$

On substituting for I_c as $I_1 - I_S$ we obtain the relation

$$\phi + (2\pi LI_1/\Phi_0)\sin\phi = (2\pi/\Phi_0)(\Phi_E + LI_1) = \phi_A \tag{6.10}$$

which is plotted in figure 6(*f*). This plot gives the *actual* phase ϕ across the junction in terms of the *applied* phase ϕ_A, the phase which would have been present if the junction carried no current. The following points should be noted (Silver and Zimmerman 1967, Kurkijarvi 1972).

(i) If $2\pi LI_1 < \Phi_0$ the slope of the plot is always positive and there is just one solution for ϕ at a given applied phase ϕ_A. This solution is always *stable*. Note that values of ϕ between $\frac{1}{2}\pi$ and $\frac{3}{2}\pi$, which would be unstable in an isolated junction driven by a source of any impedance, are now stable.

(ii) For larger values of LI_1 there are values of ϕ_A for which three or more solutions exist, such as A, B and C in the figure. The solutions such as B on negative-slope regions are unstable. The system now shows hysteresis: if it starts in state A and ϕ_A is increased it will eventually be forced to jump to the C branch, and if it starts in C and

ϕ_A is reduced it must jump back to the A branch. If the free energy is calculated, then the states nearest the line $\phi = \phi_A$ are found to be the most stable. Other stable states represent situations in which flux is trapped in the loop.

(iii) When it is small ϕ is approximately equal to $\phi_A(1+2\pi LI_1/\Phi_0)^{-1}$ so that if $LI_1 \gg \Phi_0$ then ϕ is much smaller than ϕ_A. This just represents the fact that if LI_1 is large applied changes in flux are effectively screened from inside the loop.

We shall see later that this case has important applications in the device known as the RF SQUID (§10.2) and in the measurement of current–phase relations (§9.7).

7. Time-dependent effects for the shunted-junction model

7.1. Use of current sources and the RSJ model

When we discussed the AC effect and the inverse AC effect in §5.1 we assumed that the signals were applied to the junctions using *voltage* sources. But since most Josephson devices have low impedances and are frequently fed from high-impedance microwave sources it is often more instructive to consider the case of current-source input. In this situation any input current which is not transmitted as supercurrent must be forced through the device as normal current, thus determining the voltage and hence the rate of change of phase across the junction. Thus, for the first time in this review, we find a situation where the nature of the normal current is important in determining the supercurrent. In this section we shall assume that the normal current can be described using a simple parallel resistance as in the RSJ model represented by equation (5.3) of §5.1. This is, of course, an approximation, but it contains the essential physics for most effects of interest up to the gap frequency. It appears to be a rather good approximation for certain weak links such as microbridges and SNS junctions, though not so good (as we have seen) for tunnel junctions. The extent to which the model is valid is discussed for tunnel junctions in §8.1 and for other weak links in §9. The shunt resistance can usually be assumed to be roughly equal to the normal state resistance of the device.

We shall examine below the time-dependent behaviour of the RSJ model in various situations, normally using a current source. As we shall see, the use of a current source leads to strongly nonlinear differential equations and behaviour that are often qualitatively different from what are expected for a voltage source. This nonlinearity makes analytic solution difficult, but it also frequently leads to a fascinating richness of solutions.

7.2. Reduced variables

If a current $I(t)$ is applied to a small junction of critical current I_1 we find on combining the Josephson relations (5.2) and (5.3) the nonlinear equation of motion for ϕ

$$\frac{\hbar\dot{\phi}}{2eR} = I(t) - I_1 \sin\phi \tag{7.1}$$

which in terms of the reduced parameters shown in table 1 takes the form

$$\dot{\phi} = i(\tau) - \sin\phi. \tag{7.2}$$

7.3. Constant current applied to a small junction of negligible capacitance

In this case $i(\tau)$ is a constant, i_0. The general nature of the solutions can be understood by noting that (7.2) is now the same equation as that of a particle moving under

Table 1. Reduced parameters for calculation using the RSJ model

Reduced current	$i = I/I_1$
Reduced current density	$j = J/J_1$
Reduced time	$\tau = (2eRI_1/\hbar)t = \omega_c t$
Reduced frequency	$v = (\hbar/2eRI_1)\omega = \omega/\omega_c$
Reduced voltage	$v = (RI_1)^{-1}V = \partial\phi/\partial\tau$
Reduced capacitance	$c = (2eR^2I_1/\hbar)C = \omega_c RC$
Reduced distance	$x = (2e\mu_0 dJ_1/\hbar)^{1/2}X = X/\lambda_J$
Reduced velocity	$u = (\lambda_J\omega_c)^{-1}U$

gravity in a viscous medium on a sloping washboard (figure 9). For $|i_0| < 1$ (applied current less than critical current) ϕ settles rapidly to a constant, stable value in the range $-\frac{1}{2}\pi < \phi < \frac{1}{2}\pi$. For $|i_0| > 1$ there is no static solution and the phase slips. The rate of slippage is greatest when $\phi = -\frac{1}{2}\pi$, and smallest when $\phi = \frac{1}{2}\pi$. Consequently the

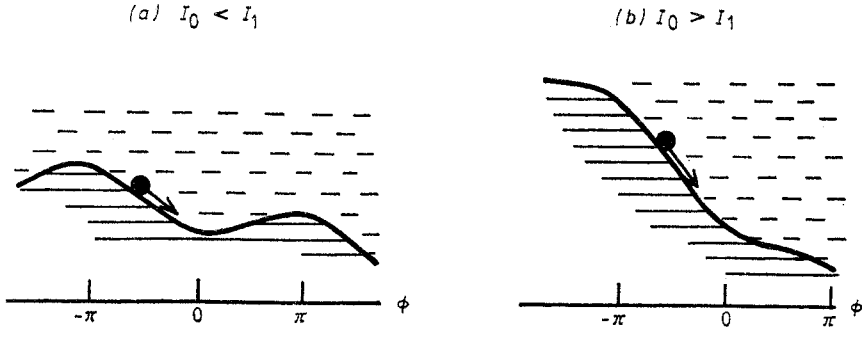

Figure 9. The washboard analogue. The tilt corresponds to the DC current injected. For the RSJ model the particle has weight but no inertia (§7.3). For a capacitative junction the particle has inertia (§7.4). Oscillations around the minimum for $I_0 < I_1$ correspond to the plasma oscillation (§7.7). Electrical noise is equivalent to Brownian motion (§7.9).

phase increases unsteadily, and this means that the supercurrent at finite voltage is not a purely sinusoidal function of time: it has a DC component and also components at all multiples of the Josephson frequency. The equation can be solved analytically and the phase is given as a function of time by the relation

$$i_0 \tan(\tfrac{1}{2}\phi) = 1 + v_0 \tan[\tfrac{1}{2}v_0(\tau - \tau_0)] \tag{7.3}$$

where $v_0 = (i_0^2 - 1)^{1/2}$. Clearly ϕ increases by 2π when $v_0\tau$ does the same, so that v_0 is the reduced frequency of a periodic variation of ϕ. The mean value of $\dot{\phi}$ which is also the mean reduced voltage is thus given by $\dot{\phi} = v = v_0$ (figure 10(*a*)); note that, unlike the situation with a voltage source, the DC voltage increases monotonically once the critical current is exceeded and no hysteresis is expected. The full expression for the voltage is (Aslamazov and Larkin 1968)

$$v(\tau) = \dot{\phi} = \frac{v_0^2}{i_0 + \cos(v_0\tau)} \tag{7.4}$$

where we have chosen the time origin so that $\dot{\phi}$ is a minimum and $\phi = \frac{1}{2}\pi$ at $t = 0$. This expression can be expanded in harmonics of the Josephson frequency as follows (Fack and Kose 1971):

$$v(\tau) = v_0[1 + 2\sum_n (-v_0 - i_0)^{-n} \cos(nv_0\tau)]. \tag{7.5}$$

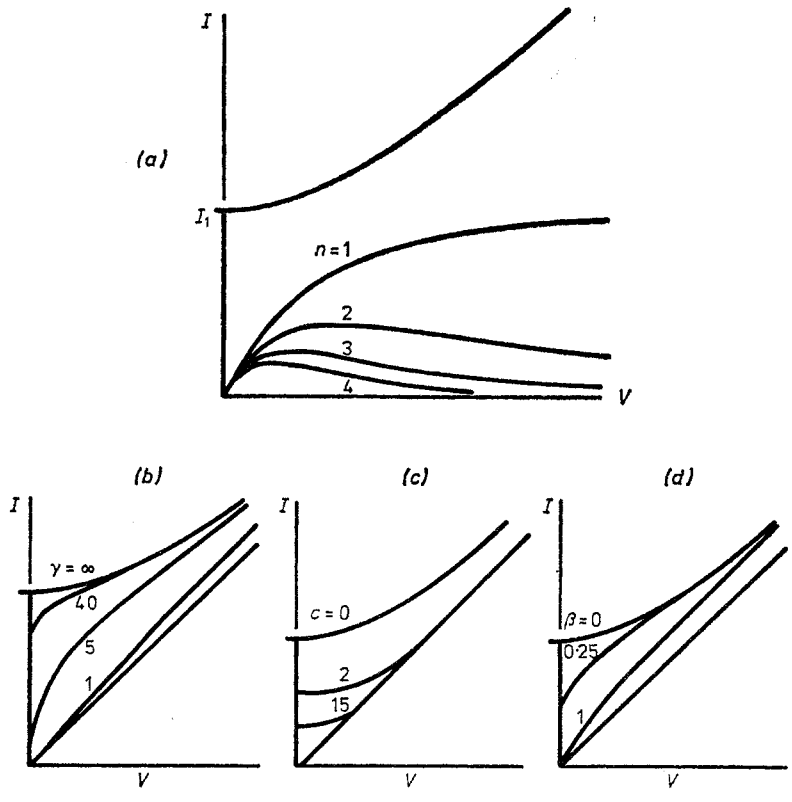

Figure 10. Predicted *I–V* characteristics. (*a*) RSJ model fed with constant current, showing also the currents flowing in the shunt resistor at harmonics of the Josephson frequency (§7.3). (*b*) Same as for (*a*), with noise rounding, where $\gamma = I_1\hbar/ekT$ (Aslamazov and Larkin 1968; §7.9). (*c*) RSJ model with shunt capacitance, where c is reduced capacity (McCumber 1968; §7.4). (*d*) RSJ model with parallel inductance and *voltage* source, where $\beta = R/(\omega_c L)$ (McCumber 1968; §7.5).

Thus we see that a junction to which a constant current is applied is expected to act as a voltage generator at all multiples of the Josephson frequency. A DC *I–V* characteristic of the type predicted has been observed in weak links of several types (see figures 11 and 13). The high-frequency voltages generated are important in microwave devices (§11).

7.4. The effect of capacitance on the I–V curve for small junctions

If a Josephson device has appreciable capacitance, as is commonly the case for tunnel junctions, then

$$I(t) = I_1 \sin\phi + V/R + \dot{V}C \tag{7.6}$$

and the reduced equation of motion for a constant input current takes the form

$$c\ddot{\phi} + \dot{\phi} = i_0 - \sin\phi \tag{7.7}$$

where c is the reduced capacitance (see table 1). The general nature of the solutions of this equation can be understood by noting that a *massive* particle sliding through a viscous liquid down a sloping washboard under gravity has the same equation of motion

(figure 9). For $i_0 > 1$ the particle will settle down to a steady average rate of slide as before. On the other hand, for $i_0 < 1$ two types of solution may be possible. There is a static solution in which the particle is at rest at a minimum of the potential (zero-voltage supercurrent) and a dynamic solution in which the particle has a steady average rate of slide, using its inertia to punch through the potential minima (finite voltage). Thus we expect to see hysteretic behaviour as i_0 is varied and this is confirmed by the computed I–V curves shown in figure 10(*c*) (McCumber 1968, Stewart 1968). Notice that the effect of the capacitance should become noticeable for $c \gtrsim 1$. For $c \gtrsim 20$ the predicted characteristic is similar to that for a DC *voltage* source; this is readily understandable when we reflect that the large capacitance has the effect of absorbing the AC supercurrents generated by the device and hence making negligible all the AC components of voltage.

Experimental checks have shown fair confirmation of this prediction in tunnel junctions, which have relatively large values of C (Scott 1970, for instance). However, as McDonald *et al* (1976) have pointed out, in good tunnel junctions the Josephson frequencies involved are near the gap frequency and the RSJ model is probably inadequate. We discuss their improved calculation in §8.1; it is not yet clear whether the experimental data for tunnel junctions lie nearer to their predictions or to those just discussed. Most other types of device have small values of C and do not show interesting effects due to capacitance.

7.5. *The effect of series inductance on small junctions*

The effect of series inductance for a *voltage* source has also been calculated (McCumber 1968) and is rather similar to the effect of parallel capacitance for a current source (figure 10(*d*)). We note that a large inductance smooths the current and makes the system behave as though it were current-source driven. The effects of series inductance may be significant in determining the observed I–V characteristics of high-resistance point contacts, which sometimes do have forms similar to those of figure 10(*d*).

7.6. *Small-signal inductance of a junction at zero voltage*

For small departures from a constant value of ϕ (which implies that the junction is biased within the zero-voltage step) we have

$$\begin{aligned} \partial I_S/\partial t &= I_1 \cos\phi_0 \, \dot{\phi} \\ &= (2eI_1 \cos\phi_0/\hbar)V. \end{aligned} \tag{7.8}$$

Thus the small changes of supercurrent behave as though they were passing through an inductance $L_J = \hbar/(2eI_1 \cos\phi_0)$. This idea is useful in discussing the RF properties of the device. The effective inductance is in parallel with the capacitance and shunt resistance.

7.7. *The plasma resonance in small junctions*

If we return to the solutions of (7.7) for $i_0 < 1$, we see that if the system is slightly disturbed from equilibrium the phase will undergo damped oscillations given by the equation

$$c\delta\ddot{\phi} + \delta\dot{\phi} + \cos\phi_0 \delta\phi = 0 \tag{7.9}$$

(corresponding to oscillations of the particle around the potential minimum on the sloping washboard shown in figure 9). If c is large these oscillations are lightly damped and we notice that their reduced frequency varies with the equilibrium value of ϕ according to the relation

$$\begin{aligned} v_p &= (\cos \phi_0/c)^{1/2} \\ &= c^{-1/2}(1-i_0^2)^{1/4}. \end{aligned} \tag{7.10}$$

In non-reduced variables the frequency ω_p is just equal to $(L_J C)^{-1/2}$, as one would expect for the equivalent circuit for small signals mentioned in the previous section. Detecting this plasma oscillation is not very easy because the small excursions of ϕ correspond to very small currents and because the junction is not easily matched to external circuits. The first observation was by Dahm *et al* (1968), who checked the effect in Sn–SnO–Sn junctions by sweeping I_0 in the presence of a small microwave signal at 4·75 GHz and detected the resonance in the second-harmonic output generated by the nonlinearity of the junction itself; the detected power was 10^{-17}–10^{-18} W. They found good agreement with the above formula for the frequency of the resonance after correction for the finite size of their junctions. Later measurements of the Q of the resonance by the same group, however, showed that the damping term was not constant as (7.9) would predict but also varied with ϕ_0. We shall discuss the significance of these later results in §8.2.

7.8. The effect of high-frequency input on small junctions

For a junction of negligible capacitance fed with a current having both DC and RF components of the form $I(t) = I_0 + I_S \cos(\omega_S t)$ the reduced equation of motion (7.2) takes the form

$$\dot{\phi} = i_0 + i_S \cos(v_S \tau) - \sin \phi. \tag{7.11}$$

This equation has not been solved analytically but has been extensively studied by digital and analogue computation (Russer 1972) and by perturbation theory (see Thompson 1973). The following features of the solution are worth noting.

(i) The mean value of $\dot{\phi}$ (the DC voltage) has a tendency to stick or lock-on at the multiples of the applied frequency, nv_S. In other words, $\bar{v}$ remains constant for a finite range of values of DC current i_0 whenever $\bar{v} = nv_S$, corresponding to a set of vertical regions in the low-frequency I–V characteristic (figure 11(a)). Within these regions the supercurrent is phase-locked to the RF input. (What happens within such a region is that if, for instance, $\bar{v}$ is slightly greater than nv_S, the phase of ϕ will gradually increase compared to the phase of the excitation. This changes the relative phases of the second and third terms of (7.11) in such a way that the effect of the third term is enhanced, which in turn reduces $\bar{v}$ until $\bar{v} = nv_S$. Thus if i_0 is suddenly increased by a small amount, $\bar{v}$ will at first increase, but the phase-locking mechanism just described will then bring $\bar{v}$ back to nv_S.)

(ii) These steps in the I–V curve correspond to the spikes in the I–V curve for the voltage-fed device which we discussed in §5.1. The correspondence can be seen most easily in the limit of high excitation frequency where $v_S \gg 1$, if we choose $i_S \approx v_S$ and examine the range of i_0 near nv_S where a step is expected. Under these circumstances the last term of (7.11) is small, and consequently we see by integration that

$$\phi = nv_S\tau + (i_S/v_S) \sin v_S\tau + \delta\phi \tag{7.12}$$

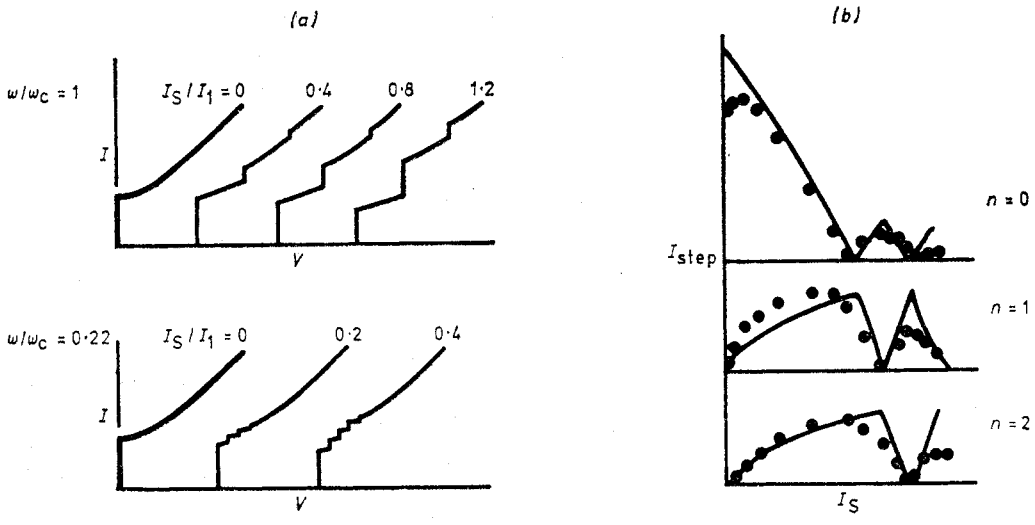

Figure 11. I–V characteristics for current-fed RSJ model with microwave excitation. (*a*) Predicted characteristics labelled with values of excitation level I_S/I_1 (Russer 1972). (*b*) Theoretical variation of step height with excitation for $\omega = 0{\cdot}22\omega_c$ compared with data for small microbridges (Gregers-Hansen *et al* 1971).

where $\delta\phi$ has a slowly varying part combined with small and unimportant high-frequency terms. If we insert this form into (7.11) we find for the low-frequency part of $\delta\phi$ the equation

$$\delta\dot{\phi} = \delta i_0 - J_{-n}(i_S/v_S)\sin\delta\phi \tag{7.13}$$

where $\delta i_0 = i_0 - nv_S$ and J_{-n} is a Bessel function. This equation in $\delta\phi$ is equivalent to equation (7.2) for an *unexcited* junction whose critical current is equal to $I_1|J_{-n}(i_S/v_S)|$. It follows that the shape of the I–V curve near a step is, in this limit, identical with the shape of a zero-order step of the same height and that the half-step height is given as a function of excitation by the Bessel function.

(iii) If, on the other hand, the reduced frequency is low, the steps interfere with one another in a complex way (figure 11(*a*)), and the variation in step height with excitation, though qualitatively similar, is no longer given by the Bessel function. Although the slope of the I–V curve between steps may be very small in this limit, it is never negative and hysteresis is not predicted.

Extensive comparisons between analogue solutions of (7.11) and measured I–V curves for small microbridges irradiated with microwaves have been made by Gregers-Hansen *et al* (1971); the quality of the agreement obtained can be seen in figure 11(*b*). It seems likely that, apart from the depression at small excitation discussed in §9.3, the residual disagreement is mainly due to the finite size of the bridge, which leads to a current–phase relationship which is not exactly sinusoidal. This, incidentally, can be shown to lead to subharmonic steps at the reduced voltages $v = nv_S/m$ where n and m are both integers, and such steps are indeed readily visible for the larger bridges. The possible effects of phase dependence of the *normal* current on I–V curves are discussed in §8.2. Similar I–V curves have been commonly observed in point contacts at microwave and higher frequencies, in Notarys–Mercereau bridges and, at lower frequencies, in SNS junctions (see §9).

The use of a Josephson device as a mixer is discussed in §11.2.

7.9. The effect of noise voltages on I–V characteristics

As we saw in §2.3, Josephson realized from the beginning that since an unbiased junction has a rather small free energy equal to $\hbar I_1/2e$, then once the thermal energy kT exceeds this value its phase will start to wander and the Josephson effects will disappear. The details of this phase wandering may be discussed in the spirit of the RSJ model by adding a Johnson noise current source in parallel with the resistor in the RSJ model. This is equivalent to adding a noise source to the right-hand side of the reduced equation of motion (7.2), having a mean square value in range dw of reduced frequency given by

$$\overline{i_N^2} = \frac{2kT}{\pi(\hbar I_1/2e)}\, dw = \frac{4}{\pi\gamma}\, dw. \tag{7.14}$$

It was pointed out by Ambegaokar and Halperin (1969) in an elegant paper that if we return once again to the mechanical analogue of the particle on the tilted washboard, the additional term is just equivalent to thermal Brownian motion. The interpretation is then quite simple (figure 9(*a*)). The noise will mean that the particle, though predominantly located near one of the potential minima, will occasionally have enough thermal energy to cross the potential barrier and will gradually drift downhill; the corresponding phase drift appears as a small finite voltage. This effect is particularly noticeable when the washboard tilt is so large that the minima have almost disappeared (I approaches I_1). If, on the other hand, the free energy $\hbar I_1/2e$ is much greater than kT, drifting is very unlikely and the supercurrent step will be *extremely* steep; this is, in fact, a typical thermally activated process and one can show that at zero bias the slope resistance will be of the order of $R \exp(-\pi\gamma)$. In a typical junction this is of the order of $R \exp(-1000)$ at helium temperatures. A similar interpretation can be shown to apply to phase drift at a Josephson step induced by microwaves. It is this extreme steepness of the steps which makes relatively easy the measurement of step voltages from which the ratio e/h can be accurately determined (§11.1).

The predictions of noise rounding made by Ambegaokar and Halperin are shown in figure 10(*b*). The theoretical predictions have been quite precisely confirmed using external noise sources (Kanter and Vernon 1970a, b). The noise actually present in devices at low temperatures is discussed in §8.4.

7.10. Time-dependent effects in large tunnel junctions

To discuss time-dependent effects in large junctions we must combine (6.7), which shows how the phase varies with position, with (7.6), which gives the total current density for a capacitative junction. The result expressed in reduced variables is

$$\frac{\partial^2\phi}{\partial x^2} - \frac{1}{u_0^2}\frac{\partial^2\phi}{\partial\tau^2} = \sin\phi + \frac{\partial\phi}{\partial\tau} \tag{7.15}$$

which is a damped nonlinear wave equation. The constant u_0 (which we write as U_0 in unreduced variables) is just the reduced waveguide velocity which the junction would have if no current flowed across it†. Because the magnetic field penetrates into the bounding superconductors U_0 is decreased by a factor of $[d/(d+\lambda_1+\lambda_2)]^{1/2}$ compared to the velocity of light; for a typical junction this factor is of the order of 0·1. The

† The reduced velocity u_0 is equal to $c^{-1/2}$ where c is the reduced capacitance.

above equation is also the equation of motion of a line of pendulums rotating around a horizontal torsion wire with light damping and we shall use this physical analogue in trying to make clear some of the many complicated solutions which it possesses. (It has also been used to describe the motion of dislocations and has been explored as a basis for nonlinear quantum field theory. When the final damping term is absent it is sometimes known as the sine–Gordon equation.)

7.10.1. Moving flux line mode (see Lebwohl and Stephen 1967, Waldram *et al* 1970). As a first approximation it is usual to ignore the final damping term in (7.15). In this case we note that if $\phi(x)$ represents a *stationary* flux line or array of flux lines as discussed in §6.5 then $\phi[(x \pm u\tau)/\alpha]$ is a stable solution of the *dynamic* equation provided $u < u_0$ and $\alpha = (1 - u^2/u_0^2)^{1/2}$. In other words, for every static solution there are corresponding dynamic solutions in which the flux pattern moves and the length scale suffers a 'Lorenz contraction' by the factor $(1 - u^2/u_0^2)^{1/2}$. This conclusion ignores damping, however, and is rather misleading. It suggests that the density of flux lines in a moving array is uniform, as in a stationary array, whereas in fact in the presence of damping a density gradient is needed to drive the flux lines along (figure 7(*h*), (*i*) and (*j*)). It may also be shown in the absence of damping that equal and opposite flux lines can *pass through* each other. This is equally misleading. Model experiments show that very little damping is needed to ensure that equal and opposite flux lines will *annihilate* one another when they meet.

If a long junction is placed in a *magnetic field* which exceeds the critical field, flux lines of the same sign enter from the edges and flow to the centre, where they come into equilibrium and form a static array. If, on the other hand, a DC *current* exceeding the critical current is applied to the junction, flux lines of *opposite* sign enter from the edges and flow to the centre where they are annihilated in a continuous flow. This flux flow, of course, implies that there is a DC voltage across the junction and this must be our model for understanding the *I–V* curve for a long junction. The question of what *I–V* characteristic is to be expected has, however, never been clearly resolved. It involves very careful computation, since the average supercurrent depends critically on the details of the launching of the flux lines from the edges of the junction and of their annihilation at the centre. Arguments given by Waldram *et al* (1970) in discussing their theoretical calculations for SNS junctions apply also to large tunnel junctions and suggest that a substantial DC supercurrent may be expected to persist at large voltages. This is certainly what is observed for large tunnel junctions and large SNS junctions and indeed for many point contacts, too. The *I–V* characteristic frequently looks as though an almost *constant* supercurrent has been added to the normal characteristic independent of the voltage applied. (In tunnel junctions the *I–V* curve is often complicated by the presence of other structures: see §7.11.)

7.10.2. Transmission line modes. A second type of solution corresponds to the plasma oscillation in small junctions discussed in §7.7. In its simplest form it can be regarded as the mode of small oscillation about the equilibrium state $\phi = 0$ (or, in the mechanical analogue, the waves of small oscillation of the line of pendulums about the vertical equilibrium position). As Josephson (1965) noted, if ϕ is small and we omit the damping term, (7.15) becomes

$$\frac{\partial^2\phi}{\partial x^2} - \frac{1}{u_0^2}\frac{\partial^2\phi}{\partial \tau^2} = \phi \tag{7.16}$$

which is now linear. This is a transmission line equation for the junction. Note that it has the dispersion relation, in non-reduced variables,

$$\omega^2 = \omega_p^2 + c_0^2 k^2 \tag{7.17}$$

which has a frequency cutoff similar to that for a waveguide (figure 12, curve A). If $k = 0$, the solution is exactly analogous to the plasma oscillation in a small junction and indeed the observations of the plasma resonance by Dahm *et al* (1968) discussed in §7.7 were, in fact, made on quite large junctions. In a sufficiently wide junction modes with higher k values fitted to the boundary conditions should also be observable. Although, as we shall see, related modes in a magnetic field have been observed, these expected transmission line modes in zero field do not seem to have been reported in the literature.

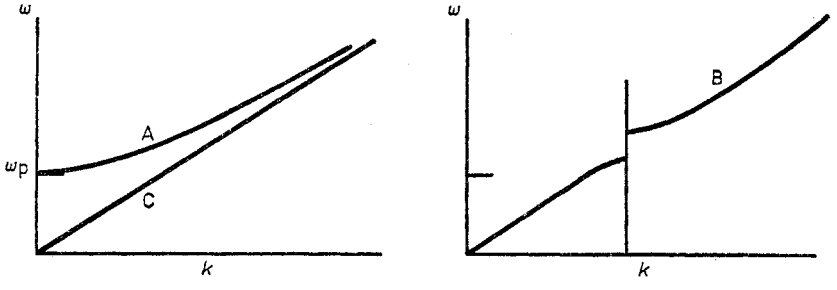

Figure 12. Dispersion relations for modes of small excitation in tunnel junctions. Curve A, no flux in junction; curve B, in presence of flux lines at spacing $2{\cdot}5\lambda_J$ (after Lebwohl and Stephen 1967); curve C, in very high flux density.

We can also ask what the modes of small oscillation about a stationary flux pattern are like (corresponding in the mechanical analogue to waves travelling along an already twisted line of pendulums). This question was discussed by Lebwohl and Stephen (1967), who actually obtained analytic solutions to the problem. Since we have a periodicity produced by the regular array of flux lines in the equation for small disturbances it is no surprise that the solutions have two branches with a frequency gap (figure 12, curve B). When the flux lines are well separated the two branches are easily interpreted. The upper branch has a large amplitude between the flux lines and corresponds to the transmission line mode in the absence of flux just discussed. The lower branch only has appreciable amplitude near the flux lines and corresponds to various modes of oscillation of the flux line array. The zero-frequency point on this branch corresponds to the uniform motion of the array discussed in the previous paragraph. The sharp peak observed by Pedersen *et al* (1972) in their observations of the plasma mode was evidently due to a geometrical resonance of the transmission line mode in the presence of a magnetic field. What happens to such modes in the presence of *moving* flux lines is discussed in §7.11.

7.10.3. The pendulum mode. Josephson (1965) also pointed out that in the presence of light damping (7.15) has a mode in which ϕ is almost independent of x (corresponding to all the pendulums moving as one). For small amplitudes, this is just the plasma oscillation but there is also a finite voltage mode (corresponding to continuously rotating pendulums). It seems likely that at high voltages the system may prefer this mode to one involving very closely spaced moving flux lines. This idea was used in a qualitative way by Scott and Johnson (1969) to explain their data on the I–V curves of

large tunnel junctions, which appeared to show a hysteretic jump from the 'displaced linear branch' characteristic of flux flow to a normal-state I–V characteristic at high voltages.

7.11. Self-excited structure in large tunnel junctions

Structure in the I–V curves of large Josephson junctions was first observed by Fiske (1964) and has been quite extensively investigated since. To understand what is happening we must remember that at finite voltage there is a *moving* pattern of flux inside the junction. The velocity of the flux pattern is known if the field and the voltage are known and is in fact equal to $V[B(t+\lambda_1+\lambda_2)]^{-1}$. Superimposed on this moving pattern will be modes of small oscillation similar to those for the fixed flux pattern discussed in the last section and including transmission line modes. The dispersion relation for the transmission line modes in these circumstances has not been calculated analytically, but if the flux density is high it will not be very different from that for a transmission line without leakage currents (figure 12, curve C) and the velocity of the transmission line modes will be close to c_0. Under these circumstances two types of behaviour may be apparent.

7.11.1. Broad peaks at voltages proportional to the field. If the system is fairly heavily damped the boundary conditions on the transmission line mode are not very important and the main effect is a broad resonance which occurs when the flux pattern is moving at the same velocity as the transmission line mode. This produces a broad peak in the energy dissipation at a voltage proportional to the magnetic field in the junction. This behaviour has been seen and successfully analysed using perturbation theory by Eck *et al* (1964).

7.11.2. Sharp steps at fixed voltages. In a more lightly damped system, the transmission line has well defined geometrical modes whose frequencies depend on the width of the junction. These modes can act as cavities to which the flux flow frequency can become locked and this produces steps at the corresponding voltages (Coon and Fiske 1965). If the magnetic field is varied, the step corresponding to the voltage at which the flux speed matches the transmission line speed is strongly enhanced (Langenberg *et al* 1966, Dmitrenko *et al* 1965). Matisoo (1969b) has seen steps in zero applied field, which he attributes to the presence of inhomogeneities in the junction. However, since any junction showing a voltage must, in fact, contain flux it seems possible that the explanation of his steps is essentially similar to that given here.

Blackburn *et al* (1971) have more recently reported detailed computations which fit the experiments of both types of behaviour reasonably well and better than the perturbation calculations do. For a discussion of the phase locking of Josephson junctions to an *external* cavity and possible applications, see the review by Richards *et al* (1973).

7.12. Time-dependent effects in large SNS junctions

In SNS junctions, the capacitative term in (7.15) is absent and the damping term dominates the time dependence. The resulting equation corresponds to that for a line of pendulums rotating around a torsion wire in a very viscous medium. In this case there is no transmission line mode and the interesting questions concern the flux flow. The equation was studied by Waldram *et al* (1970) and the following features of the results should be noted (figure 13).

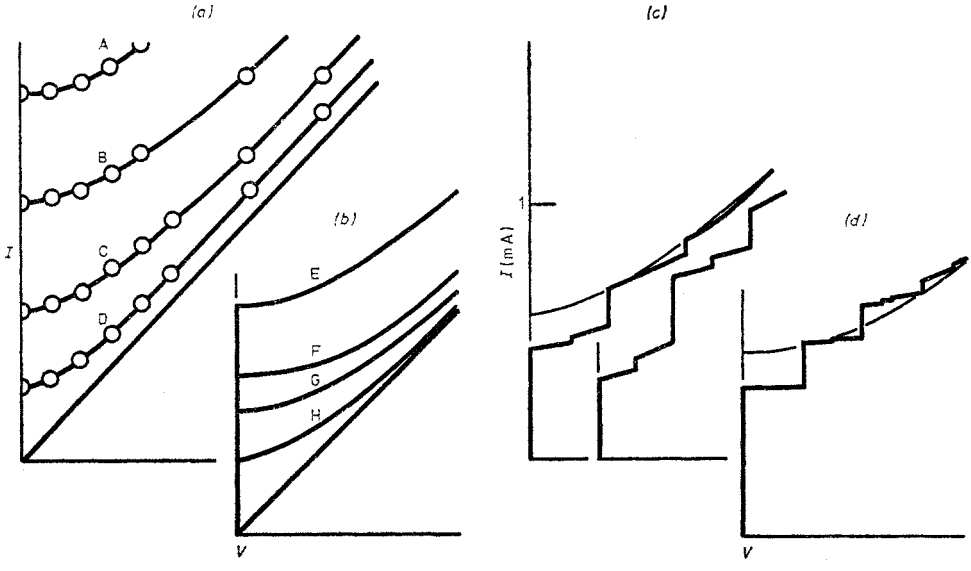

Figure 13. *I–V* characteristics for a wide one-dimensional SNS junction. (*a*) Experiment (Lumley 1974): curve A, $L/\lambda_J = 22$; curve B, $L/\lambda_J = 15$; curve C, $L/\lambda_J = 6{\cdot}5$; curve D, $L/\lambda_J = 4$. (*b*) Theory for unexcited junction (Waldram *et al* 1970): curve E, $L/\lambda_J = 13$; curve F, $L/\lambda_J = 8$; curve G, $L/\lambda_J = 6{\cdot}5$; curve H, $L/\lambda_J = 4$. L/λ_J is varied by varying the temperature. (*c*) Experiment for the same junction with two levels of microwave excitation and $L/\lambda_J = 6{\cdot}5$. (*d*) Corresponding theory. Slightly differing scales are used in the four diagrams.

(i) Numerical calculation of the flux flow situation shows that for wide junctions the *I–V* curve shows a persistent supercurrent at large voltages.

(ii) In the presence of AC excitation steps appear at submultiples as well as multiples of the Josephson voltage.

8. Further developments for tunnel junctions

We have so far done scant justice to the details of Josephson's original prediction for tunnel junctions (4.14), having worked with the RSJ model, which treats $I_1(V)$ and $\sigma_1(V)$ as constants. In this section we shall look in more detail at the full prediction and its extensions.

8.1. Werthamer's formulation of the tunnel current

Josephson's original calculation was limited to the case where the frequencies of the voltages across the junction are small compared to the gap frequency. The extension to the general case is fairly straightforward and was first performed by Werthamer (1966), using the method introduced by Ambegaokar and Baratoff (1963a, b). Werthamer's result can be written as†

$$I(t) = \mathrm{Im}\,[\exp(-\tfrac{1}{2}i\phi(t)) \int_{-\infty}^{t} \exp(\tfrac{1}{2}i\phi(t'))j_1(t-t')\,dt' + \exp(\tfrac{1}{2}i\phi(t)) \int_{-\infty}^{t} \exp(\tfrac{1}{2}i\phi(t'))j_2(t-t')\,dt'] \qquad (8.1)$$

† Readers of the original paper should note that $\phi(t)$ is written by Werthamer as $\omega_0 t + \alpha + \delta\phi(t)$ and that we have used the convolution theorem to convert his expression in terms of Fourier components $j(\omega)$ into (8.1). We have written his $j_1(\omega)$, $j_2(\omega)$ as $-\tilde{j}_1^*(\omega)$, $-\tilde{j}_2(\omega)$ to simplify the presentation.

where $\phi(t)$ is the phase across the junction at time t. The form of this result can be understood intuitively as follows. We saw in §4 that the tunnel Hamiltonian entered Josephson's calculation of the current crossing a tunnel junction *twice*, once in calculating the perturbed wavefunction and once in calculating the current carried by the perturbed wavefunction. The effect of each of these aspects of the calculation is also apparent in Werthamer's result: the phase factors in (8.1) arise when the various operators in (4.4) are applied at a given time and we see that in each term the integral over earlier times t' represents the cumulative effect of the perturbation, while the prefactor arises in the subsequent calculation of the current at time t. The first term represents the normal terms in the current and the second the Josephson terms. The response functions $j_1(t-t')$ and $j_2(t-t')$ show how the effect of the perturbation decays as the contributions of the various excited states created at time t' lose phase coherence. The functions are real. For normal metals j_2 is zero and j_1 consists of a double δ function (differential operator) at $t-t'=0$, so that in this case we simply have $I(t)\propto\dot{\phi}(t)\propto V(t)$. In superconductors the situation is, of course, more complicated and j_1 and j_2 can be related to Josephson's calculation as follows. If we have a constant voltage, or a voltage which changes only slightly in the gap time $\hbar/\Delta$, we may write $\frac{1}{2}\phi(t)$ as ωt in Werthamer's equation (8.1), where we follow his notation by writing $\hbar\omega=eV$, ω being *half* the usual Josephson frequency. We then find that

$$I(V)=\text{Im}\,\tilde{j}_1(\omega)-\sin\phi\ \text{Re}\,\tilde{j}_2(\omega)+\cos\phi\ \text{Im}\,\tilde{j}_2(\omega) \tag{8.2}$$

$\tilde{j}_1(\omega)$ and $\tilde{j}_2(\omega)$ being the Fourier transforms of $j_1(t)$ and $j_2(t)$, which is just Josephson's result. Im $\tilde{j}_1$ is the ordinary tunnel current $\sigma_0(V)V$, $-$Re $\tilde{j}_2$ is Josephson's $I_1(V)$ and Im $\tilde{j}_2$ is Josephson's $\sigma_1(V)V$.

Werthamer's formulation has the advantage that it can be used to calculate the tunnel current for the general case when the voltage may be varying rapidly. The real and imaginary parts of $\tilde{j}_1(\omega)$ and $\tilde{j}_2(\omega)$ as found by Werthamer at zero temperature are shown in figure 14(*a*) and it is worth noting the following points about his results.

(i) The terms Im $\tilde{j}_1$ and Im $\tilde{j}_2$ are odd functions of voltage and correspond to real energy-dissipating tunnelling of excitations. They are absent at $T=0$ for voltages less than the gap voltage, $2\Delta/e$, as one would expect. At higher temperatures they continue down to zero voltage, both with positive sign. The linear resistive behaviour of Im $\tilde{j}_1(\omega)$ at high voltages corresponds to the presence of a double δ function (differential operator) at $t=0$ in $j_1(t)$, as in the normal metal.

(ii) The terms Re $\tilde{j}_1$ and Re $\tilde{j}_2$ are even functions of voltage and correspond to virtual transitions dissipating no energy. They both peak at the gap voltage, showing that the response functions $j_1(t)$ and $j_2(t)$ oscillate at the gap frequency $2\Delta/h$. $-$Re $\tilde{j}_2$ can be regarded as the amplitude of the Josephson current. Its peak was first emphasized by Riedel (1964) and we see that it occurs when the Josephson frequency is $4\Delta/h$ (*twice* the gap frequency) and then falls relatively slowly with frequency. We can therefore expect to see Josephson effects at frequencies well beyond the gap frequency (see §11.2). Re $\tilde{j}_1$ has no physical effect at all when the applied voltage is constant (and therefore does not appear in Josephson's original formula). It contains an arbitrary constant, since the addition to $j_1(t)$ of a δ function at $t=t'$ has no effect on the current.

(iii) When we are dealing with frequencies comparable to or greater than the gap frequency, or voltages greater than the gap voltage, the simple RSJ model of a weak link must break down.

For input derived from a *voltage* source, the calculation of the excited I–V curve from Werthamer's formulation is relatively straightforward and has been performed by Hamilton (1972) (see §8.3). When we have the more usual *current* source the calculation is much more difficult but McDonald *et al* (1976) have recently computed the unexcited I–V curves for a range of shunt capacitances. Some of their curves are compared with that for the RSJ model in figure 14(*c*). We notice that there is not only a

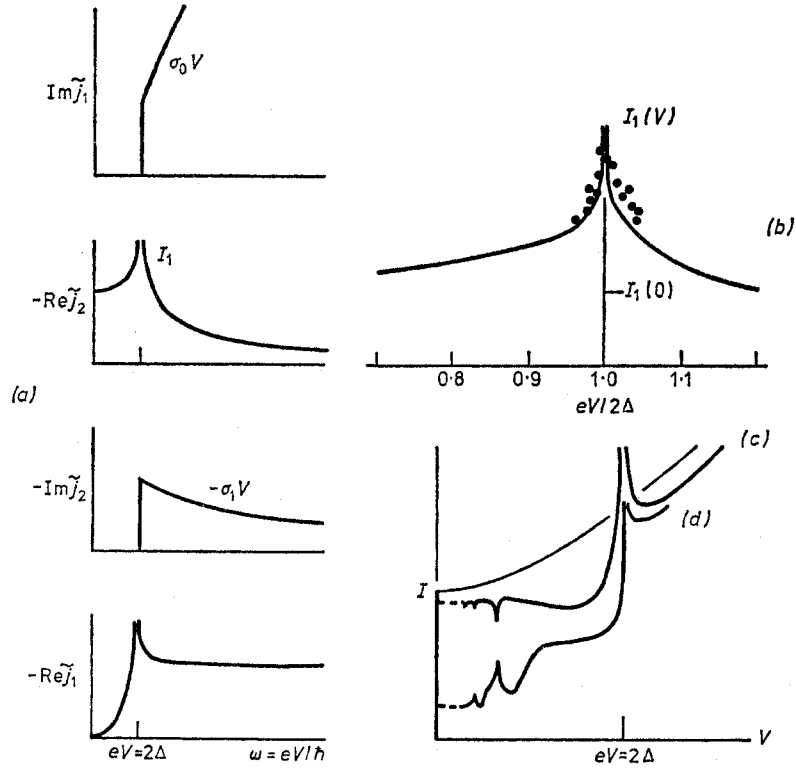

Figure 14. High-frequency effects at $T=0$. (*a*) Werthamer's response functions as a function of frequency or voltage; the first three plots represent the normal current and the amplitudes of Josephson's sin ϕ and cos ϕ term, the latter inverted (§8.1). (*b*) Representative measurements of $I_1(V)$ compared with theory (Hamilton 1972; §8.3). (*c*) I–V characteristics for ideal current-fed junction calculated by McDonald *et al* (1976). (*d*) Same as for (*c*), with allowance for effect of surface impedance (§8.1).

strong peak at the voltage associated with the Riedel peak but also structure at the odd submultiple voltages, produced by harmonic generation in the current-fed junction. Allowance by McDonald *et al* for the skin effect in the junction produced further, more rounded structure at the even submultiple voltages (figure 14(*d*)). These conclusions were anticipated by Werthamer and are most interesting, since they provide a possible explanation of the 'subharmonic structure' in tunnel junctions, first observed by Taylor and Burstein (1963). The structure was originally interpreted as due to multiparticle tunnelling, but Giaever and Zeller (1971), by using a light-sensitive tunnel junction in which the tunnel probability can be varied and also by varying other parameters, have shown convincingly that Werthamer's explanation is a better one.

Almost identical structure has recently been observed in microbridges (Gregers-Hansen *et al* 1973). McDonald *et al* find that increasing the shunt capacity removes the Riedel peak from the *I–V* characteristic which, as one would expect, rapidly becomes similar to that obtained by using the voltage-source model. No systematic calculations of *excited* characteristics under current-source conditions have been published yet, though a number of *ad hoc* modifications of analogue computations designed to make partial allowance for high-frequency effects have been reported.

8.2. Evidence for the existence and sign of the cos ϕ term

The term $\cos\phi \operatorname{Im} \tilde{j}_2(\omega)$ in the expression for the current (8.2) corresponds to real transitions, but nevertheless contains an interference factor; Josephson has referred to it as the *quasiparticle interference term.* Unlike the supercurrent term, it is associated with loss in the system and the first experimental evidence for its existence was obtained from measurements of the bandwidth of the plasma resonance in tunnel junctions by Pedersen *et al* (1972). We have already discussed the plasma resonance and its observation by the same group in §7.7. Pedersen *et al* extended this work by examining the bandwidth of the resonance as a function of the DC current bias within the zero-order step, i.e. they studied the losses as a function of the mean value of ϕ. They concluded that the variation in loss with ϕ followed Josephson's prediction within their limits of error, but only if the *sign* of the $\cos\phi$ term was reversed†. They found, in fact, that $\gamma = \sigma_1/\sigma_0 = -0{\cdot}9 \pm 0{\cdot}2$, while the microscopic theory gives $\gamma = +0{\cdot}93$ under corresponding conditions. They regarded their conclusion as partly provisional, because (i) the accuracy was not very high, (ii) an unexpected loss due to coupling to a geometrical resonance had to be subtracted out on an *ad hoc* basis, and (iii) the contribution of other forms of loss to the bandwidth was not fully established. Nevertheless, it is difficult to think of any plausible explanation of their results other than a variation in the quasiparticle current with phase having the opposite sign to that predicted by Josephson.

The effect of the $\cos\phi$ term on both unexcited and excited *I–V* characteristics was calculated (using a value of σ_1 which was independent of voltage) by Auracher *et al* (1973) who concluded that the effects would be fairly small and would in practice be difficult to distinguish from the effects of shunt capacitance. However, Falco *et al* (1973) repeated the calculation with a Johnson noise source included and found that the noise-rounding of the zero-voltage step is strongly dependent on the value of γ. On fitting this calculation to their data on the noise-rounding of steps in Notarys–Mercereau bridges they obtained the value $\gamma = -0{\cdot}8 \pm 0{\cdot}2$. This conclusion is also difficult to interpret (i) because, although it is interesting to find evidence for the presence of a $\cos\phi$ term in bridges, the theory of the normal current in bridges is essentially different from that for normal current in tunnel junctions and almost any theory is likely to lead to a variation in the quasiparticle current with ϕ which is an even periodic function, and (ii) because the calculation made by Falco *et al* included no noise source corresponding to the $\cos\phi$ term itself although, since the term is dissipative, such a source must surely be present.

Evidence for the $\cos\phi$ term in point contacts has been found by Vincent and Deaver (1974) who, by using an RF SQUID configuration of suitably low inductance, were able to bias the contact at phases between $\frac{1}{2}\pi$ and π, which are unstable for a free

† The note added in proof at the end of their paper, in which they state that the sign does after all agree with theory, was later withdrawn (Langenberg 1974).

weak link. By coupling the system to a suitable resonant tank circuit and observing the frequency and bandwidth of the resonance for small excitation as a function of DC flux applied they were able to determine the shunt conductance of the point contact as a function of ϕ for all ϕ. They obtained a good fit with theory on assuming a conductance of the form $\sigma_0(1+\gamma\ \cos\phi)$ with γ close to -1. They have a simple model for the conductance of a point contact which indeed predicts $\gamma=-0{\cdot}90$ for point contacts under their conditions but, again, we must note that their results are not necessarily related to the question of the sign of the cos ϕ term in tunnel junctions. Similar results have been reported for microbridges by Nisenoff and Wolf (1975).

On the theoretical side there has been some purely formal confusion about the sign of the cos ϕ term, but in a recent review Langenberg (1974) has concluded that there *is* a theoretical consensus that γ should be *positive* for small voltages. This is in conflict with an unpublished argument of Tinkham, based on the Krönig–Kramers dispersion relations, which appears to show that the sign must be negative. However, Josephson has himself criticized this argument. It will be interesting to see what new conclusions appear on this subject.

The experimental conclusions for tunnel junctions are not yet fully convincing. If the theory is proved wrong (for other than trivial reasons) it will be the first point at which any serious flaw has appeared in the edifice erected on Josephson's foundations. It is now a matter of some importance to make further experimental checks on the sign of the cos ϕ term, for instance by looking at voltages greater than $2\Delta/e$ (where the theory predicts that σ_1 becomes large and negative) or by applying the methods of Falco *et al* (1973) and of Vincent and Deaver (1974) to tunnel junctions.

8.3. Observations of the Riedel peak

The peak in the supercurrent amplitude Re $\tilde{j}_2$ when the Josephson frequency is twice the gap frequency, first noted by Riedel (1964), has been satisfactorily checked by Hamilton (1972), who made a careful series of measurements of excited I–V characteristics in *voltage*-biased tunnel junctions. On account of the voltage bias, spikes rather than steps appear at the Josephson frequencies and special techniques have to be adopted to eliminate hysteresis in the measurement of step height as a function of RF input. But the voltage bias also means that it is easy to determine the relation between height and $\tilde{j}_2(\omega)$ using Werthamer's formulation and Hamilton found that, as the frequency is varied, there should be an oscillation of the relative heights of the even and odd high-order spikes as individual spikes pass the Riedel peak, superimposed on the usual oscillation of height with RF power. By measuring this oscillation Hamilton was able to reconstruct the shape of the Riedel peak. A magnified portion of his results close to the peak region is compared with theory in figure 14(*b*) and we see that the theoretical singularity is broadened by about 2% in frequency, which is not unreasonable when considering the probable anisotropy of Δ and lifetime effects in the tin films which Hamilton used.

Hamilton was not able to draw firm conclusions about the behaviour of Re $\tilde{j}_2$ at frequencies much higher than the Riedel peak. The experiments of McDonald *et al* (1972) and of Blaney (1974) on mixing laser radiation in the THz region using niobium point contacts do not allow precise conclusions to be drawn, but show that in these devices Re $\tilde{j}_2$ does not fall very rapidly with frequency, in agreement with the theory for tunnel junctions.

8.4. Quantum noise in tunnel junctions

The size of the voltage fluctuations across a Josephson device is important in several applications, particularly in microwave mixing (§11.2) and in the broadening of the Josephson radiation or the radiation-induced steps used in measuring the e/h ratio (§11.1). We have already discussed in §7.9 the effects of a given level of noise on the steps, but there we assumed that the noise source was simply the classical Johnson noise of the shunt resistor in the model junction. The advent of accurate measurements of e/h encouraged theoreticians to examine in much more detail the behaviour of Josephson devices as noise sources. The first step was the calculation by Scalapino and others (see Dahm *et al* 1969) of the noise due to quasiparticle currents in a tunnel junction. They assumed that the currents were described by the first-order terms in the tunnel Hamiltonian and calculated the quasiparticle current fluctuations in a junction biased at constant voltage V. The result for the fluctuation at frequency ν is

$$\overline{I_{\mathrm{NN}}^2(\nu)}\,\mathrm{d}\nu = \left(I_{\mathrm{N}}(V+h\nu/e)\coth\frac{eV+h\nu}{2kT}+I_{\mathrm{N}}(V-h\nu/e)\coth\frac{eV-h\nu}{2kT}\right)e\,\mathrm{d}\nu \tag{8.3}$$

where $I_{\mathrm{N}}(V)$ is the DC quasiparticle tunnel current which flows at voltage V. The form of this result is easy to understand if we remember that at fixed voltage the current fluctuations at frequency ν are due to *virtual* transitions which involve the same excitations as do the *real* transitions occurring in DC current flow at the voltages $V\pm h\nu/e$. But we have to remember that while real DC current is the *difference* between the forward and backward transition rates (with a factor f_1-f_2 in the occupation numbers) both forward and backward virtual transitions contribute positively to the noise power (with a factor $f_1(1-f_2)+f_2(1-f_1)$). The ratio between these factors accounts for the terms in coth $(eV\pm h\nu)/2kT$ in (8.3). Several limits of (8.3) are worth noting.

(i) *High temperatures.* If we define an *effective* resistance $R_{\mathrm{eff}}=V/I_{\mathrm{N}}(V)$ then in the high-temperature limit we have $\overline{I_{\mathrm{NN}}^2(\nu)}=4kT/R_{\mathrm{eff}}$ the usual *Johnson noise* formula.

(ii) *High current.* If eV is much larger than both $h\nu$ and kT, we find $\overline{I_{\mathrm{NN}}^2(\nu)}=2eI_0$, the usual expression for *shot noise.*

(iii) *Low temperature, zero bias.* In this limit we have $\overline{I_{\mathrm{NN}}^2(\nu)}=4h\nu(\bar{n}+\frac{1}{2})/R_{\mathrm{eff}}$, where $\bar{n}=[\exp(h\nu/kT)-1]^{-1}$, the usual expression for *quantum-limited Johnson noise.*

In a real circuit (where the source will not have zero impedance) the voltages across the junction can be calculated by treating the noise currents just described as sources in parallel with the junction. The noise generated by the source must also be included: if the source is at room temperature its noise may well be larger than the junction noise.

A more surprising contribution was pointed out by Stephen (1968), who noted that although under *voltage* bias conditions the supercurrent is dissipation-free and therefore noise-free, under other conditions a DC supercurrent can exist at finite voltage (see figure 10), and since this supercurrent is dissipative, there must be an associated noise term. The reason for the dissipation is that under, for instance, current bias conditions there is a large AC voltage applied to the junction at the Josephson frequency and this means that pairs can make real transitions across the barrier with the stimulated emission of photons. To model this dissipation Stephen regarded the junction formally as being coupled to a cavity in which the photons were created—in the real case the 'cavity current' just means the AC currents flowing in the junction and the external circuit at the Josephson frequency. In the low-frequency

limit he found an extra contribution to the current noise source given by

$$\overline{I_{SN}^2(\nu)}\,d\nu = 2e^* I_S \coth(e^* V/2kT_0)\,d\nu \tag{8.4}$$

where in this case the term in $\coth(e^*V/2kT_0)$ comes from the photon occupation number for the model cavity and T_0 is its effective temperature, I_S is the DC part of the supercurrent and e^* is the pair charge, $2e$. In practice this term is only important at relatively large voltages, when it reduces to a *supercurrent shot noise*, $2e^*I_S\,d\nu$.

These predictions were checked by Kanter and Vernon (1970a) for noise at 150 kHz using niobium point contacts and measuring the fluctuations directly. They found reasonable agreement with theory and in particular were able to see the supercurrent shot noise, which could be suppressed by applying a magnetic field. The corresponding voltage fluctuations when the source has finite impedance lead by a simple calculation to phase fluctuations and hence frequency spreading of the Josephson emission linewidth. Dahm *et al* (1969) and Silver *et al* (1967) have measured such linewidths in tunnel junctions and point contacts and found good agreement with theory (the bandwidth near T_c is of the order of $\pi^{-1}(2e/\hbar)^2 kTR_{dyn}$ which is typically 10^7 Hz, but may fall to 10^5 Hz on self-induced steps having small values of R_{dyn}). Measurement of such linewidths has, in fact, been suggested as the basis of a noise thermometer working down to very low temperatures (Kamper and Zimmerman 1971). Rather little work has been done so far on noise at the very high frequencies where Josephson mixers are likely to be most useful.

The tunnel theory just discussed treats the motion of individual quasiparticles or the transitions involving individual pairs as independent and this means that the predictions may not apply very well to other types of device such as microbridges or SNS junctions in which correlated motions would probably smooth out shot noise in particular.

9. Other weak links

We showed in §2.3 that any pair of weakly coupled superconductors whose state varies periodically with the phase difference between them is expected to show Josephson effects. This obviously includes a wide range of devices other than tunnel junctions and in this section we shall discuss the physics of their operation.

9.1. Josephson's generalized calculation

Although his original letter was only concerned with tunnel junctions, Josephson gave in his Doctoral Thesis (see Josephson 1965) a generalized calculation applicable to any weak link structure, written in the language of thermal Green's functions which had recently been applied to superconductors by Gor'kov and others†. His result showed that the supercurrent flowing between two regions can be written quite generally as

$$I = 2ie\hat{T} \int\int [n(\boldsymbol{r}') - n(\boldsymbol{r})] \sum_{\omega} G_{-\omega}(\boldsymbol{r}', \boldsymbol{r}) \tilde{G}_{\omega}(\boldsymbol{r}', \boldsymbol{r}) \Delta(\boldsymbol{r}) \Delta^*(\boldsymbol{r}')\, d^3r\, d^3r' \tag{9.1}$$

† This calculation was not published at the time; the first published account of the method was given independently by de Gennes (1963). The technique is expounded in the book by Abrikosov *et al* (1963).

where $\hat{T}$ is the time-ordering operator, G and $\tilde{G}$ are the thermal Green's functions which describe electron propagation from r to r' in the superconducting and normal states respectively, and the function $n(r)$ specifies the regions between which the current is to be calculated: $n(r)$ is equal to 1 in the first region and 0 in the second region. The physical content of this result is that the supercurrent between the regions depends on the ordinary propagation characteristics for electrons between the regions and on the amplitudes and phases of the order parameter within the regions, but that there is no requirement that the order parameter should be finite within the weak link itself.

As Josephson pointed out, this result leads at once to a generalization of the weak link concept. If we can treat Δ as constant over the important region of integration on each side of the barrier, then (9.1) reduces to the form

$$\begin{aligned} I &= iK(\Delta_1\Delta_2^* - \Delta_2\Delta_1^*) \\ &= 2K|\Delta_1||\Delta_2| \sin\phi \\ &= I_1 \sin\phi \end{aligned} \tag{9.2}$$

where K, and hence I_1, involves an integral over Green's functions which span the boundary. Evidently we can always obtain Josephson's relation if we can treat Δ as constant on the two sides, or even simply as having constant phase. This will be so provided (i) that the barrier current is small, so that the supercurrent in the bulk superconductors is small enough to allow us to treat the phase of Δ as a constant within them, and (ii) that the integral from the barrier region itself (where Δ must be changing phase) is negligible. This formalism allows us to predict at once that several familiar structures should behave as weak links. For tunnel junctions the barrier is so thin compared to the region of integration (which extends a coherence length into the superconductors) that the barrier integral is negligible; the same applies to sufficiently small bridges and point contacts. Josephson noted that the result will apply for SNS junctions if Δ is small in the N region and that supercurrents should be able to cross a substantial thickness of normal metal corresponding to the range of the Green's functions. He also anticipated that magnetic impurities (which upset the phase cancellation between $G_{-\omega}$ and $\tilde{G}_{\omega}$) would have a strong destructive effect on the supercurrents.

Josephson's generalized formalism has been extensively exploited by theoreticians as a starting point for the calculation of junction supercurrents from first principles.

9.2. The microbridge

Careful investigation of the I–V curves of small bridges of superconductor was begun by Parks and Mochel (1964), who were looking for evidence of the quantized current vortices in thin films predicted by Tinkham (1963). They expected that when they varied the applied magnetic field, vortices would enter the bridge region one by one. They interpreted the resistance as being due to an intermediate state containing islands of superconductor in a sea of normal metal and they expected that the appearance of this state as the temperature was raised would be affected by the number of quantized vortices present, and indeed they found a periodic variation of resistance with field which appeared to confirm their idea. But Anderson then pointed out that this idea could be simplified and connected with the Josephson effect by a slight modification: it was not necessary to invoke an intermediate state to explain the finite

resistance, for the bridge could be simultaneously superconducting and resistive. This would occur if quantized vortices (which each contain one quantum of flux, $\Phi_0 = h/2e$) were *moving* across the bridge (normal to the current flow) at a rate of $V/\Phi_0 = 2eV/h$ vortices per second. This flow would simultaneously induce the voltage along the bridge and 'unwind' the phase difference along the bridge as rapidly as it was generated by the voltage (because the line integral of phase around a vortex is 2π: see §2.4). In this picture, the modulation of resistance with field would be due to the quantum interference of the supercurrents at different points across the width of the bridge (as in Rowell's experiment on tunnel junctions). Moreover, the frequency $2eV/h$ at which vortices cross the bridge is just equal to the Josephson frequency. Anderson expected that if this flow of vortices existed, it might be possible to phase-lock it to an applied microwave field; if this occurred, AC Josephson effects would be visible. He encouraged Dayem to look for such an AC effect and the results were very gratifying. The argument and the first observations were published soon after the first observations of the Josephson effect (Anderson and Dayem 1964).

Experimental work has now established the following points.

(i) Only small bridges less than 1 μm in width and length show AC effects like those in current-driven tunnel junctions. Longer bridges show weaker, less predictable AC effects (Dayem and Wiegand 1967).

(ii) Unlike tunnel junctions, fairly small bridges show steps at *subharmonic* voltages $V = n\hbar\omega/2em$ (Dayem and Wiegand 1967).

(iii) Under some conditions microwaves can *increase* the size of the zero-voltage step in microbridges (the Wyatt–Dayem effect which we consider in §9.3).

(iv) In very small bridges near T_c, the simple RSJ model applies accurately to microbridges (the requirement appears to be that the bridge should be small compared to the Ginzburg–Landau coherence length) (Gregers-Hansen and Levinsen 1971, figure 11(*b*)).

(v) At temperatures of more than a few tenths of a degree below T_c most bridges show more complicated AC effects and hysteresis appears in the I–V characteristic. This has been shown to be connected with the appearance of localized hot spots kept normal by Joule healing (Skocpol *et al* 1974).

(vi) Steps in the unexcited I–V curves for long, narrow microbridges (up to 150 μm long and about 1 μm wide) have been shown to be due to discrete localized phase-slip centres, each having essentially the same I–V curve and a resistance which corresponds to a length of about 10 μm of the bridge (considerably greater than the coherence length) which is independent of temperature but varies with resistivity. The AC effect in such bridges is the sum of the AC effects at the individual phase-slip centres (Skocpol *et al* 1974).

The theoretical situation is complicated by the existence of *three* apparently different theories of the behaviour of microbridges. These theories are, however, more closely linked than appears at first sight and they are all written in terms of Ginzburg–Landau theory, which describes the behaviour of the order parameter Ψ in situations in which it varies in space and time. First we have Anderson's picture, which we discussed above. According to Anderson any system through which vortices can pass is likely to show the Josephson AC effects, and if the vortex passes easily and does so every time the phase across the bridge increases by 2π, then we have a non-hysteretic system whose free energy is periodic in phase difference and therefore a Josephson device in the sense discussed in §2.3. It was soon realized, however, that Josephson effects were visible in bridges much too narrow to contain a complete vortex, so narrow in fact that they could be treated as *one-dimensional*; and the remaining two theories both adopt

a one-dimensional picture. We must first recognize that this is not intrinsically different from Anderson's picture—all that has happened is that the process in which a vortex crosses the bridge now appears as a process in which Ψ is reduced to zero at some point on the length of the bridge.

The first of the two theories was put forward by Baratoff *et al* (1970). It was based on ordinary time-independent Ginzburg–Landau theory (which is appropriate for calculating equilibrium current-carrying states in superconductors) and showed that under certain conditions a microbridge of superconductor would be expected to show a sinusoidal current-phase relation *when in thermal equilibrium.* This theory has been developed by Gregers-Hansen *et al* (1972) and shows that in sufficiently short bridges not only is the current proportional to $\sin\phi$ but also that near T_c the magnitude of the supercurrent is given by the *same* function of the gap parameter and the normal bridge resistance as in Josephson's theory for tunnel junctions. Both predictions agree with experiment.

The other theory, suggested by Notarys and Mercereau (1971), is apparently different. It suggests that the 'unwinding' of the flux when there is a finite voltage across a microbridge occurs when the voltage drives the ordinary supercurrent beyond the ordinary critical current; the supercurrent then collapses, superconducting order is destroyed, re-forms, and the process begins again. According to Notarys and Mercereau it is this essentially *non-equilibrium relaxation oscillation* which is associated with the Josephson frequency. The idea was taken up by Skocpol *et al* (1974) who developed a fairly complete description of the process of collapse and used it successfully to explain the resistance of the phase-slip centres which they had found in long microbridges. We can see that the two theories are more closely related than appears at first sight as follows. In situations where the order parameter varies from place to place, it obeys the first Ginzburg–Landau equation, which we shall write as

$$\xi_0^2 \frac{\partial^2\Psi}{\partial x^2} + f(|\Psi|)\Psi = \tau\left(\frac{\partial}{\partial t} + \frac{2i\mu}{\hbar}\right)\Psi \tag{9.3}$$

(see, for instance, Werthamer 1969). We have omitted the terms which depend on the magnetic field (which are not important in very narrow bridges) and we have included time-dependent terms on the right about which there is some controversy: it is not clear how far these terms are valid for ordinary superconductors having a finite energy gap. For our present purposes we can regard this equation as containing a plausible description of how Ψ changes with time, even if the details are open to question. Note that the case of thermal equilibrium (when μ is independent of position) corresponds to the solution in which (9.3) is separable in space and time and the two sides of (9.3) are both zero. The right-hand side then gives simply the Josephson relation $\hbar\dot{\theta} = -2\mu$. The left-hand side gives the equilibrium solution in space. The quantity f is sketched as a function of $|\Psi|$ and T in figure 15(*a*). Clearly, we have states of zero current in which Ψ is constant and $|\Psi|$ takes the value which makes f zero. We also have equilibrium current-carrying states where Ψ has the form $A\,e^{iqx}$ and $|\Psi|$ is smaller. The maximum current density occurs for some finite value of A, and increasing q beyond this point reduces A so rapidly that the current density falls: this is the critical current density referred to by Notarys and Mercereau. To describe what happens when the critical current is exceeded, we must solve (9.3) with the equation describing what happens to μ:

$$\begin{aligned}\partial J/\partial x &= \partial/\partial x(J_S + J_N)\\ &= (\hbar e/m)\partial/\partial x(|\Psi|^2\,\partial\theta/\partial x) + (\sigma/e)\,\partial^2\mu/\partial x^2 = 0.\end{aligned} \tag{9.4}$$

The solution of these equations is not immediately apparent, but we may gain some insight by noting that the problem has a mechanical analogue. If we have a light elastic string of uniform tension extended in the x direction whose displacement from the x axis in polar coordinates is expressed by the complex number Ψ, then (9.3) can be interpreted as an equation giving the balance of forces acting on the element of string as follows: (i) the term in $\partial^2\Psi/\partial x^2$ corresponds to the forces due to the tension in the

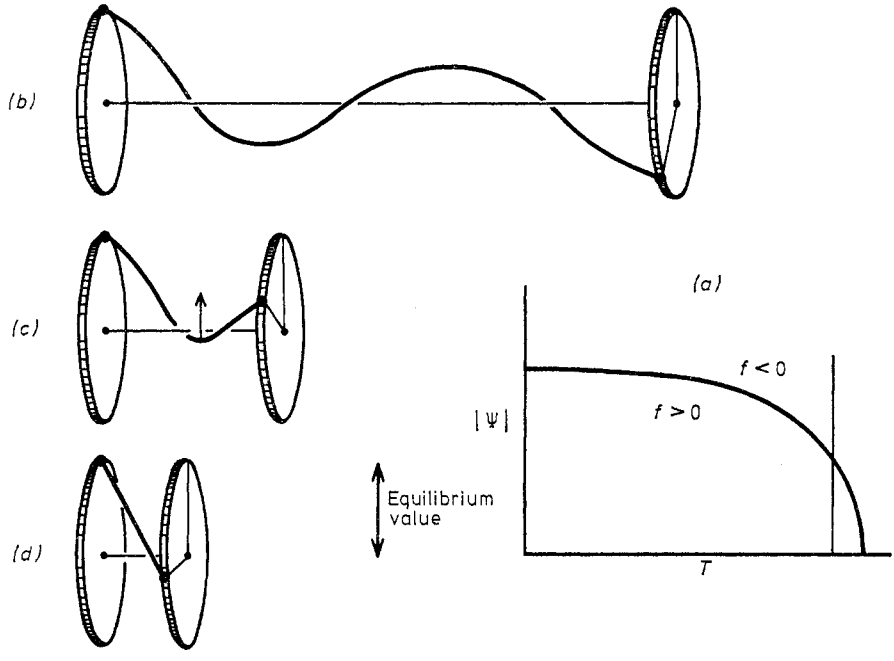

Figure 15. Ginzburg–Landau theory for microbridges. (*a*) $f(\Psi, T)$. (*b*) Mechanical analogue for long junction. (*c*) Phase slip occurs in a shorter junction. (*d*) Reversible situation in a very short junction.

string, (ii) the term in $f\Psi$ corresponds to a radial force proportional to $f(|\Psi|)$ which repels the string from the x axis at short distances but attracts it at large distances, and (iii) the right-hand term corresponds to a viscous drag force acting between the string and a medium rotating around the x axis at an angular velocity proportional to μ. If we imagine that this medium is driven to rotate only by the string and by the viscous drag between its layers then equation (9.4) just expresses the fact that the total torque acting on the medium due to the drag of the string (supercurrent term) and the viscous drag in the neighbouring medium (normal term) must be zero.

This allows us a good deal of insight into the solutions. In a *long* thin bridge a small supercurrent corresponds to a stationary, gently spiralling string (figure 15(*b*)). A larger current corresponds to a tighter spiral nearer to the axis. As the twist of the spiral is increased, a point is reached at which the repulsion from the axis cannot resist the tension in the string. In principle this instability occurs everywhere simultaneously, but in practice there will be a weak spot. At this spot the string will slip through the x axis, its motion damped by the viscous medium, which will itself rotate in the neighbourhood of the weak spot (figure 15(*c*)). This process corresponds to the phase-slip centre discussed by Skocpol *et al* (1974). In a *short* junction, on the other hand, the

boundary conditions mean that the string must be at a large distance from the x axis at each end ($|\Psi|$ fixed). If the junction is short compared to the coherence length ξ_0 then (9.3) shows that on the scale of the length of the junction the curvature of the string is negligible (figure 15(*d*)) and in this case the torque due to the string (supercurrent) will vary like $\sin\phi$. This corresponds to the solution considered by Baratoff *et al* (1970) which only applies to short microbridges.

9.3. The Wyatt–Dayem effect in microbridges

This effect in microbridges was first reported by Wyatt and co-workers (Wyatt *et al* 1966); the same anomaly was also seen by Dayem at about the same time (Dayem and Wiegand 1967). The effect, which was thought very peculiar when first observed and is still not completely accounted for, is an *increase* in the critical current with microwave power (figure 16(*a*)). This is contrary to the predictions of the RSJ model shown in figure 11(*b*) and it can be quite dramatic, especially near the critical temperature. Several workers have repeated and extended the original observations (see, for instance, Gregers-Hansen and Levinsen 1971). The details of the effect are complex, but can be crudely summarized as follows.

(i) The effect of the microwaves on the critical currents is like that of an increase in the critical temperature by a few mK, and indeed microwaves can *induce* a critical current just above the usual critical temperature.

(ii) The effect is only apparent above 1 GHz, typically, and becomes rapidly stronger at higher frequencies.

(iii) The effect appears to saturate as a function of RF power, as though the microwaves could only raise T_c by a definite total amount (see the plot of step height with RF power in figure 11(*b*) where the effect is visible).

Two recent discoveries provide useful evidence about the nature of the effect. As we have already mentioned (§8.1) Gregers-Hansen *et al* (1973) have found 'subharmonic gap structure' in the I–V curves of microbridges. When the data were

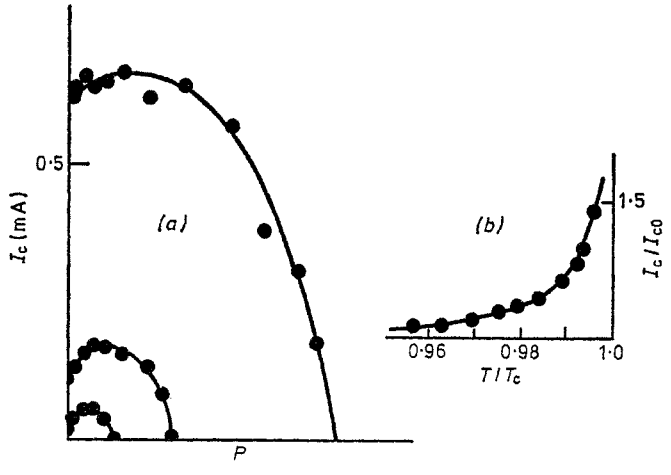

Figure 16. The Wyatt–Dayem effect. (*a*) Variation of critical current with microwave power for small tin bridge at 9·6 GHz at three different temperatures (Wyatt *et al* 1966). (*b*) Increase of critical current produced by phonon excitation in an aluminium bridge as a function of reduced temperature fitted to a modified Eliashberg theory (Tredwell and Jacobsen 1975).

examined in detail, they found that the gap parameter in the bridge region was not constant but *increased* with the Josephson frequency in much the same way as the critical current increases with microwave frequency in the Wyatt–Dayem effect. They suggested that the AC Josephson currents were having the same effect as the externally applied microwaves. More recently Tredwell and Jacobsen (1975) have shown that the critical current of microbridges can be enhanced even more strongly by high-frequency phonons than by microwaves. In the presence of a strong phonon signal a microwave signal produces no further enhancement and the RSJ model works well.

A number of explanations have been proposed. Hunt and Mercereau (1967), having discovered that the transition temperature of small superconducting bridges was depressed by an amount proportional to $V^{-1/2}$ where V is the volume of the bridge, successfully explained this effect as being due to the extra entropy in the system when, in the normal state, the relative phase of the two sides is free to fluctuate; this lowers the normal state free energy and so decreases the transition temperature. They went on to suggest that the Wyatt–Dayem effect might be explained if the microwave field had the effect of restoring the original transition temperature by inhibiting all fluctuations of the relative phase. It is, however, not clear how the microwave field could constrain the relative phase when the bridge is normal, nor does this approach explain the results of the phonon experiment. A very recent paper by Lindelof (1976) suggests that the microwave field drives the excitations away from the centre of the bridge and hence allows the order parameter to increase in magnitude. This is indeed a possible explanation, though the details of his argument may need modification. A rather different explanation was put forward earlier by Eliashberg (1970) who suggested that the effect of the microwaves is to increase the energy spread rather than the spatial spread of the excitations. So long as the microwaves do not increase the number of excitations this has the effect of increasing the order parameter (by increasing the availability for pairing of the dominant states near the gap edge). Eliashberg's theory explains neatly why the enhancement of critical current increases with frequency as it does. Moreover, it is clear that high-frequency phonons should produce a similar effect and so it is satisfying to note that Tredwell and Jacobsen (1975) report quantitative agreement between their observations and a suitably modified Eliashberg theory (figure 16(*b*)). Although no similar fit has been reported for the microwave effect, it is clear that the Eliashberg theory will at least provide a major component of the final explanation. It is also clear that analysis of the Wyatt–Dayem anomaly is unlikely to lead to any fundamental revision of our picture of the Josephson effects.

9.4. SNS junctions and related devices

By an ordinary SNS junction we mean a layer of a non-superconducting metal such as copper sandwiched between two superconductors. Josephson's generalized calculation can be applied to such a system as we have already noted (§9.1). We can see that measurable supercurrents will cross 0·1 μm or more of copper and that the Josephson relation will be obeyed. However, to calculate the behaviour of the normal currents and supercurrents in detail we need to know the Green's functions to be inserted into (9.1) and to calculate them we need in turn to know how the order parameter behaves within the sandwich. This involves us in the theory of the *proximity effect*, the spreading of superfluid properties into normal metals. The Ginzburg–Landau theory which helped us in understanding microbridges is not adequate in this regime and we must turn to the non-local form of the microscopic theory developed by Gor'kov and

applied to this problem by de Gennes and others (see de Gennes 1966). This theory is a substantial one and we shall only refer briefly to a few of its features.

(i) The spatial variation of the order parameter is the solution of Gor'kov's equation

$$\Delta(\boldsymbol{r}) = \int K(\boldsymbol{r}, \boldsymbol{r}')\Delta(\boldsymbol{r}')\, \mathrm{d}^3 r' \tag{9.5}$$

which replaces the BCS self-consistent equation (3.6). The kernel K, like the term $V/2E_K$ in (3.6), is proportional to the interaction parameter V and also depends on the nature of the one-particle excitations in the neighbourhood of $\boldsymbol{r}, \boldsymbol{r}'$, which in turn depends on Δ: the equation has to be solved self-consistently. When Δ is small (as it is near the critical temperature of the sandwich) K is independent of Δ and the solutions are relatively easy to obtain (de Gennes 1964). For a discussion of how to find solutions in the general case see Hook and Waldram (1973).

(ii) In a metal such as copper where the interaction parameter is small the critical current falls off exponentially with thickness, the decay length being of the order of $(\hbar v_F l/kT)^{1/2}$ in impure materials (typically 10^{-8} m or more). But if the 'normal' metal is in fact a superconductor only just above its transition temperature, the decay length can be much greater.

(iii) The small value of V in a metal such as copper means that the excitations in it are more or less normal. The SNS junction therefore carries large normal currents at voltages below the gap voltage which do not fall exponentially with the junction thickness. Thus in an SNS junction Josephson's relation $eI_1R = \frac{1}{2}\pi\Delta$ connecting the critical current and the resistance does not apply.

The physics of SNS junctions has been examined by Clarke (1969) who has found good agreement with the microscopic theory. The theory predicts, and experiment confirms, that of all Josephson devices the SNS junction is the closest to the simple RSJ model; we have already discussed some of the data in §§6.5 and 7.12 (figures 8 and 13).

The SNS sandwich is unlikely to be useful as a device for two reasons: its resistance is typically 10^{-6} Ω, which makes matching it to conventional circuits almost impossible, and its I_1R product is typically only 10^{-8} V, corresponding to frequencies in the MHz region. There is, however, a related device which does not suffer so severely from these limitations, known as the Notarys bridge (Notarys and Mercereau 1971). This device contains a bridge region overlayed by a layer of normal metal, which depresses the transition temperature through the proximity effect. Harris has recently achieved similar results by implanting magnetic ions and gives a clear discussion of the physics involved (Harris 1975). At low temperatures such devices behave like ordinary microbridges, but when the bridge region is above its bulk transition temperature (the rest of the sample being still superconducting) they behave like SNS junctions with a large decay length so that the bridge region may be several μm long. It can also be up to 10 μm wide, so that it is much less likely to burn out accidentally than an ordinary microbridge. Depending on its dimensions the resistance can approach 1 Ω, but the I_1R product is generally still poorer than it is for tunnel junctions and short microbridges.

9.5. Modified tunnel junctions

Two particular modifications of the tunnel junction seem likely to become technically important.

9.5.1. Semiconductor tunnel junctions. The main difference between a semiconducting sandwich at low temperatures and an SIS junction is that, since the band gap is smaller,

the tunnel decay length is greater and for a given current density the barrier can be much thicker. Huang and van Duzer (1975) have made junctions with critical currents of 30 mA using silicon barriers more than 0·1 μm thick. These devices are potentially very important on account of three features: they should be more reproducible and reliable than tunnel junctions, their capacitance is smaller for a given critical current, and their I_1R product can be close to the theoretical limit.

9.5.2. Granular microbridges. The granular microbridge reported by Deutscher and Rosenbaum (1975) is made of small superconducting granules in an insulating matrix. Supercurrent passes by Josephson tunnelling between the granules, making the matrix behave like a bulk superconductor of high resistivity and low critical current density. This means that the bridge dimensions can be made of the order of 10 μm without reaching the long-bridge regime, even at low temperatures. This device appears to be reliable and reproducible and has very small capacitance combined with useful resistance and critical current. Though little work on it has yet been published, it appears very promising and has already been used in a working RF SQUID.

9.6. Point contacts

Point contacts are made by lightly pressing a sharp superconducting point onto a flat superconducting plane; the material used is almost always niobium. In spite of their extensive use in both SQUID and microwave applications, little certain is known about their mode of operation, though the device is presumably a cross between a very small, thin tunnel junction and a microbridge. The fact that small contacts under light pressure usually show some structure at the gap voltage (especially those which are most effective as mixers in the submillimetre waveband) suggests that tunnelling is involved, but since the form of the I–V characteristic can be drastically modified by varying the mechanical history of the contact, it is clearly dangerous to generalize. Point contacts were extensively developed by Zimmerman and others for use in SQUIDS (see Silver and Zimmerman 1967) and by Grimes and later workers for microwave applications (see Grimes and Shapiro 1968). The following features of point contacts make them useful.

(i) They can be adjusted *in situ* to obtain the required critical current etc, and although rather fragile, can now be made very reliable by encapsulation after adjustment.

(ii) They are very easy to make (except for ultra-high-frequency applications, when only very sharp tips seem to work).

(iii) They have excellent I_1R products, negligible capacitance, and can be made with resistances up to 50 Ω, which makes matching relatively easy.

(iv) They are so far the only devices to have shown Josephson effects at frequencies well beyond the gap frequency.

9.7. Current–phase measurements

The question of how accurately Josephson's relation $I_S = I_1 \sin \phi$ is obeyed in any particular weak link is not altogether easy to answer. The agreement of quantum interference patterns with prediction is confused by the effects of self-fields and non-uniformity in junctions, and time-dependent effects are confused by uncertainty about the behaviour of the normal currents. If the periodic function is markedly non-sinusoidal, steps or spikes should appear at *submultiples* of the Josephson voltage in the

inverse AC effect. Such steps are indeed seen in *large* junctions of most types, but this again can be understood as being due to self-field effects. *Small* tunnel junctions, SNS junctions and microbridges do not show submultiple steps.

Early attempts (Fulton and Dynes 1970) to measure directly the relation between I_S and ϕ in the time-independent state were subject to some uncertainty and accurate measurements have only been reported fairly recently (Jackel *et al* 1974, Waldram and Lumley 1975). The measurements are made in the configuration discussed in §6.6 in which the weak link is in parallel with a bypass loop. The problem is to determine the flux within the loop and hence ϕ (from (6.9)) when a given current is flowing in the link. The latter authors solved this problem by working in a thin-film geometry in which stray flux from the current leads was less than 2×10^{-3} flux quanta. Then for a fixed input current I_1 the externally applied flux Φ_E was varied until the circulating current I_c (measured using a separate SQUID) was zero. Under these conditions the only flux in the loop is the applied flux and the whole of the input current I_1 is flowing through the device, so that the current–flux and hence the current–phase relations could be determined, in this case to an accuracy of about 0·5%. LI_1 was made sufficiently small for the system to be stable at all phases, as described in §6.6. Direct measurement has shown that in small SNS junctions and point contacts the Josephson relation is accurately obeyed. The main interest in this field is to extend precise measurements to systems such as long microbridges and other devices where measurable deviations from Josephson's result may be expected.

9.8. Josephson effects in superfluid helium

After the discovery of the Josephson effects in microbridges, Anderson suggested that analogous phenomena should occur in the flow of superfluid ^{3}He through a small hole, and Richards and Anderson (1965) soon published the results of an experiment which appeared to demonstrate the existence of the inverse AC effect. They allowed superfluid helium to drain from one reservoir into another through a small hole and plotted for a series of sample times the rate of change of level (current) against level difference (analogue of voltage). In the presence of high-frequency acoustic excitation the current showed a fairly convincing series of spikes (as would be expected, since we have in this case the analogue of a voltage source) at multiples and submultiples of the Josephson level difference. They also found that in the presence of the acoustic signal the level difference sometimes remained *constant* for long periods (this is also to be expected: the phase of the Josephson current relative to that of the ultrasonic excitation should be able to adjust itself when biased on a step so as to keep the level difference constant, the normal flow being cancelled by a superflow). Similar constant level differences were found and studied by Khorana (1969).

However, doubt has been thrown on the interpretation of these experiments, especially by the careful studies of Muzinsky (1973) who did an essentially similar experiment and again found static level differences. But in his case he discovered that (i) the ultrasonic excitation generates a *temperature* difference across the hole (which in helium would make an important extra contribution to the chemical potential), (ii) that the static level differences did not vary correctly when further temperature differences were deliberately introduced, (iii) that the effect was more closely linked with the *absolute* level of the helium than with the level *difference*, and (iv) that the effect had the wrong frequency dependence. In his experiments the static levels were almost certainly associated with acoustic resonances inside the reservoirs and in spite of careful search-

ing he found no trace of the true effect. It remains possible that the other observers really did see it in their somewhat different geometries, but until observations have been made which meet the important criteria which Muzinsky laid down, the Josephson effect cannot be regarded as confirmed in helium.

10. Applications using quantum interference

We discuss in the final two sections of this review some important applications of the Josephson effect. We shall concentrate on the most useful and elementary devices only.

10.1. The DC SQUID

We saw in §6.2 that the critical current of a pair of Josephson devices in parallel is sensitive to the magnetic flux which the loop so formed encloses. Such an arrangement can be used to detect flux changes of a small fraction of a flux quantum and has become known as a *DC superconducting quantum-interference detector* or DC SQUID. The theory and practice of the use of DC SQUIDS was largely worked out by Mercereau and his co-workers (see reviews by Mercereau (1970) and Clarke (1973)). They are particularly useful as null detectors in the measurement of very small magnetic fields and voltages.

To understand how a SQUID works we must note that in most practical SQUIDS the self-field cannot be ignored. In fact, if $L_S I_1 \gg \Phi_0$, where L_S is the self-inductance of the SQUID loop, a relatively small imbalance in the currents flowing through the two junctions is sufficient to cancel the effect of a few flux quanta applied to the loop and to a good approximation a circulating current in the SQUID loop will almost cancel any small applied flux. There must be a small residual phase difference, however, for otherwise $I_A - I_B$ would be zero and there would be no circulating current. Thus we can write for a symmetrical SQUID

$$\begin{aligned} I_A &= I_1 \sin(\phi_0 + \tfrac{1}{2}\alpha) \\ I_B &= I_1 \sin(\phi_0 - \tfrac{1}{2}\alpha) \end{aligned} \tag{10.1}$$

where α represents the small residual phase difference and ϕ_0 will be close to $\frac{1}{2}\pi$ when the total current $I_A + I_B$ is maximized. If we remember that $\frac{1}{2}L_S(I_A - I_B)$ must be close to the applied flux Φ_E and that $I_A + I_B$ is maximized with respect to ϕ_0 we find, after a little algebra, that the critical current is equal to $2I_1$ when $\Phi_E = 0$ and equal to $2I_1 - \Phi_0/L_S$ when $\Phi_E = \frac{1}{2}\Phi_0$. Thus in this limit the modulation depth of the critical current as Φ_E is varied is only Φ_0/L_S and not $2I_1$ as it would have been if the self-inductance could have been ignored. If we take a typical value of the critical current I_1 to be 100 μA, then we find that the SQUID will indeed be self-field limited unless its inductance is less than about 2×10^{-11} H. A few SQUIDS have been made for special purposes (by vacuum evaporation of two junctions in parallel onto a single glass slide) whose inductances were as low as this, but the much more common arrangement is to use a double point contact circuit made by splitting a solid block of niobium in which a small hole has been drilled (figure 17(*b*)), for which the inductance will be more like 5×10^{-10} H. Thus the modulation depth is typically a few microamps. The variation in critical current is normally detected by biasing the double junction with a sinusoidal or sawtooth current input which just exceeds the critical current at its peak; the integrated voltage output is then used to detect variations in the critical current. In a practical circuit a change of about 10^{-3} flux quanta in the applied flux can be detected.

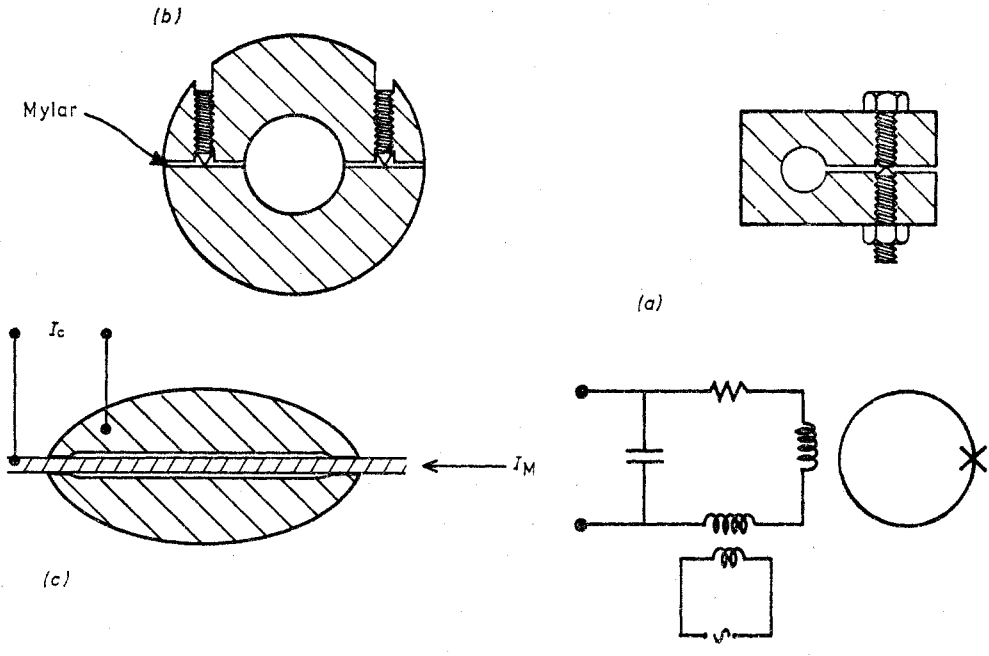

Figure 17. SQUIDS. (*a*) RF SQUID and circuit. (*b*) DC SQUID. (*c*) SLUG. The current to be measured, I_M, passes along the centre wire and the critical current I_c is measured between this wire and the solder blob.

To use the SQUID as a *current detector* we can insert a coil carrying the current into the hole in the SQUID. A small superconducting coil of 50 turns might have a mutual inductance with the SQUID loop of 10^{-8} H, giving a current detection sensitivity of $M/10^{-3}\Phi_0$ or 5×10^{-11} A. This is useful as a DC current detector, but not beyond the range of existing instruments. The SQUID really comes into its own as a null detector in low-voltage potentiometers. In a potentiometer circuit the out-of-balance current is $\Delta V/R$, where R is the total resistance in the loop formed by the detector and the voltages being compared and the detector reading settles down with a time constant $\tau = L/R$ where L is the self-inductance of the same loop. Thus we have two practical constraints:

$$\Delta V/R \gtrsim \Delta I, \qquad R/L \gtrsim 1/\tau_0 \tag{10.2}$$

where ΔI is the current sensitivity of the detector and τ_0 is the maximum available observing time. The SQUID can produce an impressive performance as a voltage detector for three reasons.

(i) On combining these conditions we find that $\Delta V \gtrsim (L/\tau_0)\Delta I$. If we allow an observing time of 1 s and assume that the inductance of the potentiometer circuit can be brought down to, say, 10^{-7} H we find that the *theoretical* DC voltage sensitivity in the absence of noise can be as low as 5×10^{-18} V: the SQUID gains as a voltage detector because it *combines* good current sensitivity with the possibility of very low inductance.

(ii) Although this limiting sensitivity can only be achieved for a particular value of R (10^{-7} Ω in the example quoted) by using a superconducting transformer the SQUID detector can in principle be matched to any reasonably low resistance.

(iii) Being superconducting, the SQUID adds no resistance of its own to the circuit.

A particular form of SQUID developed by Clarke (1966), who calls it the superconducting low-inductance galvanometer or SLUG, is particularly robust and convenient for voltage measurements. It consists of an ordinary solder blob formed on a niobium wire (figure 17(*c*)). The current to be measured passes along the wire. Josephson contacts between the blob and the wire form through the oxide on the wire, often near the ends of the blob; in this geometry the 'hole' is the cylindrical space between the blob and the wire and the induced flux passes around the wire. The current sensitivity of the SLUG is only about 1 μA which is much less than could be achieved in an ideal SQUID and its very small inductance is wasted because the external circuit inductance cannot normally be reduced below 10^{-8} H, so SLUGS have a voltage sensitivity no better than 10^{-15} V. Since the RMS Johnson noise in 10^{-7} Ω at 4 K is about 2×10^{-15} V, however, this performance is, in fact, close to the useful limit in most circumstances and in practice conventional SQUIDS are not much more sensitive than SLUGS for most purposes. Clarke *et al* (1971) have also suggested ways of increasing the SLUG sensitivity for special applications. SLUGS and SQUIDS have made possible many low-voltage experiments which were previously impossible.

To use the SQUID as a *field detector* we link the input coil in the SQUID hole to a pick-up coil, using superconducting wire for the whole circuit. If, as is likely to be the case, the inductance of the pick-up coil and external circuit is appreciably larger than that of the SQUID itself, the flux transfer into the SQUID loop for a given external circuit is maximized when the number of turns in the input coil has been increased to the point where its self-inductance is equal to that of the external circuit. The flux transfer ratio is then about equal to $(L_s/L_{ext})^{1/2}$ and the total flux transferred is of the order of $(L_s/L_{ext})^{1/2}(AN)B$ where AN represents the area-turns in the pick-up loop. Since $L_{ext}^{1/2}$ is also proportional to N, nothing is gained by having many turns in the pick-up loop and the flux transferred depends mainly on the geometry. Using figures for a typical small pick-up loop and SQUID one finds a theoretical field sensitivity of about 10^{-13} T. Practical SQUID magnetometers do, in fact, reach this sort of performance.

10.2. RF SQUIDS

The RF SQUID consists of a *single* device in a superconducting loop (for a review, see Giffard *et al* 1972). Unlike the DC SQUID this structure has no DC critical current which can be measured by attaching leads to it but it can still be made sensitive to the static magnetic field by applying to it in addition an oscillating field of several flux quanta from a coil in a tuned circuit, resonant usually in the MHz region (figure 17(*a*)). The SQUID is arranged so that $2\pi L_s I_1$ is several flux quanta. The characteristic shown in figure 6(*f*) and discussed in §6.6 is then quite strongly 'folded back' and the RF field, which provides an oscillating term in ϕ_A, will drive the SQUID around a complex hysteresis loop. The loss in this loop depends on the number of hysteresis jumps made and it is this which is sensitive to the *static* part of ϕ_A. This means that the Q of the resonant circuit coupled to the SQUID loop varies periodically with the static flux applied to the loop in much the same way as the critical current does in the DC SQUID and can be used in a similar way to detect changes of a small fraction of a flux quantum.

This idea has been extensively developed by Zimmerman and his co-workers, and for most purposes RF SQUIDS are more convenient than DC SQUIDS. They can have somewhat higher basic flux sensitivities, especially if the tank circuit frequency is high, and only one Josephson device is involved so that problems of critical current stability are much less severe. The considerations involved in matching external circuits to the

SQUID hole (normally a small hole in a niobium block—see figure 17(*a*)) are essentially similar to those for a DC SQUID are discussed in the previous section. An RF SQUID and associated circuits with a basic flux sensitivity of $2 \times 10^{-4}\Phi_0$ in the frequency range 0·1 Hz–5 kHz and corresponding voltage and field sensitivities of 10^{-13} V and 10^{-14} T can now be obtained commercially. RF SQUIDS are now important tools in magnetometry, and applications include NMR, CMN thermometry and geophysical field-gradient measurements.

10.3. Josephson devices as computer elements

Josephson devices have a number of attractions as high-speed switches and memories for use in computers and are now under active development by many workers, particularly at IBM Laboratories. Matisoo (1967) was the first to demonstrate that tunnel junctions can be switched very fast (in less than 1 ns) from the superconducting to the normal state. In a typical application a *gate current* passes through the device itself (the gate) and a *control current* passes through a conducting strip which lies over the device in such a way that its magnetic field enters the barrier and can quench the supercurrent by inducing quantum interference. In such a switching operation the voltage across the device builds up in a time controlled by two constraints: (i) the speed with which the control flux enters the junction and quantum interference is set up which, with the small circuit inductances that are possible, is extremely fast, and (ii) the speed of development of the DC voltage after quenching, which depends on the capacitance of the junction and the magnitude of the gate current. In a tunnel junction the voltage rises initially by charging the capacitance and then saturates with the sudden onset of normal current at the gap voltage, $2\Delta/e$. The transition time is given by $(2\Delta/e)C/I_g$ which can easily be made substantially less than 1 ns (Stewart 1969). A number of practical one-bit memory devices based on this idea have been proposed (for instance Clark and Baldwin 1967, Anacker 1969). The information is stored as a circulating supercurrent. In Clark and Baldwin's device, for instance, the junction is in parallel with a superconducting bypass. The memory may be written by pulsing the gate current forwards or backwards. As the gate current rises, the supercurrent divides in such a way as to keep small the flux in the loop formed by the device and the bypass. The pulse is large enough to ensure that in this process the device current exceeds its critical value and when this happens the gate current is 'steered' into the bypass by the finite voltage developed across the device. Once this steering is complete the voltage falls and the device becomes superconducting again. There is now a net flux in the loop generated by the bypass current and when, finally, the gate pulse passes, this flux is left behind with a net circulating current in the loop. The memory can be interrogated by applying suitable pulses to a control strip. The 'steering' time (which has to be added to the switching time) depends on the inductance of the loop, but can also be kept down to less than 1 ns.

Apart from the basic advantage of high speed, Josephson devices have several other advantages.

(i) No power is consumed by the memory during storage.

(ii) They have a substantial output voltage of a few mV.

(iii) Useful current gain: the current switched can be larger than the control current.

(iv) High density: a memory of 10^6 bits can be stored on 1 cm^2 without excessive heating.

(v) They are potentially cheap.

The main drawback is the difficulty of producing the thin oxide layers for tunnel junctions sufficiently reliably. Recent work on switches based on semiconductor junctions (Huang and van Duzer 1975) and microbridges using granular superconductors (Deutscher and Rosenbaum 1975) may allow this problem to be avoided. Further developments investigated recently include the use of two or three devices in parallel to improve the current gain by making the quantum interference more sensitive to the control pulse (Zappe 1975) and the use of a single wide junction as a memory instead of a junction plus a loop, the information being stored as a flux line inside the junction (Guéret 1975).

A rather different idea suggested by Anderson and developed by Fulton and Dunkleberger (1973) is the *flux shuttle*. This consists of a very long tunnel junction to which are attached a number of control electrodes. The junction can contain flux lines, as discussed in §6.5. Using the control electrodes small currents can be injected into finite lengths of the junction, which has the effect of trapping the flux lines in a series of magnetic potential wells. The flux lines can be made to move along the junction by moving these potential wells and can be injected at one end by a control electrode when required. This device can act as a very fast *shift register*, in which a sequence of bits may be stored and moved along to be read either on emergence at the end or *in situ*, as required.

It seems likely that the advantages of Josephson devices will be seen to outweigh the problems of refrigeration and that computers based on them will be built during the next few years.

11. Applications using the AC effects

As in the previous section I shall concentrate attention on what applications seem to be of most long-term significance and on the most technically advanced work reported. Solymar's book (1972) discusses the earlier high-frequency work in detail and some key references for further reading are mentioned in the text.

11.1. Precision measurements of e/h and voltage

The measurement of the ratio of the fundamental constants e/h by comparing the voltages of the steps in the I–V characteristic of a Josephson device with the frequency of the signal producing them was first suggested by Pippard almost as soon as the effect had been discovered. The first very high-precision measurement was made by Parker *et al* (1967) using X-band microwaves applied to a wide range of tunnel junctions and point contacts. The quoted accuracy was 6 ppm. The major source of error was not due to any fundamental limitation but simply to the difficulty of comparing the step voltages of less than 1 mV with the existing voltage standards. In the most recent version of the experiment (Finnegan *et al* 1971) up to 500 steps are measured using a number of junctions in series and the accuracy has reached 0·12 ppm. The precision is still not limited by the finite slope of the steps which, as we noted in §7.9, are extremely steep for the step height of 50 μA which was used. These measurements have led to a substantial revision of the best fit to the values of a number of fundamental constants, the largest change being an increase of 91 ppm in Planck's constant and the most significant a decrease of 20 ppm in the dimensionless fine-structure constant, which ap-

parently resolves an inconsistency between theory and experiment in quantum electrodynamics which had been worrying theoreticians for some time. Measurements of the same type will almost certainly be used in the future to maintain, or even to define, the voltage standard in terms of a frequency standard. For a review of work on this subject, see Langenberg and Taylor (1971).

To justify the measurement it was of course necessary to confirm the exactness of Josephson's relation $h\nu = 2eV$ which connects the step voltage with the frequency. Several authors have suggested that there may be frequency-pulling effects or noise effects which can alter the effective value of ν or quantum electrodynamic effects which can alter the effective value of e. All of these arguments have been refuted; there seems every reason to believe that (i) the relation $h\nu = 2\Delta\mu_c$ is an exact quantum conservation condition, and (ii) that the relation $V = \mu_c/e$ is an exact description of what a real potentiometer measures when placed across a junction. Clarke (1968) has performed a simple and ingenious experiment which shows that the voltages across two SNS junctions of different materials both biased on the same step of their characteristics and joined in a ring† are equal to within 1 part in 10^8, and other experiments have shown that, to within 1 ppm, the experimental value of e/h is independent of step order, temperature, magnetic field, frequency, materials, and also on whether tunnel junctions, point contacts or solder-drop junctions are used in the observation. The measurements of e/h and voltage are therefore on very firm ground both theoretically and experimentally.

11.2. Microwave mixing

Josephson devices can be used as microwave mixers of high efficiency and low noise (see Richards *et al* 1973). Technical development has not yet proceeded very far, but it has been demonstrated that in the millimetre waveband they are at least the equal of other existing devices. In the submillimetre band less data are available, but they may well prove to be the best mixers available and receivers based on them will probably soon be developed. Mixing can occur in at least the following modes.

(i) With external local oscillator, biased off the Josephson steps.

(ii) With external local oscillator, biased within a step (see §11.3).

(iii) Using the Josephson frequency as local oscillator (with or without cavity stabilization).

(iv) With external local oscillator, using hysteretic devices biased at the edge of a hysteresis region.

Early experiments on mixing were reported by Shapiro and co-workers (see Grimes and Shapiro 1968). Richards and others at Berkeley have investigated both the theory and the practice of mixing in a thorough series of papers (see Taur *et al* 1974) for frequencies up to one-twentieth of the gap frequency, using mainly niobium point contacts. They have found remarkably close agreement with the simple resistively shunted junction model in noise performance as well as in mixing efficiency. For the likely applications the first mixing mode described is probably the best and it is also easy to understand: the signal beats with the local oscillator, and this produces a modulation of the step height at the intermediate frequency (cf figure 11(*b*)). If the

† There are, however, difficulties in deducing that the same would necessarily be true if the junctions were separate.

system is biased outside the vertical regions it behaves at the intermediate frequency as a current source of amplitude $(\partial i/\partial i_L)_V i_S$ and source resistance $(\partial V/\partial i)_{i_L}$. Calculating the power available is therefore simply a matter of calculating how the I–V characteristic behaves as a function of local oscillator current, as discussed in §7.8. The answer is a function of bias point, local oscillator power and source impedance. When these are optimized Taur *et al* (1974) find that:

(i) At low signal frequencies the conversion efficiency is excellent and indeed conversion gain can occur (the power coming from the DC source), but at frequencies beyond the critical frequency given by $\omega_c = 2eI_1R/\hbar$ the conversion efficiency falls off as $(\omega_c/\omega_S)^2$. For niobium ω_c is 1·14 THz so in the submillimetre waveband there is a strong incentive to use materials of even higher T_c.

(ii) For a given signal frequency, little efficiency is lost by using a local oscillator at a submultiple of the signal frequency, though more local oscillator power and more precise biasing are necessary. This is a very significant technical advantage at the highest frequencies.

(iii) The mixer noise temperature referred to the input is equivalent to about five times the actual temperature of the device and is more or less independent of the conversion efficiency. Thus the fall in efficiency at high frequencies does not worsen the ratio of signal to mixer noise, though of course it makes the noise of later stages more important.

(iv) The optimum local oscillator power required is small, typically about $\frac{1}{2}$ μW if perfectly matched.

Mixing using the internally generated Josephson frequency as local oscillator has a worse signal-to-noise ratio and is less efficient. It may also suffer from unacceptable frequency blurring unless quite exceptional measures are taken to stabilize the DC current source. Hysteretic mixing can give conversion gain factors as high as 50 but only at the cost of poor noise performance and narrow bandwidth.

At frequencies beyond the gap frequency the validity of the RSJ model is suspect. For tunnel junctions Werthamer's theory suggests at first sight that the fall in the Josephson current amplitude beyond the Riedel peak would further degrade the mixing performance at high frequencies. However, careful examination of (8.1) shows that this is not necessarily so. If an appropriate large DC bias is used one can arrange that $e^{\pm i\phi}$ has terms linear in the signal which have frequencies near the Riedel peak and actually take advantage of it; the corresponding transition is shown in figure 4(*c*) for a particular case. Conventional tunnel junctions are, however, useless at such high frequencies because of their large shunt capacitance and it is clear that relatively large microbridges in which the Josephson effect is a consequence of the Ginzburg–Landau theory will probably cease to operate when the frequency reaches the inverse of the Ginzburg–Landau relaxation time, which may be at the gap frequency or lower (Højgaard Jensen and Lindelof 1975). The only devices to have shown convincing Josephson effects beyond the gap frequency are high-resistance point contacts; these devices commonly show some structure in their I–V curves at the gap voltage and may be intermediate in nature between tunnel junctions and very small microbridges. Steps and Josephson mixing have been seen in such niobium point contacts by a number of observers at frequencies up to five times the gap frequency, and indeed a technique is being adopted by standards laboratories in which point contacts are used to generate very high harmonics of microwave frequency standards for comparison with laser standards in the submillimetre region. The mixing efficiency and noise performance at these very high frequencies has not yet been explored.

11.3. Parametric amplification

We saw in §7.6 that a junction biased within the zero-order step has a small-signal inductance L_J equal to $\hbar/(2eI_1 \cos \phi)$. Since this is a function of ϕ, it can be modulated by a signal at another frequency and it has been noted that the familiar properties associated with variable parameters should arise. The simplest useful effect is just mixing, but unless the intermediate frequency is unusually high this process is not competitive with the mixing when biased outside the step (see §11.2). A more interesting possibility is the use of resonant signal and idler circuits with an external pump signal, as in a conventional parametric amplifier. From a simple model calculation one finds that the parametric gain can be written as $\beta(1-\beta)^{-2}(\omega_I/\omega_S)$ where ω_I and ω_S are the idler and signal frequencies and β is given by

$$\beta = \frac{\omega_c^2}{\omega_I \omega_S} \sin \phi_0 J_1(\phi_p) \tag{11.1}$$

where ϕ_0 is the equilibrium phase across the junction (which can be adjusted by the DC bias), J_1 is the Bessel function, and ϕ_p is a phase proportional to the pump amplitude, which can also be adjusted. Similar effects probably occur when the junction is biased within any of the vertical steps induced by the pump frequency. According to this simple model any required gain can be achieved provided $\omega_I < (\omega_c^2/\omega_S) J_{1\,\max}^2$. This means that, if we use a local oscillator as pump and use as the load in the idler circuit the input of an IF amplifier, we can in principle get mixing with any required gain provided the IF frequency is *low* enough (and provided $\omega_I = \omega_p - \omega_S$, not $\omega_I = \omega_S - \omega_p$). This idea was presented and experimentally checked by Zimmer (1967) and by Feldman *et al* (1975) for the slightly more complicated condition $2\omega_p = \omega_I + \omega_S$, in which the coupling between signal and idler is via the second harmonic of the pump frequency. This had two advantages: no DC bias was required, and it was possible to arrange that ω_p, ω_I and ω_S were almost equal and could conveniently be handled by the same resonant circuit. Feldman *et al* used an array of microbridges (to improve matching) and worked at 10 GHz. Gains of up to 16 dB and amplifier noise as low as 8 K were measured and the agreement with the RSJ model with suitably adjusted parameters was good. Useful parametric gain at 30 MHz using the Josephson oscillation as pump has been reported by Kanter and Silver (1971). If these ideas can be applied at higher frequencies the technical implications would be important.

Acknowledgments

I must express my thanks to B D Josephson for advice in planning this article and for a critical reading of it which exposed a number of deficiencies, and to P D A Orr, who also read and criticized part of the manuscript. I must, however, make clear that I am responsible for what is written and for whatever errors remain. I am also grateful to a number of authors for allowing me to see work in advance of publication.

References†

† ABRIKOSOV A A, GORKOV L P and DZYALOSHINSKI I E 1963 *Methods of Quantum Field Theory in Statistical Mechanics* (Englewood Cliffs, NJ: Prentice-Hall)

AHARONOV Y and BOHM D 1959 *Phys. Rev.* **115** 485

AMBEGAOKAR V and BARATOFF A 1963a *Phys. Rev. Lett.* **10** 486

† Books and review articles helpful for further reading are indicated thus.

—— 1963b *Phys. Rev. Lett.* **11** 104
AMBEGAOKAR V and HALPERIN B I 1969 *Phys. Rev. Lett.* **22** 1364
ANACKER W 1969 *Trans. IEEE* **MAG-5** 968
ANDERSON P W 1958 *Phys. Rev.* **112** 1900
—— 1964 *Lectures on The Many-Body Problem* vol 2, ed E R Caianiello (New York: Academic Press) p113
—— 1966 *Rev. Mod. Phys.* **38** 298
†—— 1967 *Progress in Low Temperature Physics* vol 5, ed C J Gorter (Amsterdam: North-Holland) pp1–43 (a review of Josephson effects)
ANDERSON P W and DAYEM A H 1964 *Phys. Rev. Lett.* **13** 195
ANDERSON P W and ROWELL J M 1963 *Phys. Rev. Lett.* **10** 230
ASLAMAZOV L G and LARKIN A I 1968 *Zh. Eksp. Teor. Phys. Pis. Red.* **9** 150 (Engl. trans. *Sov. Phys.–JETP Lett.* **9** 87)
AURACHER F, RICHARDS P L and ROCHLIN G I 1973 *Phys. Rev.* B **8** 4182
BARATOFF A, BLACKBURN J A and SCHWARTZ B B 1970 *Phys. Rev. Lett.* **25** 1096
BARDEEN J, COOPER L N and SCHRIEFFER J R 1957 *Phys. Rev.* **108** 1175
BLACKBURN J A, LESLIE J D and SMITH H J 1971 *J. Appl. Phys.* **42** 1047
BLANEY T G 1974 *Rev. Phys. Appl.* **9** 279
†DE BRUYN OUBOTER R and DE WAELE A Th A M *Progress in Low Temperature Physics* vol 6, ed C J Gorter (Amsterdam: North-Holland) pp243–90 (a review of quantum interference)
CHAMBERS R G 1960 *Phys. Rev. Lett.* **5** 3
CLARK T D and BALDWIN J P 1967 *Electron. Lett.* **3** 178
CLARKE J 1966 *Phil. Mag.* **13** 115
—— 1968 *Phys. Rev. Lett.* **21** 1566
—— 1969 *Proc. R. Soc.* A **308** 447
†—— 1973 *Proc. IEEE* **61** 8–19 (a review of DC and RF SQUIDS)
CLARKE J, TENNANT W E and WOODY D 1971 *J. Appl. Phys.* **42** 3859
COHEN M H, FALICOV L M and PHILLIPS J C 1962 *Phys. Rev. Lett.* **8** 316
COON D D and FISKE M D 1965 *Phys. Rev.* **138** A744
DAHM A J, DENENSTEIN A, FINNEGAN T F, LANGENBERG D N and SCALAPINO D J 1968 *Phys. Rev. Lett.* **20** 859
DAHM A J, DENENSTEIN A, LANGENBERG D N, PARKER W H, ROGOVIN D and SCALAPINO D J 1969 *Phys. Rev. Lett.* **22** 1416
DAYEM A H and WIEGAND J J 1967 *Phys. Rev.* **155** 419
DEUTSCHER G and ROSENBAUM R 1975 *Appl. Phys. Lett.* **27** 366
DIETRICH I 1952 *Z. Phys.* **133** 499
DMITRENKO I M, YANSON I K and SVISTUNOV V M 1965 *Zh. Eksp. Teor. Fiz. Pis. Red.* **2** 10 (Engl. trans. *Sov. Phys.–JETP Lett.* **2** 10)
DOWMAN J E, MACVICAR M L A and WALDRAM J R 1969 *Phys. Rev.* **186** 452
ECK R E, SCALAPINO D J and TAYLOR B N 1964 *Phys. Rev. Lett.* **13** 15
EHRENBERG W and SIDAY R E 1949 *Proc. Phys. Soc.* B **62** 8
ELIASHBERG G M 1970 *Zh. Eksp. Teor. Fiz. Pis. Red.* **11** 186 (Engl. trans. *Sov. Phys.–JETP Lett.* **11** 114)
FACK H and KOSE V 1971 *J. Appl. Phys.* **42** 320
FALCO C M, PARKER W H and TRULLINGER S E 1973 *Phys. Rev. Lett.* **31** 933
FELDMAN M J, PARRISH P T and CHIAO R Y 1975 *Proc. 14th Conf. on Low Temperature Physics* vol 4, ed M Krusius and M Vuorio (Amsterdam: North-Holland) pp188, 192
FERRELL R A and PRANGE R E 1963 *Phys. Rev. Lett.* **10** 479
FINNEGAN T F, DENENSTEIN A and LANGENBERG D N 1971 *Phys. Rev.* B **4** 1487
FISKE M D 1964 *Rev. Mod. Phys.* **36** 221
FULTON T A and DUNKLEBERGER L N 1973 *Appl. Phys. Lett.* **22** 232
FULTON T A and DYNES R C 1970 *Phys. Rev. Lett.* **25** 794
DE GENNES P G 1963 *Phys. Lett.* **5** 22
—— 1964 *Rev. Mod. Phys.* **36** 225
†—— 1966 *Superconductivity of Metals and Alloys* (New York: Benjamin)
GIAEVER I 1960 *Phys. Rev. Lett.* **5** 147
—— 1965 *Phys. Rev. Lett.* **14** 904
GIAEVER I and ZELLER H R 1971 *Physica* **55** 455
†GIFFARD R P, WEBB R A and WHEATLEY C J 1972 *J. Low Temp. Phys.* **6** 533–610

GREGERS-HANSEN P E and LEVINSEN M T 1971 *Phys. Rev. Lett.* **27** 847
GREGERS-HANSEN P E, HENDRICKS E, LEVINSEN M T and PICKETT G R 1973 *Phys. Rev. Lett.* **31** 524
GREGERS-HANSEN P E, LEVINSEN M T and FOG PEDERSEN G 1972 *J. Low Temp. Phys.* **7** 99
GREGERS-HANSEN P E, LEVINSEN M T, PEDERSEN L and SJØSTRØM C J 1971 *Solid St. Commun.* **9** 661
GRIMES C C and SHAPIRO S 1968 *Phys. Rev.* **169** 397
GUÉRET P 1975 *Trans. IEEE* **MAG-11** 751
HAMILTON C A 1972 *Phys. Rev.* B **5** 912
HAMILTON C A and SHAPIRO S 1971 *Phys. Rev. Lett.* **26** 426
HARRIS E P 1975 *Trans. IEEE* **MAG-11** 785
HARRISON W A 1961 *Phys. Rev.* **123** 85
HØJGAARD JENSEN H and LINDELOF P E 1975 *Proc. 14th Int. Conf. on Low Temperature Physics* vol 4, ed M Krusius and M Vuorio (Amsterdam: North-Holland) p152
HOOK J R and WALDRAM J R 1973 *Proc. R. Soc.* A **334** 171
HUANG C L and VAN DUZER T 1975 *Trans. IEEE* **MAG-11** 766
HUNT T K and MERCEREAU J E 1967 *Phys. Rev. Lett.* **18** 551
JACKEL L D, BUHRMAN R A and WEBB W W 1974 *Phys. Rev.* B **10** 2782
JAKLEVIC R C, LAMBE J J, SILVER A H and MERCEREAU J E 1964a *Phys. Rev. Lett.* **12** 159
—— 1964b *Phys. Rev. Lett.* **12** 274
JOSEPHSON B D 1962a *Phys. Lett.* **1** 251
—— 1962b *Trinity College Fellowship Thesis*
—— 1964a *PhD Thesis* University of Cambridge (partly published as next reference)
†—— 1965 *Adv. Phys.* **14** 419–51 (a review of Josephson effects)
—— 1964b *Rev. Mod. Phys.* **36** 216
†—— 1974 *Science* **184** 527 (the Nobel lecture)
KAMPER R A and ZIMMERMAN J E 1971 *J. Appl. Phys.* **42** 132
KANTER H and SILVER A H 1971 *Appl. Phys. Lett.* **19** 515
KANTER H and VERNON F L 1970a *Phys. Rev. Lett.* **25** 588
—— 1970b *Phys. Lett.* **32A** 155
KHORANA B M 1969 *Phys. Rev.* **185** 299
KURKIJARVI J 1972 *Phys. Rev.* B **6** 832
LANGENBERG D N 1974 *Rev. Phys. Appl.* **9** 35
LANGENBERG D N, SCALAPINO D J and TAYLOR B N 1966 *Proc. IEEE* **54** 560
† LANGENBERG D N and TAYLOR B N (ed) 1971 *Proc. Int. Conf. on Precision Measurement and Fundamental Constants, NBS Publ. No. 343* (Washington, DC: US Govt Printing Office)
LEBWOHL P and STEPHEN M J 1967 *Phys. Rev.* **163** 376
LEVINSTEIN H J and KUNZLER J E 1966 *Phys. Lett.* **20** 581
LINDELOF P E 1976 *Solid St. Commun.* **18** 283
LUMLEY J M 1974 *PhD Thesis* University of Cambridge
MATISOO J 1967 *Proc. IEEE* **55** 172
—— 1969a *J. Appl. Phys.* **40** 1813
—— 1969b *Phys. Lett.* **29A** 473
MCCUMBER D E 1968 *J. Appl. Phys.* **39** 3113
MCDONALD D G, JOHNSON E G and HARRIS R E 1976 *Phys. Rev.* B **13** 1028
MCDONALD D G, RISLEY A S, CUPP J D, EVENSON K M and ASHLEY J R 1972 *Appl. Phys. Lett.* **20** 296
MCMILLAN W L and ROWELL J M 1969 *Superconductivity* vol 1, ed R D Parks (New York: Dekker) p561
MEISSNER H 1960 *Phys. Rev.* **117** 672
† MERCEREAU J E 1970 *Rev. Phys. Appl.* **5** 13–20 (a review of DC SQUIDS)
MUZINSKI D L 1973 *J. Low Temp. Phys.* **13** 287
NISENOFF M and WOLF S 1975 *Phys. Rev.* B **12** 1712
NOTARYS H A and MERCEREAU J E 1971 *Physica* **55** 424
OWEN C S and SCALAPINO D J 1967 *Phys. Rev.* **164** 538
PARKER W H, TAYLOR B N and LANGENBERG D N 1967 *Phys. Rev. Lett.* **18** 287
† PARKS R D (ed) 1969 *Superconductivity* 2 vols (New York: Dekker)
PARKS R D and MOCHEL J M 1964 *Rev. Mod. Phys.* **36** 284
PEDERSEN N F, FINNEGAN T F and LANGENBERG D N 1972 *Phys. Rev.* B **6** 4151

PRANGE R E 1963 *Phys. Rev.* **131** 1083
RICHARDS P L and ANDERSON P W 1965 *Phys. Rev. Lett.* **14** 540
† RICHARDS P L, AURACHER F and VAN DUZER T 1973 *Proc. IEEE* **61** 36–45 (a review of mixing)
† RICKAYZEN G 1965 *Theory of Superconductivity* (New York: Wiley)
RIEDEL E 1964 *Z. Naturf.* **19A** 1634
ROWELL J M 1963 *Phys. Rev. Lett.* **11** 200
RUSSER P 1972 *J. Appl. Phys.* **43** 2008
SCOTT A C and JOHNSON W J 1969 *Appl. Phys. Lett.* **14** 316
SCOTT W C 1970 *Appl. Phys. Lett.* **17** 166
SHAPIRO S 1963 *Phys. Rev. Lett.* **11** 80
SILVER A H and ZIMMERMAN J E 1967 *Phys. Rev.* **157** 317
SILVER A H, ZIMMERMAN J E and KAMPER R A 1967 *Appl. Phys. Lett.* **11** 209
SKOCPOL W J, BEASLEY M R and TINKHAM M 1974 *J. Low Temp. Phys.* **16** 145
SMITH P H, SHAPIRO S, MILES J L and NICOL J 1961 *Phys. Rev. Lett.* **6** 686
† SOLYMAR L 1972 *Superconductive Tunnelling and Applications* (London: Chapman and Hall)
STEPHEN M J 1968 *Phys. Rev. Lett.* **21** 1629
STEWART W C 1968 *Appl. Phys. Lett.* **12** 277
—— 1969 *Appl. Phys. Lett.* **14** 392
TAUR Y, CLAASSEN J H and RICHARDS P L 1974 *Rev. Phys. Appl.* **9** 263
TAYLOR B N and BURSTEIN E 1963 *Phys. Rev. Lett.* **10** 14
THOMPSON E D 1973 *J. Appl. Phys.* **44** 5587
TINKHAM M 1963 *Phys. Rev.* **129** 2413
TREDWELL T J and JACOBSEN E H 1975 *Phys. Rev. Lett.* **35** 244
VINCENT D A and DEAVER B S 1974 *Phys. Rev. Lett.* **32** 212
WALDRAM J R and LUMLEY J M 1975 *Rev. Phys. Appl.* **10** 7
WALDRAM J R, PIPPARD A B and CLARKE J 1970 *Phil. Trans. R. Soc.* A **268** 265
WERTHAMER N R 1966 *Phys. Rev.* **147** 255
—— 1969 *Superconductivity* vol 1, ed R D Parks (New York: Dekker) p321
WYATT A F G, DMITRIEV V M, MOORE W S and SHEARD F W 1966 *Phys. Rev. Lett.* **16** 1166
YANSON I K, SVISTUNOV V M and DMITRENKO I M 1965 *Zh. Eksp. Teor. Fiz.* **48** 976 (Engl. trans. *Sov. Phys.–JETP* **21** 650)
ZAPPE H H 1975 *Appl. Phys. Lett.* **27** 432
ZIMMER H 1967 *Appl. Phys. Lett.* **10** 193